The role of T-box transcription factor TBX3 in rhabdomyosarcoma

By Danica Anne (Smuts) Sims

(SMTDAN013)

SUBMITTED TO THE UNIVERSITY OF CAPE TOWN

In fulfilment of the requirements for the degree

MScMed in Medical Cell Biology

Division of Human Biology

Faculty of Health Sciences

University of Cape Town

April 2016

Supervisor: Professor Sharon Prince

Co-supervisor: Dr Jade Pereira de Andrade Peres

Declaration

I, Danica Anne (Smuts) Sims, hereby declare that the work on which this dissertation/thesis is based is my original work (except where acknowledgements indicate otherwise) and that neither the whole work nor any part of it has been, is being, or is to be submitted for another degree in this or any other university.

I empower the university to reproduce for the purpose of research either the whole or any portion of the contents in any manner whatsoever.

Signed by candidate

Danica Anne (Smuts) Sims

April 2016

Acknowledgements

It does not feel right to have only my name on the final degree, because I know how many people have made it possible for me to achieve this. Without your generous support, unwavering encouragement and endless patience, the success of this project would have never been realised:

Professor Sharon Prince, it has been an absolute pleasure and privilege to be a part of the "T-box" lab these past three years. From the very first moment you lectured me in my undergraduate human physiology course about the cell cycle I knew that I wanted learn from and work with you. Under your unparalleled guidance, knowledge, experience and supervision I have grown tremendously and I know that training in your lab will make me the best scientist I could ever be. I will never forget to pay attention to all the details and links but also remember to stand back and look at the big picture. It has been incredibly exciting to contribute my small piece to the larger puzzle your laboratory is building. Thank-you for investing so much time in me and in my future.

Dr Jade Peres, you took me as a fresh (to put it mildly) honours student and somehow managed to smooth out the roughness and mold me into a "real" researcher. Thank-you for guiding me day in and day out, for practically training me, instilling confidence in the skills I have learned but also balancing it with checking over my shoulder to make sure that I don't make an unnecessary mistake. Thank-you too for reading through all my attempts at writing, giving me feedback and encouraging me.

Many thanks to the members of the ***Prince lab*** – I will sorely miss being a part of this family. I think that there are few laboratories like ours in which there is ready laughter, encouragement and help (and an excuse to use any vaguely happy occasion to eat some cake!). It was comforting knowing that I was surrounded by friends who were passionate about what they were researching and always keeping an eye out for one another. The T-box lab has a reputation for excellence and I was so proud to be a member. Thank-you

Jenna, Joy-Mari, Rehanna, Jade, Tarryn, Sandra, George, Alexis, Serah, Melissa, Irene and Lawrence for your daily support.

A special thank-you to Mrs Susan Cooper for assistance with the confocal microscope, to Mr Rodney Lucas for his assistance during the mouse work, to Mrs Morea Peterson for embedding and staining the mouse tumours, to Professor Dhiren Govender for analyzing the histopathology of the tumour sections and to Professor Dirk Lang for taking photographs of the tumour sections.

Lastly I would like to thank my husband ***Ray***. No words will never be enough to describe how grateful I am for your eternal patience, understanding, love, support, encouragement, prayers, belief in me and for your sacrifice and service – I could not have wished for a better friend to have shared this often difficult but wonderful adventure with me. I am utterly certain that I would not have been able to achieve all that I have without you by my side. I am so excited for our next adventure together – whatever it may be!

This work was kindly supported by the Harry Crossley Research Fellowship and National Research Fellowship, without whose generous contributions would not have made this year of study possible, thank-you. The opinions expressed and conclusions arrived at are my own and not necessarily to be attributed to the NRF.

"*Great are the works of the LORD; they are studied by all who delight in them*." Psalm 111:2.

Research outputs from this Masters

Original Publication:

Willmer T, Cooper A, **Sims D**, Govender D, Prince S (2016) The T-box transcription factor 3 is a promising biomarker and a key regulator of the oncogenic phenotype of a diverse range of sarcoma subtypes. Oncogenesis 5, e199; doi:10.1038/oncsis.2016.11.

Oral presentations:

Prince S, Willmer T, **Smuts D**, Peres J, Parkes J and Govender D (2015) The T-BOX transcription factor 3 is a promising biomarker and therapeutic target in a diverse range of sarcoma subtypes. AORTIC 2015, entitled "AORTIC Roadmap to Cancer Control in Africa", 18 - 22 November 2015, Marrakech, Morocco.

Smuts D, Peres J, Prince S (2015) The oncogenic role of TBX3 in rhabdomyosarcoma. Health Sciences Faculty Postgraduate Research Day, University of Cape Town, 2 September 2015.

Smuts D, Peres J, Prince S (2015) The role of TBX3 in rhabdomyosarcoma. Medical Biochemistry seminar series, University of Cape Town, 26 May 2016.

Table of Contents

Abbreviations

3Dlg3: disks large homolog

AKT: protein kinase B

ARMS: alveolar rhabdomyosarcoma

BSA: bovine serum albumin

Caperα: Coactivator of AP1 and Estrogen Receptor

CASK: Calcium/calmodulin-dependent serine protein kinase

CDK: cyclin dependent kinase

CDKI: cyclin dependent kinase inhibitors

cDNA: Complementary DNA

ChIP: chromatin immunoprecipitation

CSCs: cancer stem cells

Cx40: connexin 40

DDX3: DEAD box helicase 3

DMEM: Dulbecco's-modified Eagle medium

DNA: dioxyribonucleic acid

Dppa3: developmental pluripotency-associated protein 3

EMT: epithelial-to-mesenchymal transition

ERMS: embryonic rhabdomyosarcoma

ESCs: embryonic stem cells

FACS: fluorescence assisted cell sorting

FBS: fetal bovine serum

FGF: fibroblast growth factor

G1: gap 1 phase of the cell cycle

G2: gap 2 phase of the cell cycle

G-418: geneticin

GSK3: glycogen synthase kinase 3

HDAC: histone deacetylase

H & E: haematoxylin and eosin

HGF: hepatocyte growth factor

Hh: hedgehog

HPV: Human papillomavirus

Hsc: Heat shock cognate

Hsp: Heat shock protein

IGF: insulin-like growth factor

IP: immunoprecipitation

iPSC: induced pluripotent stem cells

KIT: mast/stem cell growth factor receptor Kit

Klf4: kruppel-like factor 4

lncRNA: long non-coding RNA

M: mitosis/meiosis phase of the cell cycle

MAPK: mitogen-activated protein kinases

MDM2: mouse double minute 2 homolog

MEFs: mouse embryonic fibroblasts

mESC: mouse embryonic stem cells

MET: MET proto-oncogene receptor tyrosine kinase

miR/miRNA: micro-RNA

MMP: matrix metalloproteinase

mtbx3: mouse Tbx3

mRNA: messenger RNA

mTOR: mechanistic target of rapamycin

MTT: methylthiazol tetrazolium

Nfκb1: nuclear factor of kappa light polypeptide gene enhancer in B-cells 1

Nkx2-5: NK2 homeobox 5

Nppa: natriuretic peptide A

PAX3/7–FKHR/FOXO: paired box 3- forkhead box O1

PBS: phosphate buffered saline

PBS/T: 1X phosphate buffered saline /0.1% Tween-20

PCR: polymerase chain reaction

PDGF: platelet derived growth factor

PKCδ: protein kinase C-δ

PI: propidium iodide

PI3K: phosphoinositide 3-kinase

PLCg: phospholipase Cg

PMA: phorbol 12-myristate 13-acetate

POMC: pro-opiomelanocortin

qRT-PCR: quantitative real-time polymerase chain reaction

RA: retinoic acid

RNA: ribonucleic acid

RNAi: RNA interference

RMS: rhabdomyosarcoma

ROS: reastive oxygen species

rpm: revolutions per minute

Rb: retinoblastoma

RT: room temperature

RTK: receptor tyrosine kinase

S: synthesis phase of the cell cycle

SDS-PAGE: sodium-dodecyl-sulphate polyacrylamide gel electrophoresis

SHCTRL: positively transfected stable shCTRL control cell line

shRNA: short hairpin RNA

SHTBX3: positively transfected stable shTBX3 knockdown cell line

siCTRL: positively transfected transient siCTRL control cell line

siRNA: short interfering RNA

siTBX3: positively transfected transient siTBX3 knockdown cell line

Taz: Tafazin

TBX: T-box

TGF-β: transforming growth factor beta

UCA1: Urothelial Cancer Associated 1

UMS: ulnar mammary syndrome

VEGF: vascular endothelial growth factor

Wnt: wingless

List of Tables and Figures

Abstract

Cancer remains one of the leading causes of death worldwide due to late diagnosis and ineffective treatment options. To address this problem requires the elucidation of the molecular mechanisms, including the signaling pathways and transcription factors that drive cancer initiation and progression. In this regard, our laboratory has been particularly interested in the embryonically important T-box family of transcription factors which has been heavily implicated in promoting initiation and progression of a long list of cancers. For example, the overexpression of the T-box factor TBX3, has been reported to function in promoting immortalization, migration, invasion and tumour formation in a number of epithelial-derived malignancies. Furthermore, our laboratory recently reported that TBX3 is also overexpressed in a wide range of sarcoma subtypes including rhabdomyosarcomas. This suggests that TBX3 may also contribute to the development and/or progression of sarcomas and potentially may serve as a biomarker for their diagnosis and targeted therapy. This is exciting because sarcomas are diverse and heterogeneous cancers with varying clinical behaviours, high rates of metastasis and recurrence and are notoriously resistant to current chemotherapies. However, whether TBX3 is a molecular driver of these mesenchymal-derived cancers remains to be determined. This project therefore aimed to elucidate the role of TBX3 overexpression in embryonal rhabdomyosarcomas (ERMS) which is the most common soft tissue sarcoma in children and adolescents. To this end, ERMS cell culture models were established in which TBX3 was either stably knocked down or stably overexpressed and the resulting cells were tested for several features of the cancer phenotype using *in vitro* and *in vivo* experiments. The results show that TBX3 promotes cell proliferation, anchorage independent growth and cell migration *in vitro* and tumour formation and invasion *in vivo.* This study also provides evidence that nucleolin binds to, and co-operates with, TBX3 to promote proliferation and migration of ERMS cells. Furthermore, data from initial experiments reveal that Hsc70 interacts with TBX3, to possibly increase its protein stability, and that oncogenic c-Myc and AKT1 positively regulate TBX3 levels in ERMS. This, albeit preliminary data, suggest that Hsc70, c-Myc and AKT1 are responsible, in part, for the overexpression of TBX3 in ERMS. Together findings from this study implicate TBX3 as an oncogene in ERMS and suggest that TBX3, nucleolin, Hsc70, c-Myc and AKT may be used in combination as biomarkers for the diagnosis and targeted therapy of ERMS.

Chapter 1. Literature Review

1.1. Introduction

The wonder of life is the process of a single fertilized egg developing into a complex, multicellular, fully functional organism. This intricate dance requires precise and controlled co-ordination of gene expression by transcription factors and signaling pathways. Disruption in this delicate choreography can have catastrophic consequences regarding the development and homeostasis of an organism. For example, the T-box family of transcription factors play an important role in embryonic development and the patterning of many tissues, and mutations in several members of this family result in congenital disorders. Furthermore, their deregulated expression has also been implicated in many carcinomas and more recently in sarcomas, including some of the most aggressive and treatment resistant malignancies. Sarcomas are aggressive, malignant tumours that develop in bone and soft tissues with a relatively poor prognosis. They are a complex group of cancers derived from the mesenchyme and there are more than 75 sarcoma subtypes that exhibit different biologies and clinical behaviours. Sarcomas are difficult to treat and are largely resistant to current chemotherapeutics. This is in part, because there is a lack of adequate diagnostic markers for early and accurate classification of subtypes, 30% of sarcomas metastasize and 20% recur. Therefore elucidating the status, role and regulation of key molecular drivers of the various sarcoma subtypes will greatly benefit the field in terms of diagnostics and more effective combination-targeted treatment options. Of particular interest to the current project is the T-box factor TBX3 and its potential role in rhabdomyosarcoma, a childhood sarcoma of the skeletal muscle.

1.2. T-box transcription factor family

Transcription factors are master regulators of gene expression and are key players in embryogenesis where they regulate, amongst other processes, cell proliferation, apoptosis, cell migration and invasion into surrounding tissues. Considering that these processes are

also key features of oncogenesis, it is not surprising that the deregulated expression and activity of transcription factors are a feature of cancer initiation and progression (Lewis, 2000). An example is the T-box transcription factor family which derive their name from a highly conserved DNA binding domain, known as the T-box, present in all its members (Kispert *et al*. 1995). T-box factors are highly conserved across a wide range of metazoans including nematodes, fruit flies, fish, frogs, chicken, mice and humans (**Figure 1.1**) (Kavka & Green, 1997; Papaioannou, 2001).

Brachyury (Greek *brakhus* for short and *oura* for tail) is the first member of the T-box family that was described in 1927 by the Russian surgeon and scientist Nadine Dobrovoskaia-Zavadskaia. She observed that mice with homozygous loss of *Brachyury* died *in utero* whereas heterozygous mice failed to complete full tail development and consequently had short tails (Dobrovolskaia-Zadvadskaia, 1927). MacMurry and Shin (1988) showed that deletions of different allelic forms of Brachyury result in a gradient of protein levels and that this impacted on the severity of the short tail phenotype. This was the first study to illustrate that T-box proteins exhibit dosage sensitivity. The mouse Brachyury was later cloned (Hermman *et al.*, 1990) and subsequent homologues were identified in several vertebrates and invertebrates confirming the existence of the ancient T-box family (**Figure 1.1**) (Klava & Green, 1997; Smith, 1999). Phylogenetic and genomic analyses have traced the origins of this gene family back to a common ancestor that, through gene duplication events, further diverged along individual lineages. This has allowed different T-box family members to acquire unique functions and spatial and temporal expression patterns, while retaining a conserved T-box domain (Agulnik *et al*., 1996; Minguillon & Logan, 2003). In mammals the T-box family consists of 18 members and they have been grouped into the following five subfamilies: Brachyury (also known as T), T-brain1 (Tbr1), TBX1, TBX2 and TBX6 (Agulnik *et al*., 1996; Papaioannou *et al*., 2014).

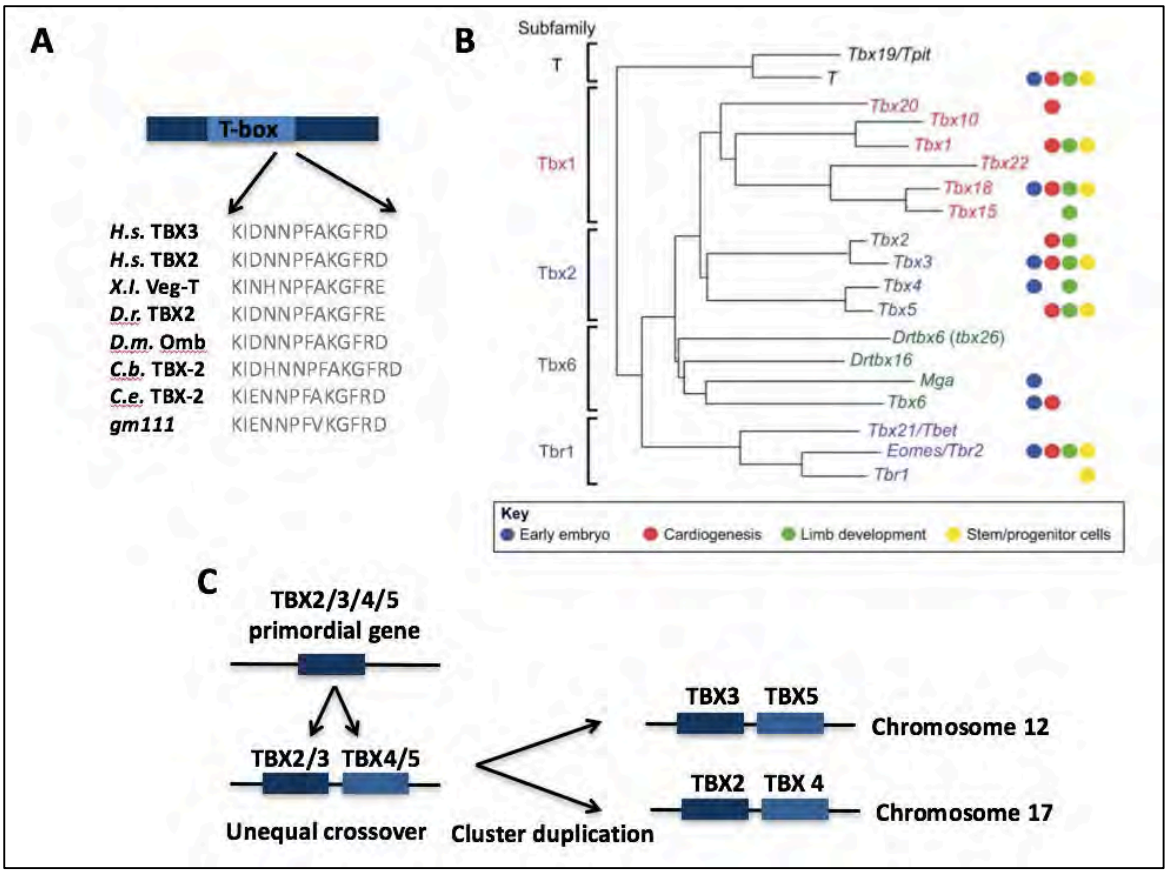

Figure 1.1: Evolutionary history of the T-box gene family. ***(A)*** Conservation of the T-box domain across a number of T-box factors in different species. *H.s., Homo sapiens; X.l., Xenopus laevis; D.r., Danio rerio; D.m., Drosophila melanogaster; C.b., Caenorhabditis briggsae; C.e., Caenorhabditis elegans* (taken from Papaioannou *et al*., 2014). ***(B)*** Phylogenetic analysis of the T-box family in vertebrates. These T-box genes are present in human and mouse with the exception of the zebrafish genes Drtbx16 and Drtbx6 (taken from Papaioannou *et al*., 2014). ***(C)*** Most of the loci where T-box factors reside are dispersed in the genome, yet some clustering has been observed in mammals, for example TBX2 and TBX4 on chromosome 17, and TBX3 and TBX5 on chromosome 12 (adapted from Agulnik, 1996; Bamshad, 1997; Minguillon & Logan 2003; Naiche *et al*., 2005).

The T-box family members have best been characterized for their critical roles in embryonic development where they function in early embryogenesis, germ layer specification, limb patterning and organogenesis (reviewed in Papaioannou, 2014). For example, TBX4 and Eomesodermin contribute to trophoectoderm and allantois formation (Russ *et al.*, 2000), TBX6 specifies patterning of the somites, TBX2, TBX3, TBX5 and TBX20 contribute to heart development, and TBX3, TBX4 and TBX5 are involved in limb formation (Naiche & Papaioannou, 2003; Naiche *et al.*, 2005). Their essential roles in development are further observed in the congenital disorders that arise from mutations in T-box genes as described

in **Table 1.1** (reviewed in Packham & Brook 2003 and Papaioannou, 2014). The rare autosomal dominant disorder, ulnar mammary syndrome (UMS) results from mutations in the TBX3 gene and will be discussed later under section 1.4.2 dealing with TBX3 in development.

The T-box domain present in all T-box factors is approximately 200 amino acids long and does not have any sequence similarities to any known transcription factor DNA-binding domain (Kispert & Herrmann, 1993). Early *in vitro* studies of Brachyury found that the T-box recognizes and binds the "TCACACCT" DNA sequence, called the T element, found within the nearly palindromic sequence [TTT(G/C)ACACCTAGGTGTGAAATT], as either a monomer or dimer (Kispert & Herrmann, 1993; Muller & Herrmann, 1997; Smith, 1999; Wilson & Conlon, 2002). Muller and Herrmann (1997) used X-ray crystallography to show that the T-box interacts with both the major and minor groves of their target DNA. Whereas some T-box factors, including Brachyury, TBX1, TBX5, TBX6, TBX19 and TBX20 act as transcriptional activators (Ataliotis *et al*., 2005; Zaragoza *et al*., 2004; Gonzalez *et al*., 2013; Maira *et al*., 2003; Lingbeek *et al*., 2002; Stennard *et al*., 2005; Casey *et al*., 1998), others such as TBX2, TBX3, TBX15, TBX18 and TBX22 function predominantly as repressors (Prince *et al*., 2004; Jacobs *et al*., 2000; Andreou *et al*., 2007; Carlson *et al*., 2001; Farin *et al*., 2013). In addition there is evidence that Brachyury, TBX2, TBX3, TBX5, TBX20 and Mga can act as both transcriptional activators and repressors (Carreira *et al*., 1998; Casey *et al*., 1998; Sakabe *et al*., 2012; Prince *et al*., 2004; Wilmer *et al.*, 2016; Lu *et al*., 2011; Carlson *et al*., 2001; Takeuchi *et al*., 1999; Zaragoza *et al*., 2004; Stennard *et al*., 2005; Singh *et al*., 2005; Kawamura *et al*., 2008; Hurlin *et al*., 1999). This begs the question as to what switches the activating versus repressing activity of these T-box factors. Furthermore, while all T-box factors bind and regulate the same consensus T-element *in vitro*, *in vivo* evidence reveals that T-box factors regulate different target genes, are functionally distinct and are able to bind highly variable and degenerate sites (Lingbeek *et al*., 2002; Boogerd *et al*., 2012). Together this suggests that T-box factor target gene specificity and transcriptional activity may, in part, be determined by co-factors and that they may regulate their target genes via

Table 1.1: Developmental disorders resulting from loss of T-box transcription factors.

T-box factor	Congenital disorder	Characteristics	Reference
TBX1	DiGeorge syndrome	Cardiac abnormalities, cranio-facial anomalies/dysmorphology, palatal defects, hearing impairment, learning difficulties, behavioural problems, parathyroid deficiency, thymus hypoplasia, hypocalcemia and abnormal vertebrae	Merscher *et al.*, 2001; Vitelli *et al.*, 2003; Jerome & Papaioannou 2001
TBX2	Unnamed syndrome	Microcephaly, postnatal growth retardation, hand, foot and limb abnormalities, and heart defects	Ballif *et al.*, 2010, Nimmakayalu *et al.*, 2011
TBX3	Ulnar mammary syndrome	Lost or duplicated posterior limb structures, breast, tooth and genital abnormalities	Bamshad, 1997
TBX4	Small patella syndrome	Patella a/hypoplasia, pelvic and lower limb/foot structural anomalies	Bongers *et al.*, 2004
TBX5	Holt-Oram syndrome	Cardiac defects, skeletal malformations, altered forelimb patterning, digit abnormalities	Li *et al.*, 1997
TBX15	Acromegaloid facial appearance syndrome	Facial abnormalities: thick lips, thickened upper eyelids, bulbous nose and overgrown intra-oral mucosa	Agulnik *et al.*, 1998
TBX19	Isolated ACTH deficiency	Adrenal insufficiency	Liu *et al.*, 2001
TBX22	Cleft palate	X-linked cleft palate (speech, feeding, dentition defects) with ankylogossia (tongue-tied)	Braybrook *et al.*, 2002

co-factor binding sites (Lu *et al.*, 2011; Papaioannou, 2014). Indeed, several of lines of evidence underscore the importance of co-factors in regulating T-box factor functions during development and a few examples are mentioned below.

In nematodes, the T-box factor MLS-1 requires interaction with UNC-37 in specifying uterine muscle and loss of UNC-37 results in a phenotype similar to that of a MLS-1 mutant (Miller & Okkema, 2011). Kawamura *et al*. (2008) observed that the transcriptional activity of T-box proteins TBX24 and Ntl were switched from transcriptional activation to repression by their interaction with Ripply1 in zebrafish embryos. Furthermore, the phenotype arising from aberrant Ripply1 expression is similar to that of a homozygous Ntl mutant (Kawamura *et al*., 2008). In pituitary gland cells TBX19/Tpit is only able to activate pro-opiomelanocortin (POMC) gene expression by co-operation with Pitx binding to a contiguous site within a regulatory region of the promoter (Lamolet *et al.*, 2001). Indeed, mutations in either Tpit or Pitx's binding sites result in a loss of POMC transcription (Lamolet *et al.*, 2001). During zebrafish heart development Sox4 plays a critical role in mediating the transcriptional regulation of Connexin43 (Cx40) expression by TBX3 (Boogerd *et al.*, 2011). Moreover, Nkx2-5 interacts with Tbx2, Tbx3, Tbx5 and Tbx20 to influence their regulation of their cardiac target genes during mouse heart development (Bakker *et al*., 2008; Habets *et al*., 2002; Hoogaars *et al*., 2008; Hoogaars *et al*., 2004a; Stennard *et al*., 2003; Hiroi *et al*., 2001). Furthermore in rat brain development the protein partner complex Tbr1/Calcium/calmodulin-dependent serine protein kinase (CASK) regulates a number of target genes containing T-elements, for example Reelin (Hsueh *et al*., 2000; Wang *et al.*, 2004). In addition, TBX5 requires direct association with co-activator Tafazin (TAZ), and histone acetyltransferases p300 and PCAF, to stimulate TBX5 dependent promoters in cardiac and limb development (Murakami *et al*., 2005). Lastly, both the Smad and Groucho proteins interact and regulate the transcriptional activity of a number of T-box factors (Singh *et al*., 2009; Messenger *et al*., 2005; Miller & Okkema 2011; Kawamura *et al*. 2008; Farin *et al*., 2013) and T-box factors have also been reported to associate with chromatin remodeling factors to regulate their target genes at an epigenetic level (Murakami *et al*., 2005; Lu *et al.*, 2011; Miller *et al.*, 2011; Kumar *et al.*, 2014).

In addition to their critical roles in embryonic development, a growing list of studies have also linked inappropriate T-box factor expression to oncogenesis and several T-box factors, including Brachyury, Eomes, TBX1, TBX2, TBX3, TBX4, TBX5 and T-bet (TBX21), have been implicated to directly promote and/or suppress tumour formation (He *et al*., 2002; Yu *et al*., 2010; Trempus *et al*., 2011; Atreya *et al*., 2007; Reinert *et al*., 2011; Park *et al*., 2008; Fernando *et al*., 2010; Yang *et al*., 2009; McCune *et al*., 2010). For example, Brachyury and TBX2 promote epithelial-to-mesenchymal transition and Brachyury, TBX2 and TBX3 have all been observed to increase cell migration, invasion and metastasis (Atreya *et al*., 2007; Yang *et al*., 2009; Fernando *et al*., 2010; McCune *et al*., 2010; Reinert *et al*., 2011; Wansleben *et al*., 2014). On the other hand, TBX4 has been linked to decreased metastasis and better overall survival in pancreatic ductal cell adenocarcinoma (Qi *et al.*, 2008; Zong *et al*., 2011) and in colon cancer TBX5 has been reported to decrease substrate dependent and independent proliferation and migration as well as to induce apoptosis (Yu *et al*., 2010). TBX3, however, is able to act as both a tumour promoter and tumour suppressor depending on the context and this will be discussed in more detail later (Wilmer *et al*., 2016).

1.3 TBX3

1.3.1. Gene and protein structure

TBX3 is located on chromosome 12 at position 12q23-24.1, spans a distance of 13.9 kb, consists of 7 exons, produces a transcript of 5.2 kb and encodes a 723 amino acid long peptide (Bamshad *et al.*, 1997; Rowley *et al.*, 2004). Due to alternative splicing four TBX3 mRNA transcripts have been identified but only two, TBX3 and TBX3+2a, encode full length and functional proteins that localize to the nucleus (Bamshad *et al*., 1999). Alternative splicing between exons 2 and 3 yields the TBX3+2a transcript that produces a protein with an extra 20 amino acids within the T-box DNA binding domain (**Figure 1.2**) (Bamshad *et al.*, 1999). TBX3 and TBX3+2a are expressed in different ratios which appears to be species and tissue specific and there is debate as to whether the difference in their DNA binding domain leads to functional differences (Carlson *et al.*, 2001; Fan *et al.*, 2004; De Benedittis & Jiao, 2011). Fan *et al.* (2004) observed that whereas TBX3 was able to bind a T-element probe *in*

vitro and to repress senescence in mouse embryonic fibroblasts (MEFs), TBX3+2a was unable to bind and instead accelerated senescence in MEFs. The authors therefore concluded that the TBX3 and TBX3+2a isoforms were functionally distinct and suggested that the extra 20 amino acids in the DNA binding domain of the TBX3+2a isoform may either disrupt its ability to bind target DNA or may result in it regulating different target genes. Consistent with the latter possibility, Zhao *et al.* (2014) showed that whereas overexpression of both isoforms in mouse embryonic stem cells induced differentiation by repressing pluripotency factor Nanog, only TBX3+2a could directly bind the Nanog promoter. On the other hand, Hoogaars *et al.* (2008), using DNA binding and structural studies, found that both isoforms were able to bind a consensus T-element in the $p21^{Cip1/Waf1/CDKN4a/SDII}$ (referred to as p21) and cardiac natriuretic peptide A (Nppa) promoters as well as interact with the homeobox factor Nkx2-5. The authors also found that the ectopic expression of either isoform inhibited heart chamber formation and repressed cardiac chamber markers Nppa and Cx40. In addition, the Prince laboratory has found that both TBX3 and TBX3+2a are able to bind the p21 promoter and have comparable ability to repress *p21* expression (unpublished data; Wilmer *et al.*, 2016b). Together the above studies suggest that the TBX3 and TBX3+2a isoforms may exhibit functional differences depending on cellular context.

TBX3 functions predominantly as a transcriptional repressor and indeed it represses $p14^{ARF}$/$p19^{ARF}$ (referred to as p14/p19), p21, Nppa, E-cadherin, and phosphatase and tensin homolog (PTEN) (Burgucu *et al*., 2012; Brummelkamp *et al*., 2002; Lingbeek *et al*., 2002; Rodriguez *et al*., 2008; Hoogaars *et al*., 2008). Through deletion constructs and luciferase assays Carlson *et al.* (2001) mapped the functional domains of TBX3 and described two repression domains (R1 and R2) as well as an activation domain (**Figure 1.2**). Importantly, TBX3 C-terminal mutants linked to the UMS phenotype, in which the repression domain R1 is lost, results in increased protein decay and loss of function (Carlson *et al.*, 2001). It is important to note that TBX3 can activate Gata6 (Lu *et al*., 2011) in the context of heart development but whether this involves the putative activation domain identified by Carlson *et al.* (2001) is not known. Carlson *et al.* (2001) also mapped the location of TBX3's DNA binding domain and its nuclear localization signal to the N-terminus (**Figure 1.2**). In co-crystallisation experiments, Coll *et al.* (2002) showed that TBX3 binds its target DNA as two

monomers with each monomer binding to its consensus palindromic sequence. The authors thus speculated that physiologically TBX3 may be able to bind T-elements as a single monomer.

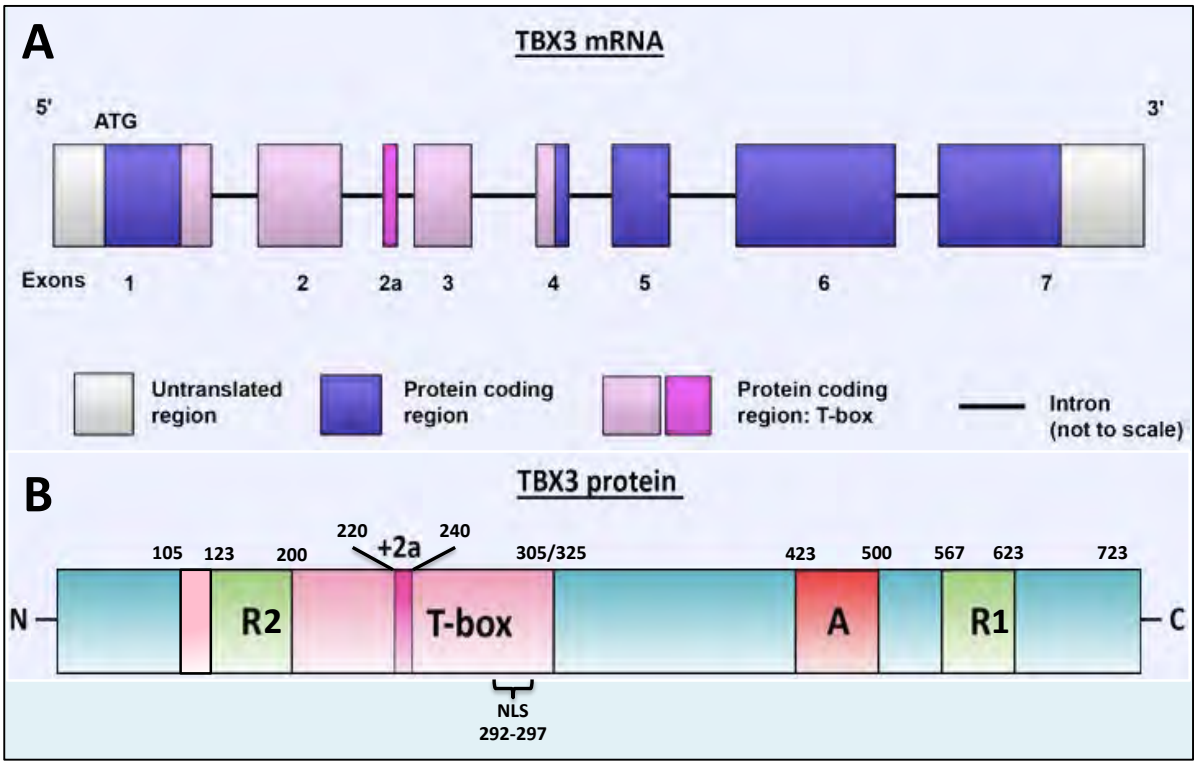

Figure 1.2: Schematic representation of human TBX3 mRNA and protein. ***(A)*** Several transcripts exist due to alternative splicing, yet the most common isoforms studied are the dominant TBX3 transcript with 7 exons of 5.2kb encoding a protein of 723 amino acids, and the TBX3+2a transcript, containing an additional 20 amino acids. ***(B)*** The functional protein domains depicted above are: R1 and R2 (green), Repression domains 2 and 1 at amino acid positions 105-200 and 567-623, T-box (light pink + R2), DNA binding domain at 105-305/325, and A (red), Activation domain at 423-500, NLS, Nuclear localization signal, at 292-297. The amino and carboxy termini are indicated by N and C respectively (Carlson *et al*., 2001).

1.3.2 TBX3 and development

During mouse development, TBX3 is expressed during the morula stage and in the extraembyronic tissue and the yolk sac (Bertolessi *et al*., 2015). Furthermore, it plays a role in mouse mammary gland formation, heart development and limb outgrowth. In mammary gland development it specifies the mammary buds, placode epithelium and branching ducts and during heart development it specifies the atrioventricular canal, the ventricular septum

and the conduction system (Davenport *et al.*, 2003; Naiche *et al.*, 2005). TBX3 is also expressed in a number of human organs including the foetal heart, liver, spleen, lung and kidney, and adult prostate, lung, placenta, ovary, testis, small intestine, adrenal gland, thyroid, breast, bladder, uterus, nervous system, mammary gland and salivary gland (Bamshad *et al.*, 1999; Carlson *et al.*, 2001; Davenport *et al.*, 2003; He *et al.*, 2002). The critical developmental role of TBX3 is demonstrated in the embryonic lethality associated with a homozygous mutation in mice, due to malformation of the yolk sac and cardiac abnormalities, and in the human ulnar mammary syndrome (UMS) that results from heterozygous mutations in the human *TBX3* gene (Hermann *et al.*, 1990; Bamshad *et al.*, 1997; Davenport *et al.*, 2003).

UMS is an autosomal dominant condition caused by haploinsufficiency of TBX3 due to deletions, frameshifts or missense mutations (Bamshad *et al.*, 1999; Frank *et al.*, 2003). It is characterized by heart, jaw and posterior limb defects (ulnar, metacarpals and phalanges), apocrine-gland defects including mammary gland hypoplasia and loss of areola, dental, hair and urogenital malformations and abnormalities (Bamshad *et al.*, 1997; Bamshad *et al.*, 1999; Packham & Brook, 2003). It is noteworthy that while TBX3 is expressed in a number of developing tissues not all of them are affected in UMS suggesting that different cell types display differing sensitivities to the level of TBX3. Aberrant TBX3 associated with UMS include truncated versions of the protein, such as loss of the R1 repression domain which is associated with decreased or no transcriptional repression activity (Carlson *et al*., 2001). Klopocki *et al*. (2006) described a novel 1.28 Mb deletion encompassing TBX3 in a single patient that resulted in a UMS-like phenotype accompanied by dysmorphic facies and mental retardation. In mice homozygous TBX3 mutants die *in utero* and display mammary gland aplasia and malformations of the limbs, similar to the human UMS phenotype, and heterozygous mutants exhibit mammary gland aplasia and minor genital anomalies (Davenport *et al.*, 2003). Additionally, in mice with homozygous deletions of the T-box an abnormal mRNA transcript and a non-functional protein that localized predominantly to the cytoplasm was produced (Frank *et al.*, 2013).

Kumar *et al.* (2014) sought to further understand the mechanisms by which TBX3 mutations result in UMS and from mass spectrometry of TBX3/protein-partner immunoprecipitation

samples the authors found that TBX3 interacts with RNA binding and splicing factors *in vivo*. Furthermore, whereas TBX3 was able to directly bind T-box binding motifs in the mRNA transcripts of Disks large homolog (3Dlg3) and Nuclear factor of kappa light polypeptide gene enhancer in B-cells 1 (Nfκb1) and regulated their splicing, UMS-associated TBX3 mutations disrupted this splicing regulatory function. TBX3 was also reported to be capable of recruiting other RNA binding and splicing factors to RNA containing T-elements, such as RNA helicase and DEAD box helicase 3 (DDX3). It was therefore hypothesized that in addition to mutations resulting in haploinsufficiency of TBX3, mutations in TBX3 that disrupt its transcriptional regulation and pre-mRNA splicing activities may also contribute to UMS. Together, the phenotypes resulting from mutations in TBX3 have suggested the importance of this gene in the development of, at the very least, the heart, mammary glands and limbs.

1.3.3 TBX3 and stem cell biology

Consistent with TBX3 being expressed in the inner cell mass of the blastocyst and its involvement in cell fate determination, it has been implicated to play pivotal roles in stem cell renewal and differentiation (Papaioannou, 2014). Indeed, TBX3 has been grouped with the pluripotency transcription factors Klf4/5, Nanog and Oct3/4 as a stem-ness factor (Russell *et al.*, 2015; Waghray *et al.*, 2015; Weidgang *et al.*, 2016). Furthermore, studies have reported that TBX3 contributes to mouse embryonic stem cell (mESC) renewal and that loss of its expression results in differentiation (Inavona *et al.*, 2006; Zhao *et al.*, 2014). In mESCs TBX3 forms part of the core pluripotency signaling pathway; it is downstream of the Wingless (Wnt) and phosphoinositide 3-kinase/Protein kinase B (PI3K/ATK) pathways that stimulate its expression, and the MAPK pathway, which antagonizes its expression to maintain balance (Niwa *et al.*, 2009; Russell *et al.*, 2015; Waghray *et al.*, 2015; Weidgang *et al.*, 2016). Zhao *et al.* (2014) reported that both TBX3 and TBX3+2a isoforms are overexpressed in mouse pluripotent stem cells and Inavona *et al.* (2006) found that TBX3 expression is needed to block differentiation into mesoderm, ectoderm and neural crest cells in mESC and that its downregulation, due to retinoic acid (RA) signaling, resulted in differentiation. Furthermore, a study by Niwa *et al.* (2009) illustrates that TBX3 maintains pluripotency by activating downstream Nanog. Moreover, TBX3 has been found to improve

reprogramming efficiency and germ-line competency of induced pluripotent stem (iPS) cells (Han *et al.*, 2010). Interestingly, micro-RNAs (miRs) have been implicated in regulating differentiation by repressing TBX3. For example, miR-137 represses TBX3 and causes accelerated neural stem cell differentiation (Jaing *et al.*, 2013) and miR-93 represses TBX3 causing limited adipocyte precursor self-renewal (Cioffi *et al.*, 2015). Weidgang *et al.* (2016) states that TBX3's expression sustains stem-ness and directs early embryogenesis and cell fate specifications through either (1) transcriptional regulation of differentiating gene programmes or (2) modification of chromatin structures, such as transcriptionally downregulating Dppa3 (Waghray *et al.*, 2015) and targeting histone H3 to regulate GATA6's methylation (Lu *et al.*, 2013).

TBX3 has also been linked to cancer stem cells (CSCs) and this will be discussed in the next section.

1.3.4 TBX3 and cancer

Considering the commonalities between developmental and oncogenic processes it is not surprising that TBX3 has been implicated in many cancers. For example, TBX3 is overexpressed in melanoma, breast, pancreatic, liver, ovarian, head and neck squamous cell cancer and several sarcoma subtypes (Hoek *et al.*, 2004; Fan *et al.*, 2004; Yarosh *et al.*, 2008; Liu *et al.*, 2011; Rodriguez *et al.*, 2008; Douglas & Papaioannou, 2013; Lomnytska, 2006; Hansel *et al.*, 2004; Renard *et al.*, 2007, Humtsoe *et al.*, 2011; Burgucu *et al.*, 2012; Wansleben *et al.*, 2014; Willmer *et al.,* 2016). Importantly, increased levels of TBX3 has been implicated in several aspects of cancer pathogenesis including bypassing senescence to establish a state of immortality, promoting proliferation and bypassing apoptosis as well as enhancing tumour formation, invasion and metastasis (**Figure 1.3**) (Wansleben *et al.*, 2014). Interestingly, there are a few recent studies that suggest a tumour suppressor role for TBX3 in certain cancer contexts, which will be discussed in more detail in section 1.3.4.3.

1.3.4.1 TBX3 in senescence, apoptosis and proliferation

TBX3 in senescence

Cancer pathogenesis is a progressive evolution that occurs when cellular homeostasis is disrupted and cells acquire oncogenic capabilities such as replicative immortality, sustained cell proliferation and resisting cell death (Hananhan & Weinberg, 2011). The first indication that TBX3 may directly contribute to cancer progression came from studies which showed that it was able to immortalize MEFs by inhibiting senescence (Carlson *et al*., 2001). Senescence is a safeguard programme that describes irreversible exit from the cell cycle and occurs in two forms: replicative and premature (Kuilsman *et al.*, 2010; Campsi, 2013). Replicative senescence occurs in all somatic cells once they have reached the end of their finite lifespan and is triggered by the shortening of their telomeres (Kuilsman *et al.*, 2010; Campsi, 2013). Premature senescence, also known as accelerated senescence, occurs in response to stressful stimuli such as DNA damage, oncogene overexpression and inflammation, forcing the cell to withdraw from active cell division before it causes more damage (Schmitt *et al*., 2007; Kuilsman *et al.*, 2010; Campsi, 2013). Expression of the negative cell cycle regulators p53 and p21 are required to initiate senescence whereas p16 and Rb are needed to maintain it (Schmitt *et al.*, 2007; Campsi, 2013). Brummelkamp *et al.* (2002) showed that TBX3 can bypass senescence through its ability to repress p14/p19 and Yarosh *et al*. (2008) later revealed that this occurs in part by TBX3 recruiting histone deactyelaces (HDACs) 1, 2, 3 and 5 to epigenetically silence the p14/p19 promoter. The p19-murine double minute 2 (MDM2)-p53 pathway plays an important role in protecting cells against oncogenic transformation. For example in response to cellular stress, p14/p19 acts to stabilize p53 by sequestering ubiquitin ligase MDM2 and preventing its association with p53 (Sherr & Weber, 2000; Sharpless & DePinho, 1999). This allows p53 to upregulate important cell cycle checkpoint initiators, pro-senescence and/or pro-apoptosis factors. Thus when p14/p19 is repressed, MDM2 is released and ubiquitinates p53 leading to increased shuttling of p53 out of the nucleus and its proteolytic degradation by the proteasome 26S in the cytoplasm (Sherr & Weber, 2000; Sharpless & DePinho, 1999; Brummelkamp *et al.,* 2002). Consequently the levels of p53 target genes that promote

senescence such as p21 are decreased. Kumar *et al.* (2014b) recently reported on an alternative mechanism by which TBX3 may be bypassing senescence. They showed that the TBX3/Co-activator of AP1 and Estrogen Receptor (CAPERα) complex directly repressed transcription of tumour suppressor long non-coding RNA (lnRNA) Urothelial Cancer Associated 1 (UCA1) that resulted in destabilization of p16 leading to bypass of Rb-mediated senescence in primary cells and mouse embryos.

TBX3 in apoptosis

The inhibition of apoptosis, a form of programmed cell death which limits uncontrolled cell proliferation, translates into an increase in the risk of cancer progression as well as in resistance to anti-cancer drugs (Schmitt *et al.*, 2007). Several studies have suggested that TBX3 may also contribute to oncogenesis by promoting the evasion of apoptosis. Carlson *et al.* (2002) reported that TBX3 expression enables cells to evade c-Myc and Ras-induced apoptosis through repressing the p19/MDM2/p53 pathway. Furthermore, when TBX3 was silenced in rat bladder cancer cells, human colon carcinoma and osteosarcoma cells, there was an increase in cell death by apoptosis, decreased cell survival and increased sensitivity to the chemotherapeutic doxorubicin (Ito *et al.*, 2005; Renard *et al.*, 2007). In addition, Humtsoe *et al*. (2012) observed that TBX3 expression protected head and neck squamous cell carcinoma cells against anoikis, a specific form of cell death induced by anchorage-dependent cells detaching from the surrounding extracellular matrix. Contrary to the aforementioned studies, Platonova *et al.* (2007) showed that neither the overexpression nor the knock-down of TBX3 affected apoptosis in mammary epithelial cells. This indicates that the ability of TBX3 to evade apoptosis may be cell context specific and therefore illustrates the need for a more in-depth analysis of the role of TBX3 in apoptosis.

TBX3 in proliferation

Several studies have described TBX3 as a pro-proliferative factor, for instance, Suzuki *et al.* (2008) and Platonova *et al.* (2008) observed that TBX3 promoted proliferation of hepatic progenitor and mammary epithelial cells through repression of p19 that was matched with a corresponding decrease in p21 levels. Findings from Wilmer *et al.* (2016b) also revealed that

TBX3 represses p21 through directly binding to a T-element in its promoter leading to increased proliferation in chondrosarcomas. High levels of TBX3 also correlated with proliferation, invasion, metastasis and tumour size in uterine and cervical primary tumour samples (Lyng *et al.*, 2006). Another mechanism by which TBX3 stimulates proliferation appears to involve its ability to transcriptionally inhibit the tumour suppressor PTEN in head and neck squamous cell carcinoma (Burgucu *et al*., 2012). PTEN acts as a tumour suppressor by negatively regulating the PI3K/AKT pathway and pro-oncogenic processes, such as proliferation, cell survival and migration (Chalhoub & Baker, 2009). Interestingly, TBX3's repression of PTEN occurred at a non-canonical site, indicating that perhaps TBX3's binding or activity was mediated via a co-repressor protein partner (Burgucu *et al*., 2012).

It must be mentioned that TBX3 has also been reported to repress proliferation to promote migration in melanoma and breast cancer cells (Li *et al.*, 2013; Peres *et al.*, 2010; Peres & Prince, 2013). This phenomenon is known as the proliferation/migration dichotomy of tumour cell invasion (Fedotov & Iomin, 2007). Peres *et al.* (2010) observed that knocking down TBX3 via a short-hairpin RNA (shRNA) approach in melanoma and breast cancer cells was accompanied by an increase in p19, p21 and p53 levels and enhanced the proliferative capacity of these cells. Furthermore, Ballim *et al.* (2012) demonstrated that upregulation of TBX3 by RA signaling caused melanoma cells to proliferate significantly slower. In addition, Li *et al.* (2013) reported that transforming growth factor β1 (TGF-β1) signaling transcriptionally activated TBX3 expression, via downstream mediators Smad 3/4 and JunB binding to its promoter, and this reduced proliferation yet boosted migration of breast epithelial cells. Together the above studies suggest that the role of TBX3 in promoting or inhibiting proliferation is cell context dependent which again may be dependent on the availability of co-factors.

1.3.4.2. TBX3 in tumour formation, migration, invasion and metastasis

TBX3 has also been implicated in promoting the later stages of cancer progression, including anchorage independent cell proliferation, tumour formation, migration, invasion,

metastasis, resistance to chemotherapeutics and recurrence (**Figure 1.3**). Indeed, our and other laboratories have shown that TBX3 plays an important role in tumour formation and invasion in breast cancer, melanoma and chondrosarcoma (Peres *et al*. 2010; Renard *et al*. 2007; Rodriguez *et al*. 2008; Mowla *et al*. 2010; Wilmer *et al.*, 2016). For example, ectopically overexpressing TBX3 was sufficient to promote tumour formation and invasion of non-tumourigenic early stage radial growth phase melanoma cells in nude mice and promoted anchorage independent proliferation, tumour formation and migration in chondrosarcomas (Peres & Prince; 2013; Wilmer *et al.*, 2016). Importantly, when TBX3 was knocked down in advanced melanoma cells using a shRNA approach the cells lost their ability to form tumours and were unable to migrate and invade surrounding tissues (Peres *et al.,* 2010). Similarly, knocking down TBX3 in breast cancer and chondrosarcomas reversed several features of the cancer phenotype such as reducing colony and tumour-forming ability as well as cell migration (Peres *et al.,* 2010; Wilmer *et al.*, 2016). The ability of TBX3 to promote melanoma formation and migration was accompanied by the inhibition of the cell adhesion molecule E-cadherin which is characteristically absent in advanced melanoma to allow for cell migration (Rodriguez *et al*., 2008; Peres *et al.*, 2010). Humstoe *et al.* (2012) also observed that head and neck squamous carcinoma cells undergoing an epithelial-to-mesenchymal-like transition had high levels of TBX3 but low levels of E-cadherin. Importantly, silencing TBX3 in these cells reduced their invasiveness and induced anoikis. Furthermore, Du *et al.* (2014) found a Protein kinase C (PKC)/TBX3/E-cadherin signaling axis which enhanced bladder cancer cell migration and invasion.

Despite the compelling evidence implicating increased levels of TBX3 with several oncogenic processes, information about the mechanisms involved with its upregulation in cancer is only beginning to emerge. As previously mentioned, TGF-β1 signaling upregulated TBX3 expression in breast cancer cells which in turn promoted cell migration (Li *et al.*, 2014). Mowla *et al.* (2011) similarly found that treating breast cancer cells with phorbol 12-myristate 13-acetate (PMA) induced TBX3 levels and caused increased cell migration. Moreover, in colon and liver cancer cells TBX3 expression, induced by the constitutively active Wnt/β-catenin pathway, promoted cell survival, anchorage independent growth, tumour formation, chemotherapy resistance and was associated with poor prognosis (Eblaghie *et al*., 2004; Renard, 2007).

Cancer stem cells (CSCs) rely on developmental signaling pathways and therefore recapitulate the development process; they are particularly aggressive as they promote cell survival, self-renewal and expansion that sustains tumour growth, progression and recurrence as well as resistance to anti-cancer therapies (Clarke *et al*., 2006; Fillmore *et al*., 2010). Fillmore *et al*. (2010) reported that estrogen/FGF/FGFR/TBX3, as well as Wnt/TBX3, signaling expanded breast cancer stem cell populations, contributing to tumour-forming potential, phenotypic plasticity and resistance to chemotherapeutics, whereas silencing TBX3 decreased tumoursphere growth *in vitro*.

1.3.4.3. TBX3 as a tumour suppressor

While TBX3 functions predominantly as a tumour promoter, there is also evidence that it may act as a tumour suppressor. For example, TBX3 is epigenetically silenced in glioblastoma, bladder and gastric cancer (Kandimalla *et al*., 2012; Etcheverry *et al.*, 2010; Yamashita *et al.*, 2006) and downregulated in uterine cervical cancer (Lyng *et al.*, 2006). Microarray data and genomic analyses revealed that when TBX3 is downregulated and silenced via methylation in uterine cervical cancer and glioblastoma respectively, its lack of expression is associated with increased invasion, metastasis, tumour size and poor prognosis (**Figure 1.3**) (Yamashita *et al.*, 2006; Lyng *et al.*, 2006; Etcheverry *et al*., 2010). Based on this data it was suggested that the expression profile of TBX3 may be used as a marker of metastasis and prognosis. Similarly, Kandimalla *et al*. (2012) found that TBX3 methylation was associated with worse progression-free survival in bladder cancer. Importantly, recently TBX3 was shown to act as a tumour suppressor in fibrosarcomas, acting to reduce substrate dependent and independent cell proliferation, tumour formation and migration (Wilmer *et al.*, 2016). Together, the above studies suggest that whether TBX3 promotes cancer or functions as a break to the oncogenic process may be dependent on tissue origin and cell context, which may be linked to the availability of co-factors.

Recently, the Prince laboratory showed for the first time that TBX3 is also overexpressed in sarcomas, including rhabdomyosarcoma (Wilmer *et al.*, 2016). However, at the start of the

current project very little was known about its involvement in the development of these mesenchyme-derived cancers.

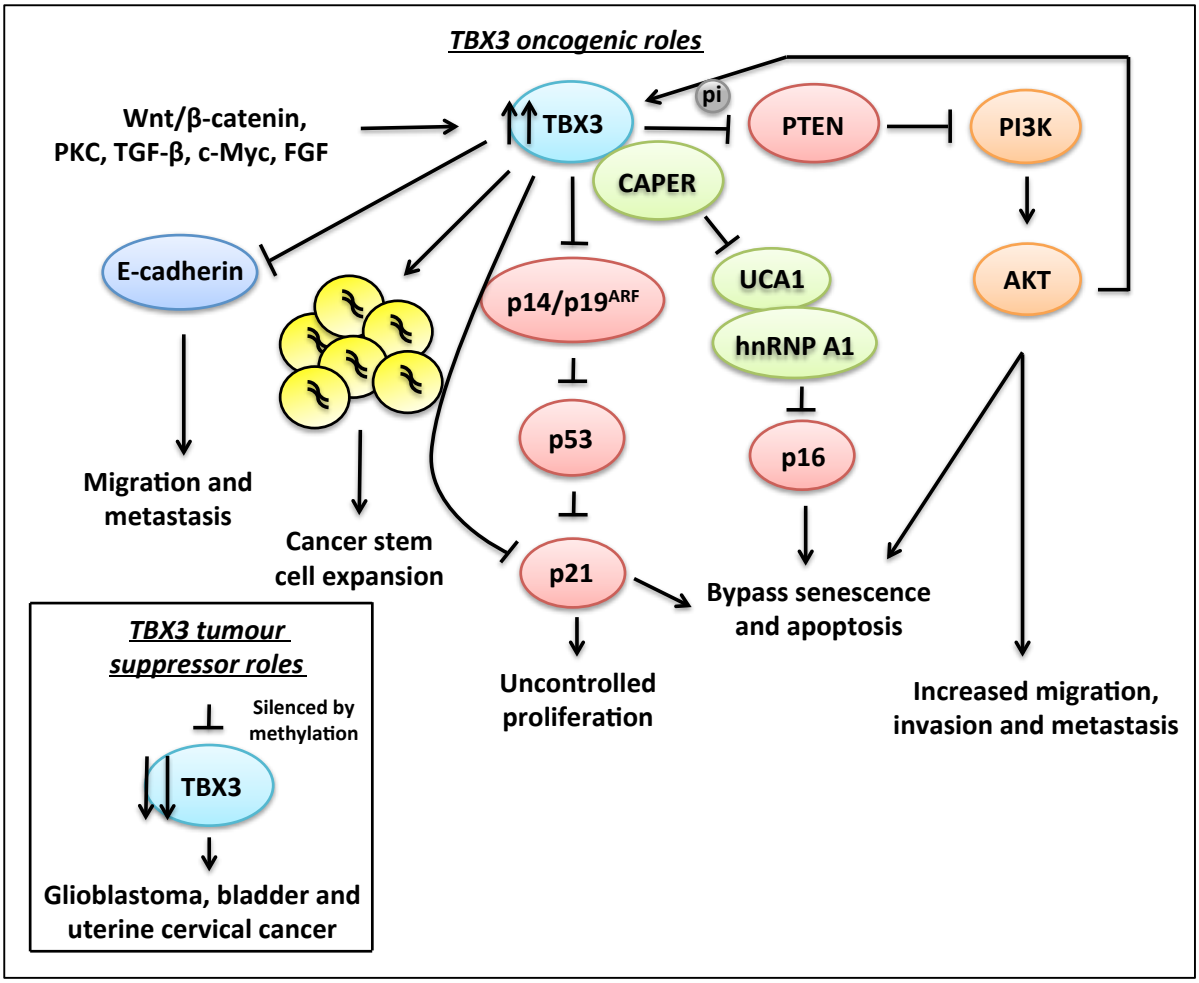

Figure 1.3: The role of TBX3 in cancer formation. TBX3 has been shown to contribute to several cancer processes including the bypass of senescence (Brummelkamp *et al.*, 2002), evasion of apoptosis, drug resistance (Carlson *et al.,* 2002; Zhang *et al.*, 2010; Humtsoe *et al.*, 2012) and the promotion of proliferation, anchorage independent growth, tumour formation, migration, invasion and metastasis (Renard *et al.*, 2007; Chen *et al.*, 2009; Peres, 2010; Mowla *et al.,* 2011; Humtsoe *et al.*, 2012; Rodriguez, 2008). TBX3 has also been viewed as a tumour suppressor as it is silenced by methylation in certain cancers (Lyng, 2006; Etcheverry *et al.*, 2011; Wilmer *et al.*, 2016) (adapted from Wansleben *et al.*, 2014).

1.4 Sarcomas

Sarcomas derive their name from the Greek words *sarcos* (fleshy) and *oma* (tumour). They are rare, histogenetically heterogenous malignant neoplasms that arise from mesenchyme-

derived tissues. Approximately 80-90% of sarcomas originate from soft tissue (muscles, joints, fat, nerves, deep skin tissues, and blood vessels) and the remaining 10-20% from bone and cartilage (Koch *et al.*, 2002; Burmingham *et al.*, 2012). They make up 1% of all existing cancers in adults, 10% in children and 8% in adolescents (Mackall *et al.*, 2002; Helman & Metzler, 2003; Ducimetiere *et al.*, 2011; Amankwah *et al.*, 2013). In general, sarcomas are highly metastatic (metastases occur in one third of all patients), they are resistant to current treatments and commonly 10-20% of all sarcomas recur (O'Neill *et al.*, 2013). While the mortality rate for patients with sarcomas has improved over the years, 40-50% of metastatic patients with soft tissue sarcomas will survive a median value of only 12 months (Italiano *et al.*, 2011; Jacob *et al.*, 2015). Importantly, sarcomas account for 21% of paediatric solid malignancies and therefore contribute to a considerable loss in years of life (Burmingham *et al.*, 2012).

Traditionally sarcomas have been classified via histopathology using light microscopy by examining cell lineage morphology, differentiation, staining for cell-specific markers and identifying resemblance to a normal tissue type (Osuna & De Alava, 2009). Thus sarcomas were named after their tissues of origin, for example, fibrosarcomas from fibrous tissue, rhabdomyosarcoma from skeletal muscle, osteosarcoma from bone, leiomyosarcoma from smooth muscle, chondrosarcoma from cartilage, liposarcoma from adipose tissue and angiosarcoma from blood vessels (Helman & Metzler, 2003). There are, however, challenges with using histopathology for classifying sarcomas as a large proportion are high-grade, poorly differentiated and pleomorphic (Doyle, 2014). Indeed, until the early 1990's the misclassification rate of sarcomas, based on histopathological diagnoses, was reported to be 20% (Harris *et al.*, 1991). Furthermore, a lack of established diagnostic markers has also made treating sarcomas difficult (Helman & Metzler, 2003). More recently, it has been postulated that sarcomas originate from mesenchymal pluripotent stem cells that undergo complex genetic alterations or chromosomal translocations thereby giving rise to a diverse range of sarcoma subtypes (**Figure 1.4**) (Teicher, 2012; Beckingsale & Shaw, 2015).

From a genetic perspective, sarcomas may be classified into two main types: sarcomas with a (1) simple (≈20%) or (2) complex karyotype (≈80%) (Mertens *et al.*, 2009). Simple karyotypes consist of specific mutations or chromosomal translocations that result in

oncogenic fusion proteins, whereas complex karyotypes are characterized by aneuploidy, as well as numerous nonspecific losses, gains and amplifications of genes and chromosomes (reviewed in Helman & Meltzer, 2003 and Osuna & De Alava, 2009).

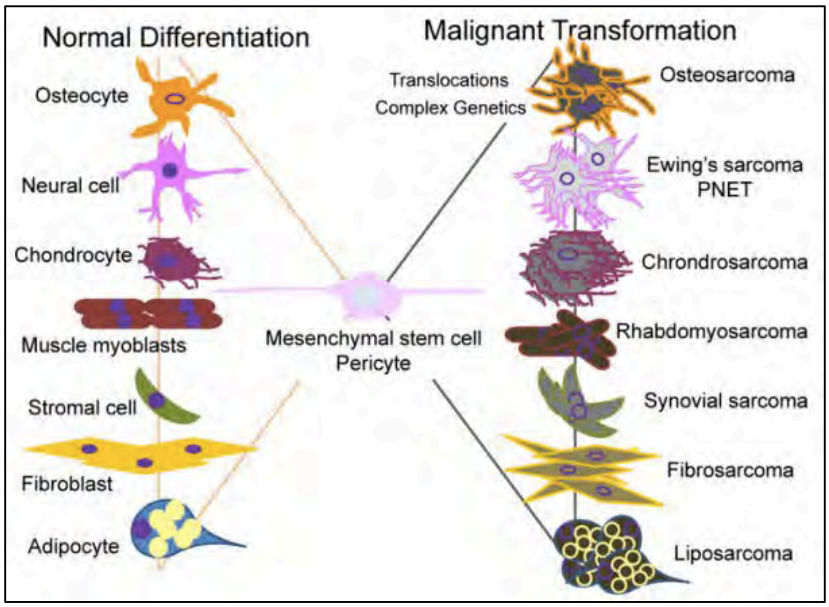

Figure 1.4: Schematic depicting the pluripotency of mesenchymal stem cells. These cells reside in all tissue and give rise to many normal differentiated cell types; however, when chromosomal translocations or complex genetic alterations occur mesenchymal stem cells, or pericytes, may give rise to the diverse types of sarcoma (taken from Teicher *et al.*, 2012).

1.5 Rhabdomyosarcoma

Rhabdomyosarcoma (RMS) is a rare malignancy of the skeletal muscle, usually presenting as a painless mass that, based on its location, can impede organ function. It is the most commonly occurring soft tissue sarcoma in children and adolescents, accounting for 3% of all childhood and 2% of all adolescent cancers in the USA (Ries *et al.*, 1999; American Cancer Society, 2014) and is the sixth most common paediatric cancer in South Africa (Van Der Schyff & Stefan, 2010; Stefan & Stones, 2012). RMS affects slightly more males than females but there is no significant difference in incidence rates between different races (Ries *et al.*, 1999; American Cancer Society, 2014). The major sites of these malignant tumours are the head and neck regions (~40%), genito-urinary tract (~25%) and trunk or extremities (~20%) (Ognjanovic *et al.*, 2009; Wang, 2012). It is postulated that RMS may arise from a myogenic precursor cell that failed to correctly and completely differentiate into muscle cells, but

because RMS tumours can originate in non-muscle sites, its etiology is under debate (Keller & Guttridge, 2013). In general, development of RMS is overwhelmingly sporadic and has no known predisposing factors (Merlino & Helman, 1999).

There are two major subtypes of RMS based on their distinct molecular and histological signatures: embryonal RMS (ERMS) and alveolar RMS (ARMS). The remaining RMS subtypes are pleomorphic RMS (PRMS) and sclerosing/spindle cell RMS (SRMS) which are very rare and affect mostly adults (Sun *et al.*, 2015). To diagnose RMS, tumour samples are stained for muscle specific markers such as α-actin, myosin heavy chain, myoglobin and Z-band proteins (Tonin *et al.*, 1991). Furthermore, whereas ERMS is histologically characterized by spindle-shaped rhabdomyoblasts cells with eccentric nuclei and eosinophilic cytoplasm, embedded in a myxoid stroma, ARMS is characterized by clusters of small, round, blue cells, densely packed around spaces resembling pulmonary alveoli, although tumours may also be solid (Merlino & Helman, 1999; Parham & Ellison, 2006; Zhang *et al.*, 2013).

Of the two major RMS subtypes, ERMS is more common (~75% of all RMS cases) and occurs mostly in children (Wang, 2012; American Cancer Society, 2014). ERMS is characterized by genetic aberrations such as loss of heterozygosity at chromosome 11p15, a region harbouring the IGF2 gene, and has a more favorable prognosis (Wang, 2012; American Cancer Society, 2014, Chen *et al.*, 2013; Hawkins *et al.*, 2014; Shern *et al.*, 2014). ARMS on the other hand occurs in adolescents and young adults, is more aggressive, has a greater rate of metastasis and recurrence and therefore a poorer prognosis (Parham & Ellison, 2006; Perez *et al.*, 2011; Kikuchi *et al.*, 2014). The majority of ARMS tumours (80%) contain the characteristic reciprocal translocations t(2; 23)(q35; q14) or t(1; 13)(q36; q14) which give rise to the chimeric oncogenic transcription factors PAX3-FKHR/FOXO1 (≈70%) or PAX7-FKHR/FOXO1 (≈10%) respectively (**Figure 1.5**). The remaining 20% are classed as being fusion-negative (Marshall & Grosveld, 2012; Quesada & Amato, 2012). The PAX transcription factors are involved in neural tube development and directing myoblast migration to upper and lower extremities, therefore it is thought that expression of this fusion protein could be responsible for the incomplete myogenic differentiation phenotype of ARMS through repression of myoblast differentiation (Osuna & De Alava, 2009; Zhu *et al.*, 2015b). Both PAX3-FKHR/FOXO1 and PAX7-FKHR/FOXO1 chimeras have been implicated in

promoting survival, transformation, proliferation, invasion and metastasis in ARMS (Marshall & Grosveld, 2012). Interestingly, PAX7-FKHR/FOXO1 is associated with lower rates of metastasis and therefore a better prognosis hinting at functional differences between the two chimeras (Osuna & De Alava, 2009).

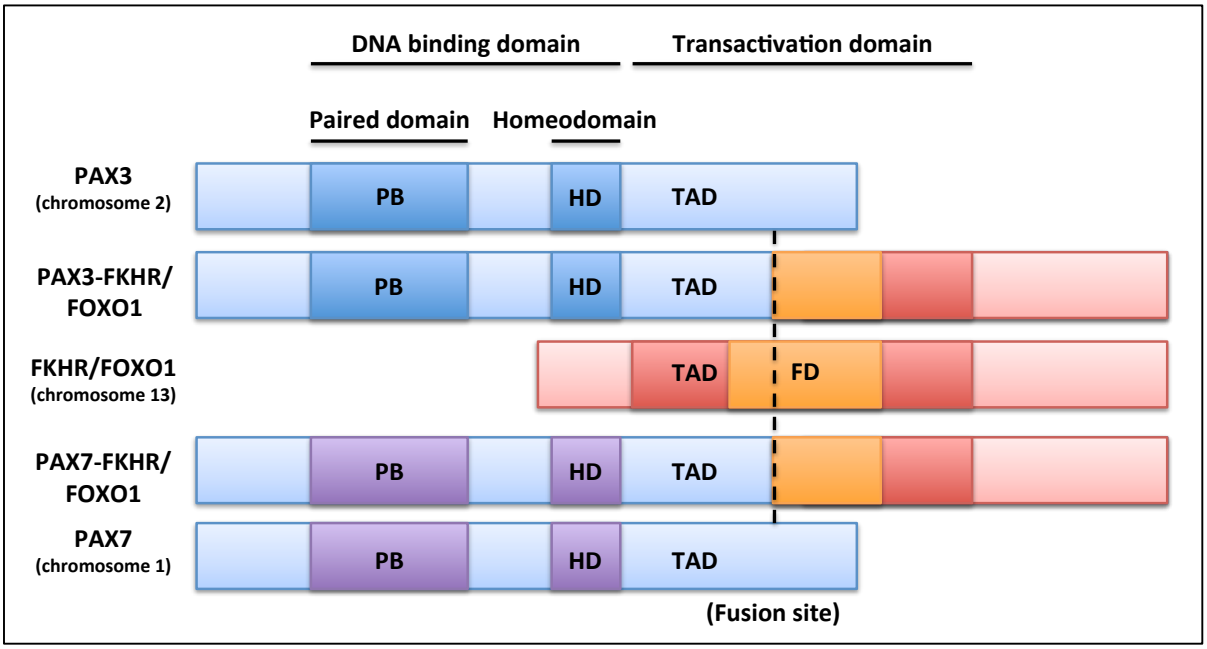

Figure 1.5: The most prevalent chromosomal translocations in ARMS. Chromosomal translocation t(2; 23)(q35; q14) creates fusion protein PAX3-FKHR/FOXO1 (top) and t(1; 13)(q36; q14) creates PAX7-FKHR/FOXO1 (bottom). These fusion proteins consist of the DNA binding domain of PAX3/PAX7 and the trans-activation domain of FKHR/FOXO1 which results in aberrant transcriptional activation of target genes. Paired domain (PB), homeodomain (HD), transactivation domain (TAD), forkhead domain (FD) (adapted from Merlino & Helman, 1999).

1.5.1 Molecular biology of RMS

ERMS and ARMS, while genetically and histologically distinct, share a phenotype of incomplete myogenic differentiation that contributes to oncogenesis. Interestingly, this is despite the expression of Myf5, MyoD, Myf6 and myogenin which are the hierarchical factors that drive muscle development. While the mechanism(s) involved in RMS is poorly understood, it has been postulated that the transcriptional activity of these myogenic factors may be inactivated (Keller & Guttridge, 2013; Winbanks *et al*., 2011). Relatedly, RMS cells maintain a level of stem-ness viewed in their ability to self-renew, rapidly proliferate,

bypass senescence and reverse quiescence (Paulson *et al.*, 2011). Indeed, cancer stem cells have been identified in RMS and the core stem cell pluripotency factors Oct4, Nanog, Sox2, PAX3 and c-Myc are expressed in RMS tumours and correlate with invasion, metastasis, resistance to anti-cancer drugs and poor overall survival (Walter *et al.*, 2011; Sun *et al.*, 2015).

Microarray and comparative genomic hybridization array technologies in ERMS revealed that it is driven by a common set of genomic defects including the inactivation of the tumour suppressors p53, p16, p14, $p15^{INK4B}$ (CDKN2B), PTEN and NF1 and the activation or amplification of the oncogenic Ras, Hh, MDM1/2, Gli1, c-Met, MYCN and FGFR1/4 (Merlino & Helman, 1999; Paulson *et al.*, 2011; Sun *et al.*, 2015). Examples of how these defects contribute to rhabdomyosarcomagenesis include loss of NF1, an inhibitor of oncogene Ras, allowing for increased proliferation, and amplification of MDM2, which interferes with MyoD activity, consequently preventing complete differentiation and contributing to the stem-ness phenotype (Sun *et al.*, 2015).

1.5.2 Signaling pathways in RMS

Many signaling pathways are deregulated in RMS and they are depicted in **Figure 1.6** (Khasi *et al.*, 2015). Accelerated cell proliferation, survival and migration in RMS is thought to be mainly due to alterations in the receptor tyrosine kinase (RTK)/RAS-RAF-MAPK/PI3K-AKT-phospholipase Cg (PLCg)- mechanistic target of rapamycin (mTOR) signaling pathway, with the RTK FGFR and IGFR pathways being particularly important (Paulson *et al.*, 2011; Shern *et al.*, 2014). Interestingly, despite the vast molecular and genetic heterogeneity in sarcomas, the RTK/Ras/PIK3CA pathway is activated in 93% of RMS tumours (Shern *et al.*, 2014). Furthermore, IGFR was reported to be overexpressed on the cell surface and in the nucleus of RMS cells and its inhibition caused decreased growth *in vivo* (Zhu *et al.*, 2015; Sun *et al.*, 2015). Likewise, FGFR was found to be overexpressed and constitutively active in RMS and to interact with oncogenic factors PI3K and mTOR and to contribute to poor differentiation, pro-proliferation, anti-apoptosis, invasion, angiogenesis, drug resistance and worse survival (Sun *et al.*, 2015). Furthermore, targeting FGF signaling in ARMS induced apoptosis (Wachtel

et al., 2014). In ARMS, PAX3/7-FKHR/FOXO1 too was found to upregulate IGF and FGF signaling, as well as transcriptionally activate MET (c-Met), which in turn activates the Ras/Raf/MAPK pathways and represses downstream cell cycle regulators p19, p21, p53 and Rb (Keller & Guttridge, 2013; Wang, 2012; Taulli *et al*., 2006; Taylor *et al*., 2009; Sun *et al.*, 2015). Other deregulated growth factor pathways implicated in RMS include TGF-β, hepatocyte growth factor (HGF) and platelet-derived growth factor (PDGF). Many of these signaling pathways converge on and inactivate negative regulators of the cell cycle to prevent cell cycle arrest required for terminal differentiation and thus enable tumour growth and metastasis (Wei & Paterson, 2001; Otten *et al.*, 1997; Ciccarelli *et al.*, 2005; Shern *et al.*, 2014).

Chen *et al.* (2013) performed genomic and RNA sequencing on human ERMS and ARMS and discovered that gain-of-function mutations in oncogenic Ras was characteristic of high-risk ERMS (Martinelli *et al.*, 2009; Paulson *et al.*, 2011). Furthermore, the authors revealed that, in ERMS, mutations in *TP53* were widespread and that the Hedgehog and Wnt pathways were altered (Chen *et al.*, 2013). Moreover, in a pleomorphic RMS mouse model in which Ras activation was combined with p53 inactivation, Ras was shown to be needed for tumour initiation (Tsumura *et al.*, 2006). This finding is supported by another study in zebrafish in which constitutive Ras activation induced ERMS (Langenau *et al.*, 2007). The authors reported that in this study, Ras upregulated the anti-apoptotic factors MDM2 and survivin that suppress p53 as well as the muscle progenitor and satellite cell factors MyoD, Myf5, Myogenin, Gli1 and Notch1. This suggests that Ras may be involved in proliferative and self-renewal pathways in ERMS. Recently it was also found that activation of Ras contributed to resistance to reactive oxygen species (ROS) and PI3K/mTOR induced cell death in ERMS (Schott *et al.*, 2015).

Ras activation is known to increase Hedgehog (Hh) signaling and, as mentioned earlier, Hh was found to be altered in ERMS (Pressey *et al.*, 2011; Chen *et al.*, 2013; Hawkins *et al.*, 2014; Shern *et al.*, 2014; Satheesha *et al.*, 2015). Together this suggests that Hh signaling may too be a common feature in ERMS. Interestingly, during the development of the myotome, Hh signaling is needed for cell survival and proliferation through suppressing apoptosis (Belyea *et al.*, 2012). Furthermore, Ptch1, Gli1, Gli3, and Myf5, downstream

signaling molecules in the Hh cascade, are expressed in ERMS and fusion-negative ARMS and are associated with worse overall survival (Zibat *et al.*, 2010; Paulson *et al.*, 2011; Nitzki *et al.*, 2015; Satheesha *et al.*, 2015). Importantly, targeting Hh reduced self-renewal in ERMS cells, induced differentiation *in vitro* and limited tumour formation *in vivo* (Satheesha *et al.*, 2015). Moreover, Satheesha *et al.* (2015) went on to show that high levels of Hh contributed to chemoresistance and inhibiting Hh signaling sensitized the ERMS cells to chemotherapeutic-induced cell death. The authors also showed Hh signaling to upregulate Nanog in ERMS and similarly increase self-renewal and tumour growth.

The developmentally important Notch and Wnt signaling have also been implicated in RMS (Vijayakumar *et al.*, 2011; Roma *et al.*, 2012). Notch is responsible for maintaining a balance between self-renewal and differentiation as it mediates cell fate determination (Belyea *et al.*, 2012). In both RMS subtypes it is thought to inhibit myogenesis, maintain stem-ness and regulate motility and invasiveness (Roma *et al.*, 2012; Belyea *et al.*, 2012). Moreover, inhibiting Notch in RMS resulted in activation of p21, myotube differentiation and hampered tumour growth *in vitro* and *in vivo* (Raimondi *et al.*, 2012; De Salvo *et al.*, 2014). In development, Wnt signaling regulates embryonic somite patterning and myogenesis through the processes of proliferation, cell migration, polarity and cell death (Annavarapu *et al.*, 2013). Not surprisingly, its deregulation contributes to invasion and metastasis of various cancers. Interestingly, while Annavarapu *et al.* (2013) reported that the Wnt/β-catenin signaling pathway was functionally active in a significant subset of RMS tumours, there is debate as to whether it plays an anti-oncogenic or pro-oncogenic role in RMS. Indeed, there have been reports that Wnt may repress proliferation and promote muscle differentiation and apoptosis while other reports have claimed that it inhibits differentiation, promotes satellite cell proliferation and facilitates RMS tumour invasion and metastasis (Roma *et al.*, 2012; Belyea *et al.*, 2012; Annavarapu *et al.*, 2013). More work is therefore required to clarify the role of Wnt signaling in RMS.

Finally, during development Hh, Wnt and Notch signaling function in the expansion of muscle stem cell subpopulations and their aberrant expression is associated with persistent stem cell maintenance, self-renewal, and tumor initiation in RMS (Takebe *et al.*, 2011; Belyea *et al.*, 2012; Roy *et* al, 2013; Satheesha *et al.*, 2015). Belyea *et al.* (2012) postulates

that the activity of these factors to maintain self-renewal increases the risk of accumulating oncogenic mutations and overall genomic instability which contributes to rhabdomyosarcomagenesis.

1.5.3 Management and treatment of RMS

Currently, the clinical criteria for classification of RMS into low-, intermediate-, or high-risk groups depend on primary tumor site, size, surgical resectability and metastasis to regional lymph nodes or distant sites (Malempati & Hawkins, 2012). Treatments for RMS include a combination of surgery, radiation and chemotherapy and while prognosis has improved, from approximately 25% in 1970 to 75% today, there is a strong drive to identify more effective targeted therapeutics, for example, based on the molecular and genetic profile of a tumour (Malempati & Hawkins, 2012). A chemical screen for drugs to repress proliferation and self-renewal in ERMS identified inhibitors of glycogen synthase kinase 3 (GSK3) (a repressor of myogenin), Raf/MEK, PI3K/AKT, Hh, HDACs and DNA damaging agents (Chen *et al.*, 2014). At the moment popular targeted therapies for RMS include mTOR and Hh inhibitors and RTK specific monoclonal antibodies or small-molecule inhibitors (see **Figure 1.6**). However, although an initial response may be observed with these treatments, the disease often continues to progress and/or tumour drug resistance develops. Furthering targeted therapies requires improved molecular classifications and diagnoses for accurate targeting, as well as greater identification of master differentiation transcription factors, cell cycle regulators and mitogenic signaling pathways that are altered in RMS. While ERMS has a better prognosis compared to ARMS, a plateau in effectiveness of current treatments (70% five-year survival rate) has been reached despite newer and more intensive chemotherapeutics and prognosis remains poor for high-risk, recurrent and metastatic ERMS (10-30% five-year survival rate) (Zhang *et al.*, 2013; Hawkins *et al.*, 2014; Sun *et al.*, 2015). There is therefore still a need to discover more effective treatments that will reduce rates of relapse and improve clinical outcomes for RMS.

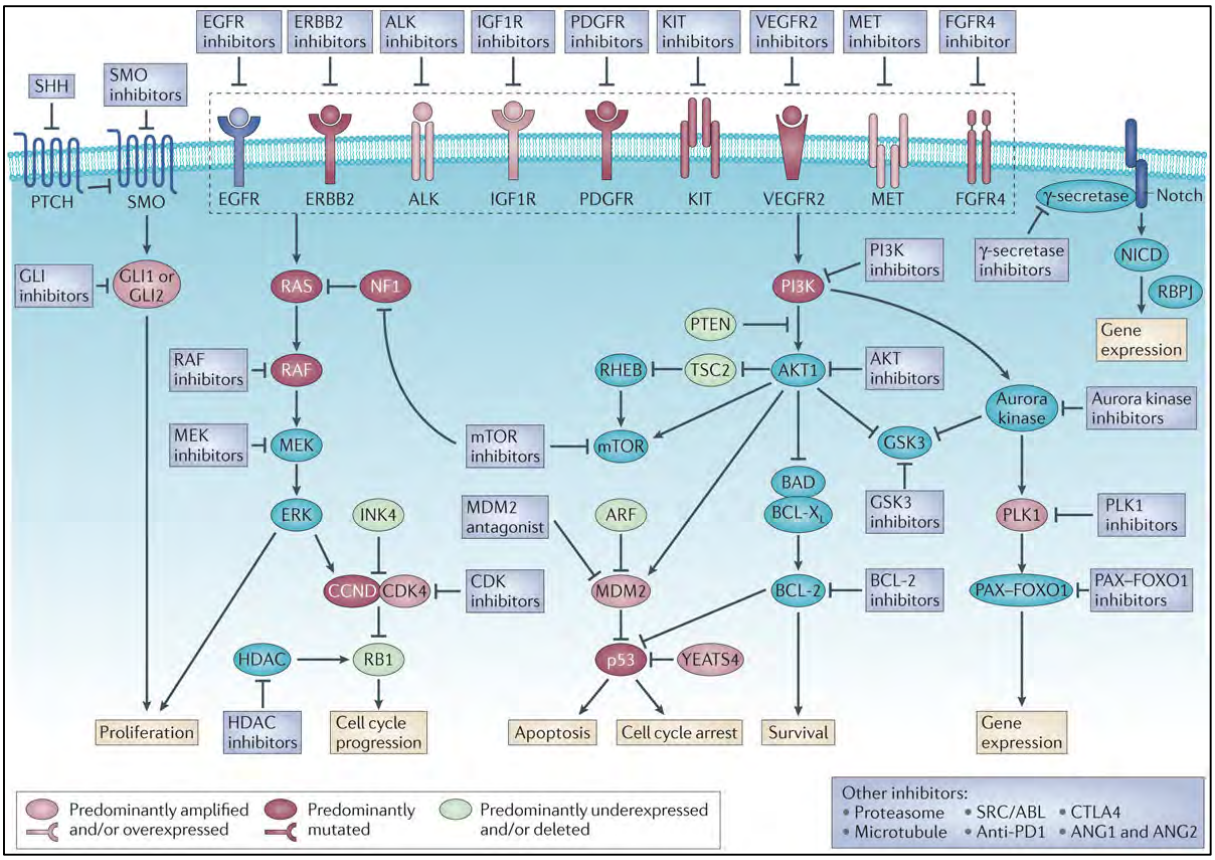

Figure 1.6: RMS pathways for targeted therapies. Diverse pathways have been implicated in RMS biology and offer potential for targeted therapeutic intervention. The diversity of targets and multitude of agents illustrates the need to leverage model systems to focus clinical trial efforts in the small RMS patient population. The drugs that target different signaling pathways are listed in boxes adjacent to the corresponding proteins, whereas other targets are listed in an independent box. ALK, anaplastic lymphoma kinase; ANG1, angiopoietin 1; BAD, BCL-2-associated agonist of cell death; CCND, cyclin D; CDK, cyclin-dependent kinase; CTLA4, cytotoxic T lymphocyte-associated antigen 4; EGFR, epidermal growth factor receptor; FGFR4, fibroblast growth factor receptor 4; FOXO1; forkhead box O1; GSK3, glycogen synthase kinase 3; HDAC, histone deacetylase; IGF1R, insulin-like growth factor 1 receptor; NICD, Notch intracellular domain; NF1, neurofibromin 1; PAX, paired box; PD1, programmed cell death protein 1; PDGFR, platelet-derived growth factor receptor; PLK1, Polo-like kinase 1; PTCH, Patched; RB1, retinoblastoma 1; RBPJ, recombination signal binding protein for immunoglobulin kJ region (also known as CSL); RHEB, RAS homologue enriched in brain; SHH, sonic hedgehog; SMO, Smoothened; TSC2, tuberin; VEGFR2, vascular endothelial growth factor receptor 2 (taken from Kashi *et al.*, 2015).

1.6 Aims of this study

The T-box transcription factor TBX3 has a critical function in embryonic development and it has also been linked to cancer. Importantly, our laboratory has recently shown that TBX3 is overexpressed in a wide range of sarcomas, including ERMS (Wilmer *et al.*, 2016). The broad objective of this study is to explore the significance of TBX3 overexpression on the oncogenic phenotype of ERMS. This will be achieved through establishing ERMS cell culture models in which TBX3 is either stably knocked down or overexpressed and the effects on key hallmarks of the cancer phenotype will be investigated. It is hypothesized that whereas knocking down TBX3 may reverse key features of the cancer phenotype, further overexpressing it may result in a more aggressive cancer phenotype. Brief characterization of TBX3 co-factors and upstream regulators will be pursued. This will be addressed through the following objectives:

Aim 1: To stably knock-down TBX3 in ERMS cells that express high levels of this protein using a short-hairpin RNA approach and to characterize the impact on key features of the transformed phenotype *in vitro* and *in vivo*.

Aim 2: To stably overexpress the two TBX3 isoforms, TBX3 and TBX3+2a, in ERMS cells and to determine the impact on key features of the transformed phenotype *in vitro* and *in vivo*.

Aim 3: To perform preliminary experiments to characterise protein co-factors that co-operate with TBX3 to drive its oncogenic activity in ERMS.

Aim 4: To perform preliminary experiments to determine whether c-Myc and AKT is responsible for upregulating TBX3 in ERMS cells.

Chapter 2. Materials and Methods

2.1 Plasmids and DNA constructs

All constructs used in this study were prepared according to standard techniques (Sambrook *et al*., 1989). The pSuper.neo/GFP vectors, either containing a shRNA specific to TBX3 (SHTBX3) or a non-specific scramble shControl (SHCTRL) sequence were previously cloned by Dr Jade Peres and are available in the Prince laboratory. The shTBX3 sequence is as follows: 5'-GATCCCCCTGCCTATAGAGATATATTCATTCAAGAGATGAATATATCTCTATAGGCAGTTTTTA- 3' and was designed based on a commercially available siRNA sequence (Qiagen, USA). Mouse expression constructs for Tbx3 harbouring a 5'-3XFLAG tag was kindly provided by our collaborator Colin Goding (Ludwig Institute, University of Oxford, UK). The pEGFP-C1 vector containing full length GFP-nucleolin was purchased from Addgene (plasmid #28176) and was provided by Michael Kastan (Takagi *et al*., 2005). The pEGFP-C1 Empty vector was previously constructed by Dr Emily Davis and is available in the Prince laboratory. For vector maps see **Appendix section 6.1**.

2.2. Cell Culture and Transfections

2.2.1 Transfections

Transfection is the process whereby cells take up and express exogenous DNA or RNA (**Figure 2.1**). Prior to performing transfections, the concentration and quality of DNA of constructs were assessed using a NanoDrop ND-100 spectrophotometer (Agilent Technologies, Boeblingen, Germany) and the integrity of the DNA confirmed by agarose gel electrophoresis. In general transfection reagents are lipid based therefore allowing for micelles to form around the nucleic acids of interest enabling them to fuse with the lipid soluble portion of phospholipid bilyer of the cell membrane, resulting in entry of exogenous nucleic acids into host cells. Three different transfection reagents were used as follows:

2.2.1.1 FuGENE HD (Roche, Germany):

Cells were transfected at a 3:1 ratio according to the manufacturer's instructions. Cells were plated at 4 x 10^5 per well of a 12-well plate (3.5 x 10^4 per well of a 24-well plate) 1 day before transfection. Three microliters (1.5 µl for 24-well plate) of the transfection reagent was added to 97 µl (48 µl for 24-well plate) serum free medium and incubated at room temperature (RT) for 5 minutes. The diluted transection reagent was added to the DNA, mixed and incubated at RT for another 15 minutes. The transfection reagent/DNA complex was added dropwise to the cells and incubated for twenty-four to forty-eight hours at 37^{o}C.

RD SHTBX3 and SHCTRL cell lines and RD Flag-mtbx3, Flag-mtbx3+2a and Flag-Empty cell lines: Cells at 60-70% confluence in 35mm dishes were transfected with 1 µg of pSuper.neo/GFP-shCtrl or pSuper.neo/GFP-shTBX3 vectors; or 1 µg 3XFLAGpCMV-mtbx3, 3XFLAGpCMV-mtbx3+2a or 3XFLAGpCMV-Empty vectors.

2.2.1.2 X-tremeGENE HP (Roche, Germany):

Operations were the same as for FuGENE HD except cells were transfected using a 2:1 ratio. Nucleolin co-operates with TBX3: RD cells were plated at 4 x 10^4cells/well in 24-well plates were transfected with 250 ng of the pEGFP-nucleolin expression vector or an equal amount of pEGFP-Empty vector.

2.2.1.3 Hiperfect®:

Transient knock-down of TBX3, nucleolin, c-Myc and AKT1 expression was achieved by siRNAs that specifically target mRNA expression of TBX3, nucleolin, c-Myc or AKT1 (siTBX3, siNuc, sic-Myc or siAKT1). RD cells were plated at 4 x 10^4 cells/well of a 24-well plate and transfected at a 60% confluency with 50 nM of siTBX3 (SI00083503, Qiagen, USA), 50 nM sic-Myc (Dharmacon, Lafayette, CO, USA and Qiagen, USA), 50nM siNuc (SI02654925, Qiagen, USA), 50 nM siAKT1 or a control (non-silencing, siCtrl) siRNA (1027310; Qiagen, USA), according to manufacturer's instructions. Briefly, siRNAs were diluted in 97 µl serum-

free medium after which using 3 µl of HiPerFect® (Qiagen, USA) was added directly to the siRNA solution, incubated at RT for 15 minutes and added to cells.

2.2.1.4 Generation of stable cell lines in which TBX3 was knocked down

RD cells express high levels of TBX3 and were therefore selected to generate cell lines in TBX3 mRNA and protein levels were stably knocked down. Cells were transfected with the pSuper.neo/GFP-shTBX3 or -shCtrl expression vectors using Fugene® (Bio-Rad, USA) as described in section 2.2.1.1. Stable transfectants were selected for with 0.8 mg/ml G-418 antibiotic (Promega, USA) 48 hours post transfection as described below.

2.2.1.5 Generation of stable cell lines in which TBX3 was overexpressed

RD cells were transfected with either 3XFLAGpCMV-mtbx3, 3XFLAGpCMV-mtbx3+2a or 3XFLAGpCMV-Empty expression vectors using FuGENE as described in section 2.2.1.1. Stably transfected clones were selected for with G-418 antibiotic (Promega, USA) 48 hours post transfection as described below.

2.2.2 Cell culture

Human embryonic rhabdomyosarcoma (ERMS) RD cells were purchased from American Tissue Culture Collection (ATCC). Cells were maintained in Dulbecco's-modified Eagle medium (DMEM) (Sigma Aldrich, USA) supplemented with 10% fetal bovine serum (FBS), 100 U/ml penicillin and 100 µg/ml streptomycin. Cells were maintained at 37°C in an atmosphere of 5% CO_2 and 65% humidity. Sterile technique was practiced, media was replaced every 2-3 days and cells were routinely subjected to mycoplasma tests. Only mycoplasma free cells were used in experiments.

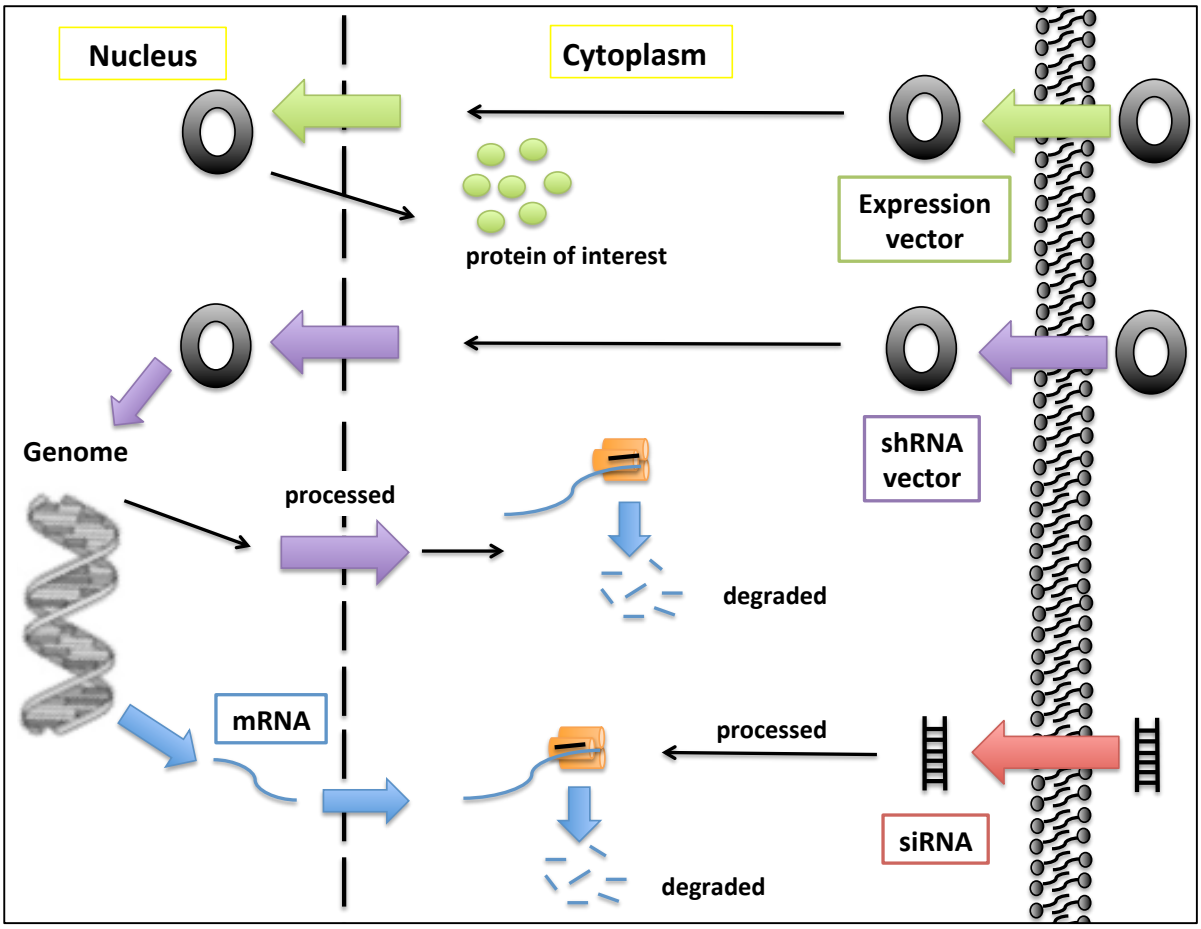

Figure 2.1: **siRNA, shRNA and expression vector processing and action.** Transfection of expression vectors, shRNA and siRNA. Expression vectors (top) are able to enter into a host cell's nucleus where it co-opts its protein synthesis machinery to express its own gene of interest off its promoter. shRNA vectors (middle) also enter into a host cell's nucleus but are able to integrate into it genome and thereby expressed through the cell's natural transcription and translation process, ultimately producing a single-stranded RNA molecule that binds and degrades complementary target mRNA. In contrast siRNA molecules remain in a host cell's cytoplasm where it too is processed into a single stranded molecule that results in the degradation of its target mRNA.

2.2.2.1 Mycoplasma test

Mycoplasma tests were performed to ensure that uninfected cells were used in experiments. Mycoplasma are parasitic bacteria that have no cell walls. These micro-organisms have very limited biosynthetic capabilities and therefore rely on their host cells for survival and replication. Mycoplasma can have deleterious effects on their host cells, including affecting their signal transduction pathways and metabolism, promoting or

inhibiting apoptosis, altering cell morphology, DNA, RNA and protein synthesis, and cell growth and even mediating cancerous transformation (Rottem *et al.*, 2012). Mycoplasma can be detected using a nucleic acid stain, Hoescht, which detects both mycoplasma and nuclei of the cell. Briefly, cells were grown on a coverslip in antibiotic-free medium for a minimum of 48 hours. The cells were then fixed by a 1:3 mixture of glacial acetic acid and methanol for 5 seconds, washed with single distilled water and air dried for 3 minutes at RT. The nuclei were stained with Hoechst 33258 (0.5 µg/ml) for 30 seconds, washed with single distilled water and mounted on a glass slide with mounting fluid (**see Appendix section 6.2**). Cells were viewed under a fluorescent microscope using the DAPI filter. Mycoplasma negative cells stained positive with Hoechst 33258 only in the nucleus, while mycoplasma infected cells showed staining in both the nucleus and the cytoplasm.

2.2.2.2 Antibiotic titration assay: Geneticin selection

To ensure that only stable transfected cells were selected 48 hours after transfection cells were treated with Geneticin (G-418) (V7983, Promega, USA), a neomycin analogue, as the pCMV and pSuper.neo/GFP expression vectors containing the TBX3 overexpression, TBX3 knock-down and control sequences, carry a neomycin resistance gene. G-418 is an aminoglycoside antibiotic that alters normal protein production by inhibiting polypeptide synthesis during the elongation step in both prokaryotic and eukaryotic cells, therefore ultimately resulting in cell death (Davies & Jimenez, 1980; Bar-Nun *et al.*, 1983; Beck *et al.*, 1982). To determine the effective concentration of antibiotic for the RD cell line a dose, or kill, curve was performed. Untransfected cells were seeded at 2.5 x 10^4 cells per well in a 6-well plate and when the cells were approximately 60% confluent they were treated with various concentrations of G-418, ranging from 0 – 1.2 mg/ml, and monitored daily. The lowest concentration, 0.8 mg/ml, which resulted in complete cell death after approximately 10 days was selected. Overexpression and knock-down were maintained through the addition of a selection agent every 2-3 days.

2.2.3 Cell Treatments

2.2.3.1 Thymidine S-phase block

TBX3 and Hsc70 expression peak during S-phase, therefore RD cells were synchronised into S-phase by a double thymidine (Sigma, USA) block (15 hours 2 mM thymidine, 9 hours release, 15 hours thymidine and a 4 hour release by 3 brief washes with fresh media and the addition of fresh media). Cells were then analysed via immunoprecipitation and immunocytochemistry.

2.2.3.2 Chemical inhibition of AKT

To inhibit the kinase activity of AKT in RD cells 4 x 10^4 cells were plated in a 24-well plate and when 60-70% confluent were treated with 10 µM of AKT-VIII chemical inhibitor (124018, Calbiochem, EMD Millipore, USA) for 1, 2 and 4 hours, followed by protein harvest and western blot analyses.

2.3 Quantitative Real-Time Polymerase Chain Reaction (qRT-PCR)

To assess the levels of TBX3 mRNA in the stable overepxression, knock-down and control cell lines quantitative real-time polymerase chain reaction (qRT-PCR) was performed. RNA was harvested, purified, and converted to complementary DNA (cDNA). Forward and reverse primers specific to TBX3 mRNA sequence were added to cDNA and cycles of PCR performed. The resultant crossover threshold (CT)/crossing point (CP) values depend on the starting amount of the cDNA, therefore the lower the CT/CP value the greater the starting amount of TBX3 mRNA and *vice versa*.

2.3.1 RNA extraction

Total RNA was extracted from cells using the High Pure RNA Isolation Kit according to the manufacturer's instructions (Roche, Germnay). Cells grown in 6 cm dishes were harvested at 70-80% confluence, after two chilled 1X Phosphate Buffered Saline (1X PBS) washes (see **Appendix section 6.3**), using 400 µl per dish of High Pure RNA Isolation Kit Lysis Buffer. The Lysis Buffer contains Triton-X 100 detergent to permeabilize the cell membranes, Tris-HCl, to regulate pH and osmolarity of the lysate, and guanidine hydrochloride, to denature proteins, inactivate RNases and promote binding of the RNA to the membrane of the spin column. Extraction was performed according to the manufacturer's instructions. Briefly, genomic DNA was removed via addition of the supplied deoxyribonucleases (DNase) and DNase incubation buffer followed by centrifugation. The phosphodiester backbone of the DNA was hydrolytically cleaved and the degraded DNA removed by washes and centrifugation, leaving behind the RNA. The RNA was eluted in nuclease free double distilled water. The wash buffers and centrifugation steps remove proteins, lipids, polysaccharides, salts and other cellular impurities from the RNA solution and, during the elution step, the polarity of the water disrupts the bonds between the RNA and membrane, enabling elution. The quality and concentration of RNA was determined by spectrophotometry using a NanoDrop® ND-1000 spectrophotometer (Agilent Technologies, Boeblingen, Germany). The resulting RNA produced was stored at -80°C.

2.3.2 Reverse Transcription

cDNA was produced from the extracted RNA samples by reverse transcription using the InProm-IITM reverse transcription system (Promega A3800) according to the manufactuers instructions. Briefly, for each sample 1 µg of RNA was combined with 0.5 µg of Oligo (dT) primer in a 5 µl volume and denatured at 70^{o}C for 5 minute, chilled on ice and combined with reverse transcription reaction mix (5X InProm-IITM reaction buffer, 25 mM $MgCl_2$, 10 mM dNTP mix, 20 units RNasin® ribonuclease inhibitor and 1 µl of ImProm-IITM reverse transcriptase) to a final volume of 20 µl. The annealing of the primers to the template RNA occurred at 25^{o}C for 5 minutes, the reactions were incubated at 42^{o}C for 1 hour for the

reverse transcription of the template, followed by 15 minute incubation at 70^{o}C to inactivate the reverse transcriptase prior to PCR. The resulting cDNA produced was stored at -20°C.

2.3.3 Quantitative Real-Time PCR (qRT-PCR)

To quantify the relative levels of cDNA between samples, qRT-PCR was conducted with the SensiMix lite kit (Quantace QT 405-05, USA) or the KAPA SYBR FAST kit (Kapa Biosystems). PCR reactions contained either 5X SensiMix Lite, 50X SYBR Green I, 1.5 µl Enzyme mix and 2 µl of combined forward and reverse primers (10 µM) per 18 µl reaction or 2X Kapa Mix, Sabax H2O, 2.5 µg/µl bovine serum albumin (BSA) and 0.4 µl of combined forward and reverse primers (10 µM) per 9 µl reaction. PCR reactions were made up as master mixes and aliquoted into glass capillaries with the addition of 2 µl or 1 µl of cDNA per capillary to give a final reacion volume of 20 µl or 10 µl for the SensiMix and KAPA SYBR FAST reactions respectively. Primers specific to TBX3 (QT00022484, Qiagen, Germany), c-Myc, and Glucuronidase Beta (GUSB) (QT00046046, Qiagen, Germany), for internal normalisation to correct for sample-to-sample variations within a PCR run, were used. The glass capillaries were centrifuged at 3000 rpm for 1 minute and placed in the LightCycler 3.0 (Roche, Switzerland). PCR cycle parameters were: denaturation (15 minutes at 95^{o}C), annealing and amplification for 35 cycles (5 seconds at 95^{o}C; 3 seconds at 55^{o}C; 5 seconds at 72^{o}C), melting step (15 seconds at 65^{o}C) and a cooling step (30 seconds at 40^{o}C). Each DNA sample was quantified in duplicate and a negative control without cDNA template was run with every assay to assess the overall specificity and monitor for contamination. Melting curve analyses was carried out to ensure product specificity and data was analyzed using the $2^{-\Delta\Delta Ct}$ method. Relative mRNA expression levels were normalized to glucuronidase beta (GUSB) for each reaction with PCR efficiency correction calculated using the formula Ratio = (Etarget)CPtarget(control–sample)/(Eref)CPref(control–sample); E: real-time PCR efficiency, CP: crossing-point. The Microsoft Excel programme was used to calculate the statistically significant differences between samples using the Student t test. P values of <0.05 were considered statistically significant.

2.4 Western blotting

2.4.1 Protein extraction

To assess protein levels western blotting was performed. Briefly cells were harvested on ice by trypsinisation taking volumes of lifted cells equivalent to that of a 90% confluent 35mm dish, were centrifuged at 2500 rpm for 2 minutes, the media discarded and the pellet re-suspended in 70ul of boiling blue buffer (see **Appendix section 6.3**). Alternatively, the cells were lysed in adjusted volumes of boiling blue buffer, according to the dish area and confluency, and scraped down using the rubber tip of a sterile plastic syringe. Cell lysates were collected into a microfuge tube, boiled for 10 minutes at 100^{o}C and stored at -20^{o}C.

2.4.2 Sodium-Dodecyl-Sulphate Polyacrylamide Gel Electrophoresis (SDS-PAGE)

Protein samples were separated by electrophoresis on 1.5 mm (thick) 8-15% resolving gels with a 5% stacking gel (see **Appendix section 6.3**). Gels were assembled in Biorad Mini PROTEAN© 3 casting apparatus, placed in the Biorad running tank and the tank was filled with 1X running buffer (see **Appendix section 6.3**). Equal amounts of sample (10-20 µl) were loaded and 6 µl of PageRuler Prestained Protein Marker (Fermentas, USA) (see **Appendix section 6.3**) was also loaded to determine the relative size of the proteins (see **Appendix section 6.3**). The running apparatus was connected to the Biorad Powerpack 200 (South Africa) and electrophoresis occurred at 100 Volts for 2 hours.

2.4.3 Protein transfer onto a nitrocellulose membrane

Electrophoresed proteins were transferred onto nitrocellulose blotting membrane (Amersham, GE Healthcare, Life Sciences, Germany). Gels were placed in a transfer 'sandwich' cassette consisting of sponges, whatman filter paper, the gel and the nitrocellulose membrane presoaked in 1X transfer buffer (see **Appendix section 6.3**) and

assembled into the correct order (**Figure 2.2**). This cassette was then placed into the transfer unit of the Biorad Mini PROTEAN© 3 transfer tank in the correct orientation to ensure that the negatively charged proteins moved from the gel onto the membrane which is placed on the positive side of the transfer sandwich. An ice pack was placed in the tank to prevent overheating and the tank was filled with 1X transfer buffer. The transfer apparatus was connected to the Biorad Powerpack 200 and protein transfer took place at 100 Volts for 90 minutes.

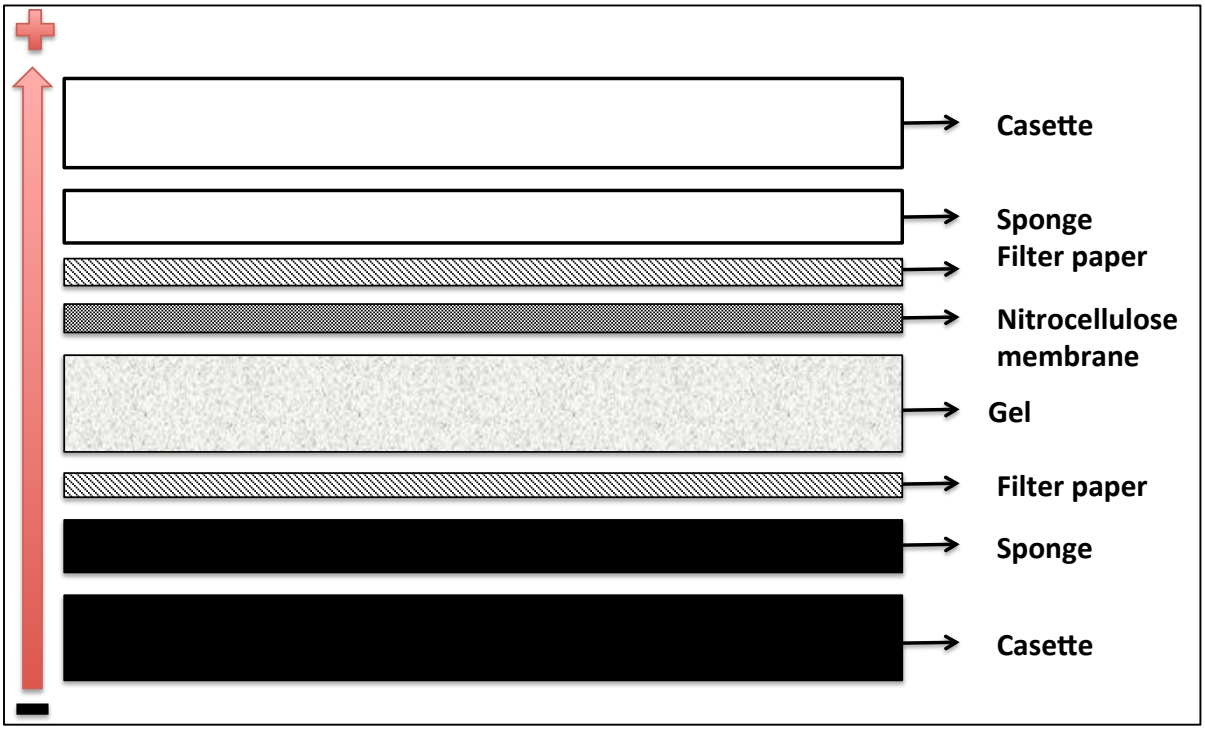

Figure 2.2: Western blot transfer sandwich. Once the SDS-PAGE has run, the gel contains size separated proteins. These proteins need to be transferred from the gel to a nitrocellulose membrane blot. The layout of the transfer sandwich and orientation of the plastic cassette is crucial in ensuring that the proteins do indeed run from the gel onto the blot for later detection.

2.4.4 Western blot detection

Following transfer, membranes were blocked for 1 hour at RT with 1X PBS/0.1% Tween (PBS/T) (see **Appendix section 6.3**) containing 5% non-fat dry milk (see **Appendix section 6.3**) and probed with appropriate primary antibodies overnight at 4°C with shaking. Primary antibodies used were as follows: rabbit polyclonal anti-TBX3 (1:500) (Zymed 42– 4800,

Zymed, San Francisco, CA) or (1:1000) (ab99302, Abcam, USA), rabbit polyclonal anti-p38 (1:5000) (M0800, Sigma, USA), mouse monoclonal Flag M2 (1:1000) (F1804, Sigma, USA), rabbit c-Myc (1:1000) (sc-N262), rabbit AKT (1:1000) (9272S), rabbit p-AKT (1:1000) (9271S), rabbit AKT1 (1:1000) (C73H10), rabbit c-Myc (1:1000) (D84C12) (Cell Signaling, USA), mouse polyclonal anti-nucleolin (1:1000) (sc-8031), mouse polyclonal anti-Hsc70 (1:1000) (sc-7298), rabbit IgG (sc-2027) (Santa Cruz Biotechnology, Santa Cruz, CA). Membranes were washed with 1X PBS/T at 2 x 5 minute and 2 x 10 minute intervals, incubated with the appropriate secondary antibody, horseradish peroxidase-conjugated anti-rabbit (1:5000) (BioRad, Hercules, CA, USA), horseradish peroxidase-conjugated anti-mouse (1:5000) (BioRad, Hercules, CA, USA) or A/G protein (1:5000) (20421, Thermo Fisher Scientific), for 1 hour at RT, then washed four times as previously described, before protein detection was performed and visualised by enhanced chemiluminescence (ECL) by addition of SuperSignal West Pico Chemilumninescent Substrate (Pierce, Rockford, IL, USA) or WesternBright (Advansta, USA) (**Figure 2.3**). Equal amounts of detection reagent A and detection reagent B were used per blot and allowed to incubate on the membrane for 5 minutes before being enclosed between two acetate sheets. The substrate for horseradish perioxidase is found within the detection reagent and therefore oxidation of the substrate is catalysed when the detection reagents comes into contact with the enzyme conjugated secondary antibody; leading to the emission of light (**Figure 2.3**). Membranes were exposed to x-ray film (autorad) and the resulting chemiluminscent signal captured by developing and fixing the autorad. Densitometric analysis was carried out to quantify the bands using Unscan-it gel 6.1. software, normalised to the p38 loading control.

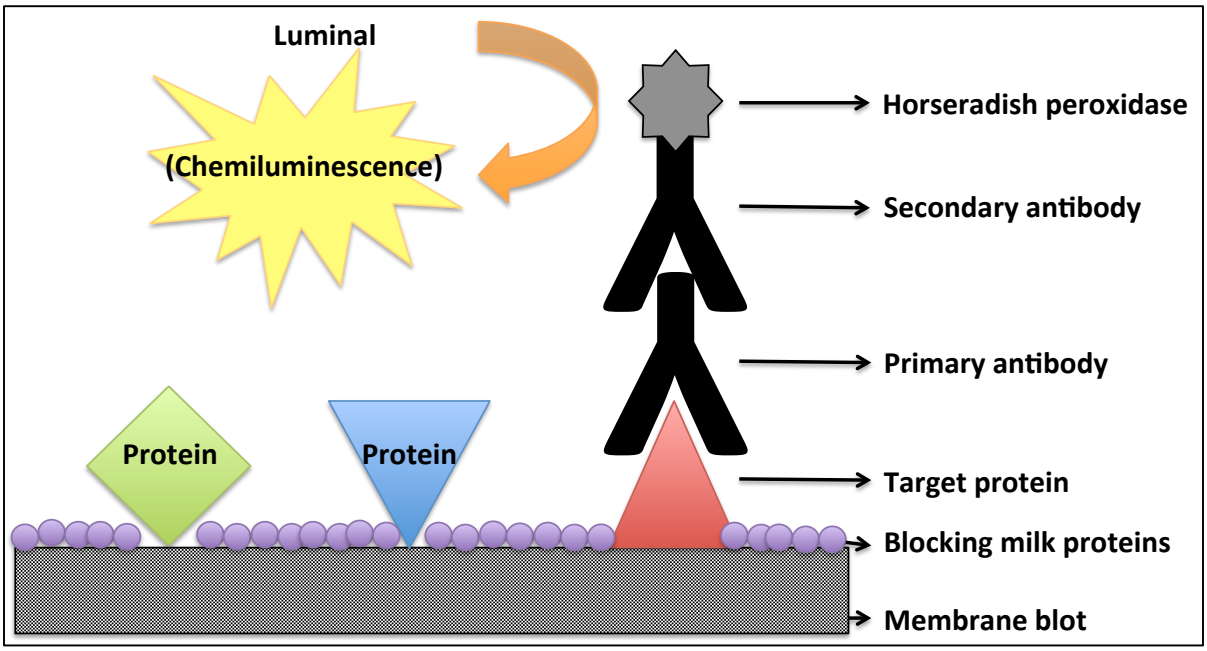

Figure 2.3: Western Blot detection by chemiluminescence. The primary antibody raised against its target protein will bind to it if present on the membrane blot containing the transferred proteins. An enzyme-conjugated secondary antibody, raised against the animal the primary was raised in, binds to the primary antibody. Enzyme substrate is added to the membrane blot and a chemical reaction takes place, resulting in a product and a light signal that is detected via exposure to an autorad film in a dark room.

2.5. Transformation assays

2.5.1 Proliferation

Two methods were utilised to determine short term cell growth, namely (1) cell viability as a measure of cell growth was determined using the 3-(4,5-dimethylthiazol-2-yl)-2,5-diphenyltetrazolium bromide (MTT) Cell Proliferation Kit (Roche, Germany) and (2) counting of cells at specific time points using a haemocytometer.

2.5.1.1 Methylthiazol tetrazolium (MTT) assay

An MTT assay is a colourimetric assay used to determine cell viability. Metabolically active cells are able to cleave yellow MTT (3-(4,5-Dimethylthiazol-2-yl)-2,5- diphenyltetrazolium

bromide, a tetrazolium ring) to purple formazan crystals in their mitochondria (**Figure 2.4**). This reduction only takes place in living cells when their mitochondrial reductase enzymes (dehydrogenases) are active. The purple MTT formazan crystals are insoluble in aqueous solutions, therefore a solubilizing solution, containing acidified isopropabol, is able to dissolve the crystals into a purple solution, which is then spectrophotometrically measured. Therefore the number of viable cells is directly related to a sample's ability to convert the yellow salt into a purple solution, which is directly related to spectrophotometric absorbance reading at the appropriate wavelength (**Figure 2.4**) (Mosmann, 1983).

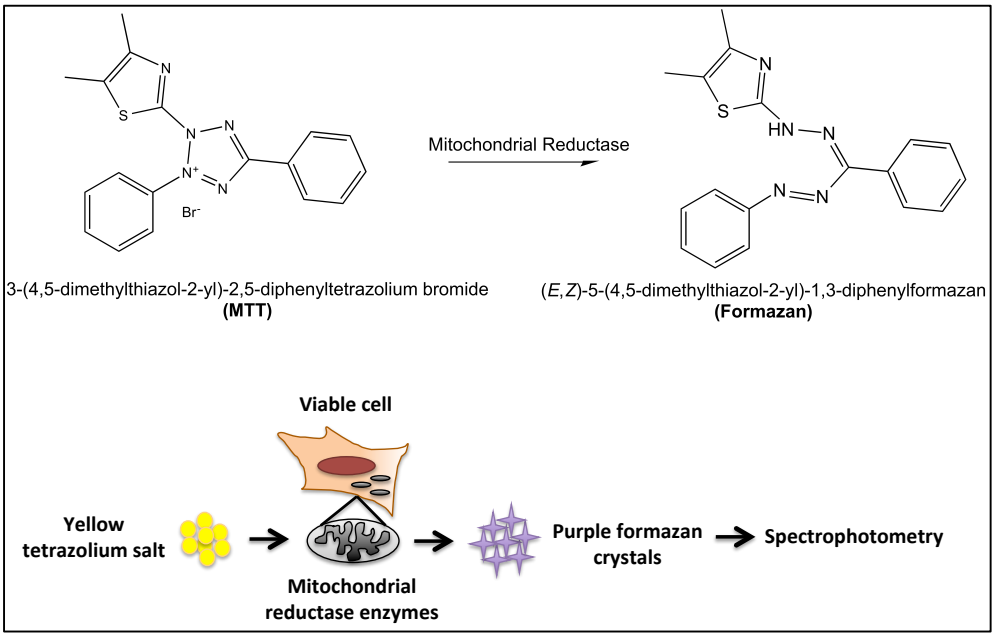

Figure 2.4: MTT reaction. In viable cells, active mitochondrial reductase enzymes result in the formation of insoluble formazan crystals from yellow tetrazolium MTT, characterized by high absorptivity at 595 nm.

To determine cell growth using the MTT Cell Proliferation Kit, cells were plated at 1 x 10^3 cells per well in quadruplicate in a 96-well plate and cell viability determined according to the manufacturer's instructions (11465007001, Roche). Briefly, cells were allowed to grow for 48 hours prior to adding 10 µl of pre-warmed MTT labelling reagent (0.5 mg/ml) per well, incubated at 37°C for 4 hours, after which 100 µl of pre-warmed solubilisation solution was added per well and incubated at 37°C overnight. The spectrophotometrical absorbance of the samples was determined at a wavelength of 595 nm using a 96-well plate reader, with the absorbance of the medium only control being subtracted from the samples.

2.5.1.2 Growth Curves

Cells were plated in triplicate in a 12-well plate at a density of 1 x 10^4 cells per well. Cells were collected by removing and keeping the media the cells had been growing in, washing the cells twice with 1X PBS, keeping the 1X PBS, and then trypsinisation. Cells were counted using a haemocytometer at days 1, 2 and 3 or 1, 4, 7 and 9.

2.5.1.3 Growth factor dependence assay

For the growth factor-dependence assay, cell proliferation was compared in medium containing either 2% or 10% fetal bovine serum (FBS), using the growth assay as described in section 2.5.1.2 above.

2.5.2 Anchorage independence assay

To determine the effect overexpressing and knocking down TBX3 has on anchorage independent growth, soft agar assays were performed. If a cell does not need anchorage to grow then it will be able to proliferate and form colonies, small clusters of cells, which can be stained and viewed with the naked eye or under the microscope. However, if a cell requires anchorage to grow, then proliferation and colony formation is not possible, and only single stained cells will be seen under the microscope.

2.5.2.1 Soft agar assay

Briefly, 35 mm tissue culture dishes were coated with a layer of 0.5% agar/medium mixture to prevent cells from attaching to the bottom of the dish. Dishes were incubated at 4^{o}C overnight to allow the agar to solidify. Cells were resuspended in 0.35% agar/medium slurry and plated on top of the 0.5% agar/medium layer at a concentration of 3 x 10^4 cells per 35 mm dish. In order to prevent dehydration of the agar/medium slurry, 1 ml of fresh medium per dish was added on top of the slurry (**Figure 2.5**). The dishes were incubated at

37°C in the presence of 5% CO_2 for 14-30 days, with fresh medium changed every 2-3 days. Cell viability was determined by overnight incubation at 37°C with p-iodonitrotetrazolium-chloride (1 mg/ml) (Sigma, USA), which forms a purple formazan dye when reduced by living cells. Pictures were taken using a non-phase contrast lens at 200X and 400X magnification (Sony cyber shot, DSC-T20) using an Axiovert fluorescent microscope (Zeiss, Germany).

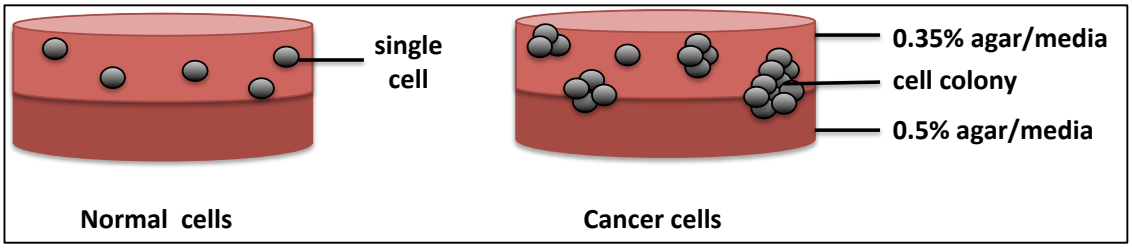

Figure 2.5: Soft agar assay. The bottom layer of the soft agar assay contains a higher percentage agar and the top layer a lower percentage agar/medium slurry in which the cells reside. The ability of the cells to proliferate anchorage independently is assessed over 14-30 days.

2.5.3 Cell migration assay

To determine the effect overexpressing and knocking down TBX3 has on cell migration, an *in vitro* two-dimensional (2D) cell motility (scratch) assay was performed.

2.5.3.1 *In vitro* 2D cell motility assay

Cells were grown to confluence in 24-well plates. A linear wound was made by scratching through the cell monolayer using a sterile 20 µl pipette tip. To remove cell debris, the growth medium was removed and then replaced, and to prevent cell proliferation Mitomycin C (Sigma, USA) was added at a final concentration of 5 µg/ml. Markings were made across the scratch line as reference points for photograph taking to ensure that the same area of the scratch was measured throughout the assay. The wound area was measured at the time of the scratching (0 hour) and thereafter at 3 hour intervals until the ninth or twelfth hour timepoint (**Figure 2.6**). Pictures were taken using a non-phase contrast lens at 20X magnification (Sony cyber shot, DSC-T20) using an Axiovert fluorescent

microscope (Zeiss, Germany). The difference in area was measured using ImageJ software (National Institutes of Health, Bethesda, MD).

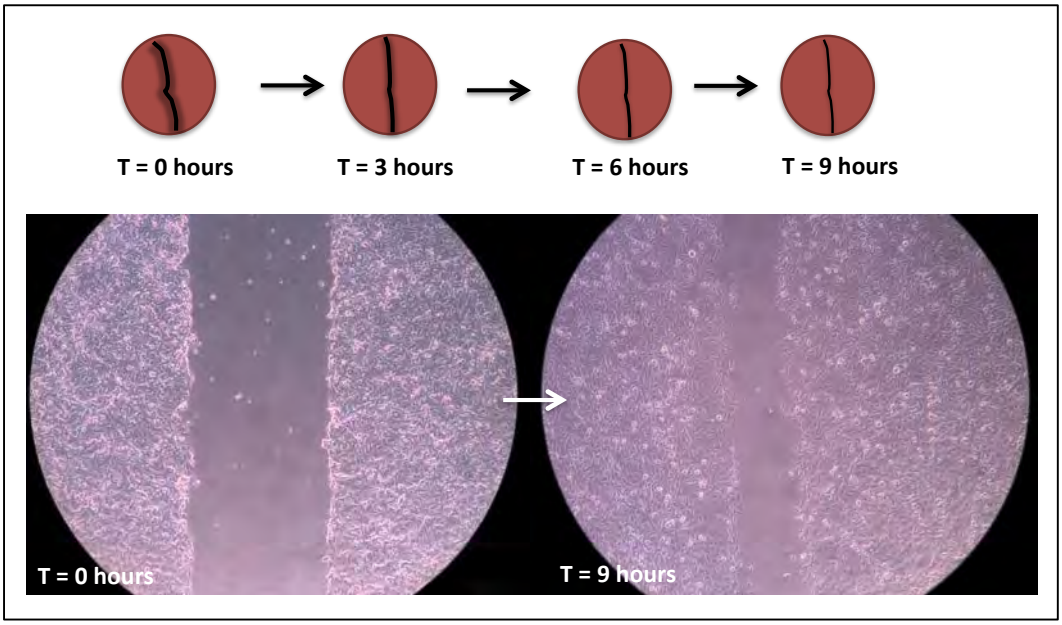

Figure 2.6: Scratch assay. A scratch is made and monitored over time to assess cell migration by wound closure.

2.5.4 Tumour forming ability in mice and tumour histology

In vivo tumour formation was assayed by subcutaneously injecting cultured cells into the right flanks of 4-6 week old UCT 21 (MF1 athymic/immunocompromised) nude mice bred and acquired at UCT's animal unit BCL2. 3 x 10^6 RD or 1 x 10^7 Flag Empty and Flag-mtbx3+2a cells were resuspended in 100 µl sterile 1X PBS and injected into both male and female mice. 7 mice were used for each cell line. Mice were maintained in pathogen-free environments and were monitored daily for tumour formation. For ethical reasons, all mice were humanely euthanised using halothane after 6 weeks. Mice were subjected to autopsies and the presence of metastatic tumours was investigated by visual assessment of the organs such as the lungs, liver and bone. All animal experiments were approved by the Institutional Committee on Ethics of Animal Experimentation (protocol number AEC 015/027).

Tumour tissue specimens for microscopy were collected in 10% formalin in 1X PBS. Samples were further processed in an automatic tissue processor (Shandon Duplex) for routine paraffin wax embedding. Tissue sections were cut, mounted onto clean glass slides, stained with haematoxylin and eosin (H & E) and viewed using a light microscope (Zeiss, Germany).

2.6 Immunofluorescence

Cells were grown on glass coverslips were washed with 1X PBS and fixed in ice cold absolute methanol at -20°C for 5 minutes. Cells were permeabilised in 0.2% Triton X-100 in 1X PBS for 10 minutes at RT. Cells were blocked for 1 hour in 10% BSA in 1X PBS at RT and incubated with the with mouse monoclonal anti-Flag M2 antibody (1:500) (F1804) (Sigma, USA) for 2 hours at 37°C or with rabbit polyclonal anti-TBX3 antibody (1:100) (ab99302) (Abcam, USA), mouse polyclonal anti-nucleolin or anti-Hsp70 (1:100; Santa Cruz Biotechnology, Santa Cruz, CA) antibodies diluted in blocking buffer at 4^{o}C overnight in a humidifying chamber. Cells were washed with 1X PBS and incubated with the Cy3 goat anti-rabbit (1:1000; Molecular probes, USA) or Alexa 488 goat anti-mouse secondary antibody (1:1000; Molecular probes, USA) for 2 hours at RT in the dark. Cells were washed again with 1X PBS and the DNA was stained by incubating the cells with 0.5 µg/ml Hoechst 33258 for 10 minutes at RT in the dark. Cells were washed, the coverslips mounted onto glass slides using Mowial mounting medium (Hoechst, Germany) containing n-Propyl gallate (anti-Fade) (Sigma, USA) and the cells were visualised by a confocal microscope (Zeiss LSM 510 Meta with NLO, Software: ZEN 2009, Lasers: Argon 488 green, solid state laser: 561 nm Red, MaiTai 2 photon laser: 750 nm for DAPI/ Hoechst, Germany) (**Figure 2.7**). Negative controls were the appropriate secondary antibodies only. Co-localisation analysis to obtain values for Mander's coefficient, weighted coefficient and Pearson's coefficient was performed using Zeiss LSM 510 Meta Software.

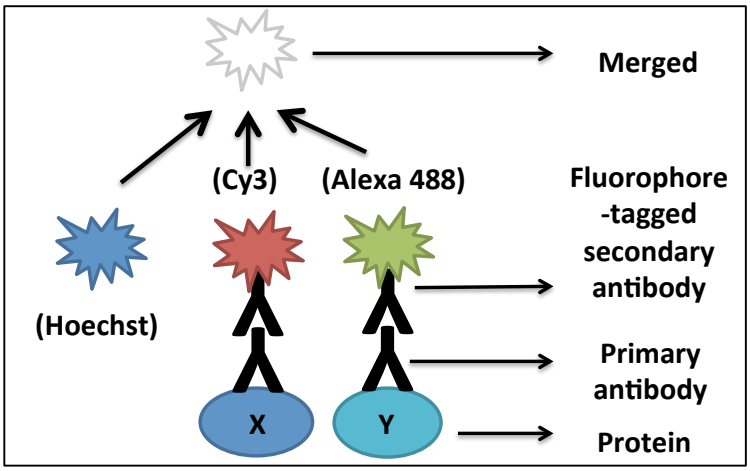

Figure 2.7: Immunocytochemistry. Using antibodies specific to certain proteins, and their complementary fluorophore-tagged secondary antibodies, immunofluorescence may by used to visualise protein location and possible interactions within a cell through measuring the fluorescence of a single fluorophore and the degree of overlap between two or more fluorophores.

2.7 Immunohistochemistry

Paraffin-embedded tissue sections were obtained from the Division of Anatomical Pathology, University of Cape Town and this study was approved by and performed in accordance with the University of Cape Town Human Research Ethics Committee. Paraffin-embedded tumour tissues from surgical specimens (before chemotherapy) were cut in 5 µm-thick sections and placed on superfrost charged slides. The tissue sections were deparaffinised in three changes of xylol and hydrated through graded ethanol series (absolute ethanol – 96% ethanol – 70% ethanol – 50% ethanol). Antigen retrieval was performed with citric acid buffer at pH 6 for 90 seconds using a pressure cooker and cooled for an additional 30 minutes. Endogenous peroxidase was quenched by incubation in 3% methanol/H_2O_2 for 10 minutes. Tissue sections were blocked with 5% goat serum (X090710, Dako, Denmark) in PBS and incubated with rabbit polyclonal anti-TBX3 (1:25; Zymed, Invitrogen, Carlsbad, CA) overnight. Goat anti-rabbit Envision reagent (K400211, Dako, Denmark) was applied for 30 minutes. The chromogenic substrate was applied (1ml buffer + 1 drop DAB) for 10 minutes (K346711, Dako, Denmark). Slides were rinsed in water and counterstained with haematoxylin for 1 minute. Nuclei were stained with Scott's solution for 1 minute, rinsed in water and dehydrated in 2 baths of 70% alcohol, 2 baths 100%

alcohol, and 3 baths xylol. The slides were mounted with glass coverslips using Entellan. All slides were observed with light microscopy (Axiovert).

2.8 Immunoprecipitation assays

2.8.1 Flag Affinity Purification

Flag-Empty, Flag-mtbx3 or Flag-mtbx3+2a RD cells were grown in 15 cm dishes to 90% confluence and harvested in 1ml of lysis buffer (see **Appendix section 6.4**). Cells were incubated for 30 minutes on a shaker at 4°C, sonicated on ice for 3 x 30 seconds, with 10 second breaks in between, and cellular debris removed by centrifugation at 12 000 rpm for 10 minutes at 4°C. The supernatant was incubated with 40 µL of anti-Flag antibody conjugated to agarose beads pre-equilibrated in 1X TBS buffer (anti-Flag M2 affinity gel, A2220, Sigma) with constant rotation for overnight at 4°C. Following binding, protein-protein complexes were pelleted by centrifugation for 30 seconds at 6000 rpm and the supernatant removed with a syringe. Beads were washed three times with 0.5 ml of 1X TBS. After the final wash, the immune complexes were resuspended in 20 µl boiling blue loading buffer and boiled for 10 minutes at 100°C. Protein samples were analysed by SDS-PAGE and western blotting using antibodies to TBX3 (1:500) (ab99302, Abcam, USA), Flag (1:1000) (F3165, Sigma, USA) and nucleolin (1:1000) (sc-8031, Santa Cruz Biotechnology, Santa Cruz, CA) (**Figure 2.8**).

2.8.2 Immunoprecipitation assays

RD cells were grown in 15 cm dishes to 90% confluence and harvested in 1ml of 150 mM RIPA lysis buffer (see **Appendix section 6.4**). Cellular debris was removed by centrifugation at 12 000 rpm for 20 minutes at 4^{o}C. The supernatant of each sample was pre-cleared by incubating with 40 µl of protein A/G Sepharose beads (Santa Cruz Biotechnology, Santa Cruz, CA) and for 30 minutes at 4°C with rotation. Antibodies to Nucleolin, Hsc70, TBX3, Flag and a non-specific IgG (Santa Cruz Biotechnology, Santa Cruz, CA) were added to separate

lysates and incubated at 4°C with rotation overnight. The immune complexes were immunoprecipitated with 20 µl of protein A/G Sepharose beads at 4°C with rotation for 4 hours, washed in cold 1X PBS four times, boiled in 40 µl boiling blue loading buffer and protein samples were analysed by SDS-PAGE and western blotting using antibodies to nucleolin (1:1000) (sc-8031), Hsc70 (1:1000) (sc-7298, Santa Cruz Biotechnology, Santa Cruz, CA), TBX3 (1:1000) (ab99302, Abcam, USA) and Flag (1:1000) (F3165, Sigma, USA) (**Figure 2.8**).

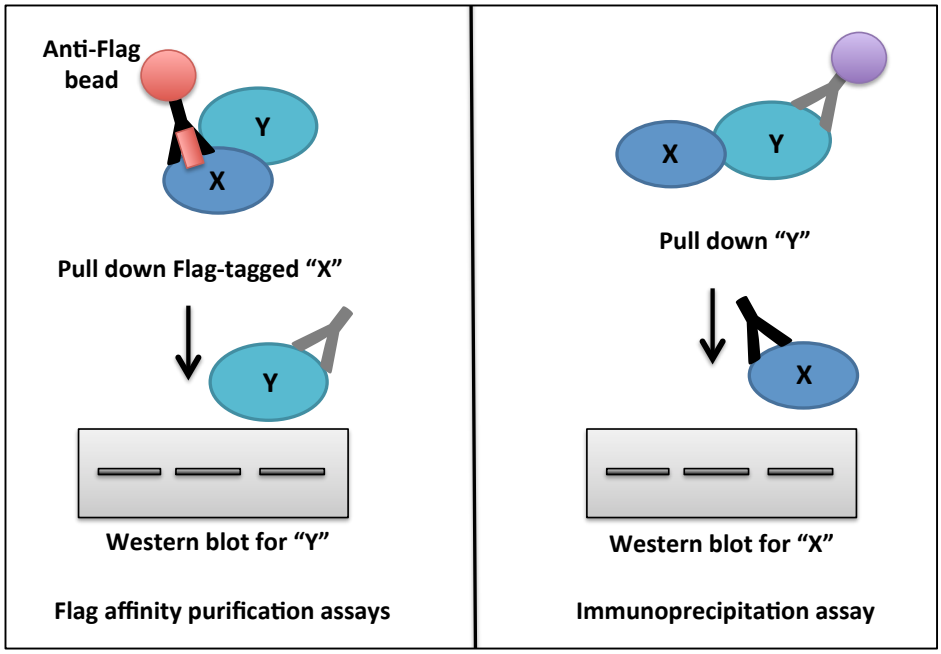

Figure 2.8: Flag affinity purification and immunoprecipitation assays. Immunoprecipitation assays aim to reveal protein-protein interactions through pulling down one protein, "Y", and then western blotting for its possible partner, "X" (right panel). A Flag affinity purification assay involves pulling down, or purifying and isolating, a Flag-tagged protein "X" and then, to determine if another protein of interest "Y" was bound to the Flag-tagged protein, a western blot is performed using an antibody against "Y" (left panel).

2.9 Statistical analyses

The Graphpad Prism 4 program was used to draw all graphs. Statistical analysis of data was performed using the 2-sample t-test (Microsoft Excel software) and $p<0.05$ (*) was considered statistically significant, $p<0.001$ (**) very significant and $p<0.0001$ (***) extremely significant.

Chapter 3. Results

Introduction

The overexpression of TBX3 has been linked to a growing list of carcinomas but whether this was true for sarcomas was only recently investigated in our laboratory. Indeed, the current study forms part of a larger study in the Prince laboratory that investigated the status, role and regulation of TBX3 in a range of sarcoma subtypes. Initial screening using qRT-PCR and western blotting revealed that, relative to normal cell lines, TBX3 is overexpressed at the mRNA and protein levels in cell lines representative of chondrosarcoma, fibrosarcoma, liposarcoma, synovial sarcoma and embryonal rhabdomyosarcoma (ERMS) (**Fig. 3.1A & B;** taken from Willmer *et al*., 2016). While two PhD students in the Prince laboratory followed up on the role of TBX3 overexpression in chondrosarcoma and fibrosarcoma, the current study investigated the role of TBX3 in ERMS. To this end, cell culture models in which TBX3 was stably knocked down, or further overexpressed, in the RD ERMS cell line were created and analyses conducted by performing a number of *in vitro* and *in vivo* transformation assays. Consistent with data obtained for chondrosarcoma, the results show that TBX3 contributes to several oncogenic processes including promoting cell proliferation, anchorage independent growth, cell migration and tumour formation. Furthermore, Tarryn Willmer, a previous PhD student in the laboratory, identified Hsc70 and nucleolin as TBX3 co-factors in chondrosarcoma and therefore the possibility that they also interact with TBX3 to mediate its oncogenic role in ERMS was investigated. Both, Hsc70 and nucleolin were shown to interact and co-localise with TBX3 in ERMS cells and nucleolin was shown to co-operate with TBX3 to drive ERMS cell proliferation and migration. Finally, preliminary identification of factors that upregulate TBX3 expression in ERMS was performed and c-Myc and AKT1 were implicated. Taken together, the findings from this study show that TBX3 is overexpressed in ERMS where it drives rhabdomyosarcomagenesis, suggesting that TBX3 may be considered as a biomarker and therapeutic target, along with its protein partners and upstream regulators, for more effective diagnosis and treatment of ERMS.

3.1 Screening TBX3 status in rhabdomyosarcoma tumour tissue

As mentioned earlier, TBX3 mRNA and protein were previously shown to be upregulated in a panel of soft tissue and bone sarcoma cell lines including the human ERMS cell line, RD (**Fig.3.1A & B**, taken from Willmer *et al*., 2016). To determine the status of TBX3 protein levels in archival patient-derived rhabdomyosarcoma tissue sections immunohistochemistry was performed. To exclude the possibility of artefactual staining, a negative control was included where sections were incubated with normal goat serum instead of TBX3 antibody and no stain was consistently observed (data not shown). Tissue from a 6-week old human embryo was used as a positive control as TBX3 is reported to be expressed in the sinus node and atrioventricular bundle (AVB) of the heart at this stage of development (Hoogaars *et al*., 2007; Hoogaars *et al*., 2004b). Indeed nuclear TBX3 staining was observed in these structures indicating that the TBX3 antibody is specific (**Fig.3.1C**). Compared to normal adjacent tissue (**Fig.3.1D**), TBX3 was upregulated in RMS and staining appeared to be nuclear (a representative figure is shown in **Fig.3.1E**).

3.2 Establishment and characterization of human embryonal rhabdomyosarcoma (ERMS) cell lines in which TBX3 was stably knocked down or overexpressed

According to Hanahan & Weinberg (2011) the 6 key hallmarks of cancer are: (1) constitutively active proliferative signaling, (2) evasion of growth suppressors, (3) resisting cell death, (4) replicative immortality, (5) inducing angiogenesis and (6) activation of invasion and metastasis. We hypothesized that knocking down TBX3 in ERMS may reverse, at the very least, some of these hallmarks whereas further overexpressing TBX3 may enhance the cancer phenotype. Therefore, this study investigated the consequences of either stably knocking down, using a short-hairpin RNA (shRNA) approach, or overexpressing TBX3 in RD cells on their cellular morphology, cell proliferation, anchorage independent growth and migration, and tumour formation in nude mice. Whereas the shRNA method

specifically target and degrade complementary mRNA, the expression vector used for overexpressing TBX3 result in co-option of a cellular host's protein synthesis machinery to overexpress the protein of interest.

Before cell culture models could be established RD cells were tested for the parasitic bacteria, mycoplasma, to ensure that only mycoplasma free cells were used for further analyses (data not shown). This is important because mycoplasma can have deleterious effects on their host cells, including affecting their signal transduction pathways and metabolism, promoting or inhibiting apoptosis, altering cell morphology, DNA, RNA and protein synthesis, and cell growth and even mediating cancerous transformation (Rottem *et al*., 2012).

The following constructs, already available in the laboratory, were used to establish the knock-down and overexpression cell culture models: the pSuper.neo/GFP containing a shTBX3 sequence targeting TBX3 (SHTBX3) or a scrambled control sequence (SHCTRL) and the pCMV expression vector containing the Flag-mtbx3, Flag-mtbx3+2a or Flag Empty control sequence. All these constructs carry the mammalian neomycin gene that confers resistance to the antibiotic G-418, a neomycin analogue, allowing a screening mechanism for successfully transfected cells. In order to determine the lowest dose of G-418 needed to kill untransfected RD cells an antibiotic titration assay, also known as a dose or kill curve, was performed. The optimal dose of G-418 required is that which kills all untransfected cells by day 10 and based on the data obtained 0.8 mg/ml of G-418 was used for drug selection and clonal expansion of the positively transfected RD cells (data not shown).

3.2.1 Establishment and characterization of human ERMS cell lines in which TBX3 was stably knocked down

To establish the TBX3 knock-down cell culture model RD cells were stably transfected with the SHTBX3 or SHCTRL constructs and forty-eight hours post transfection the cells were grown in the presence of G-418 (0.8 mg/ml) for a minimum of 10 days before drug resistant

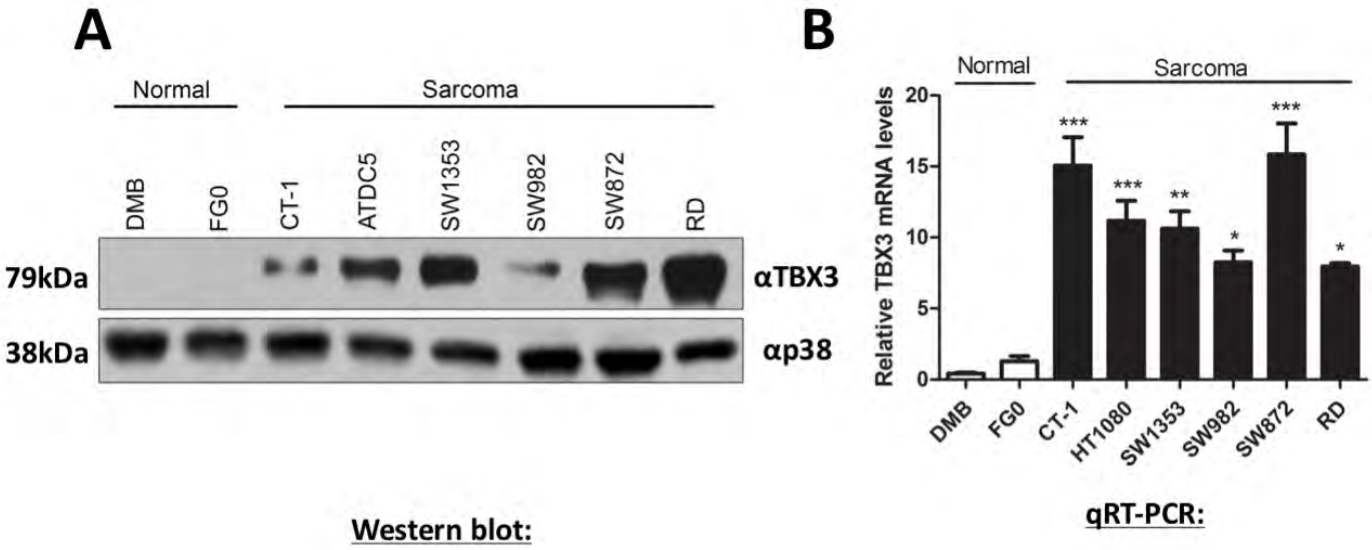

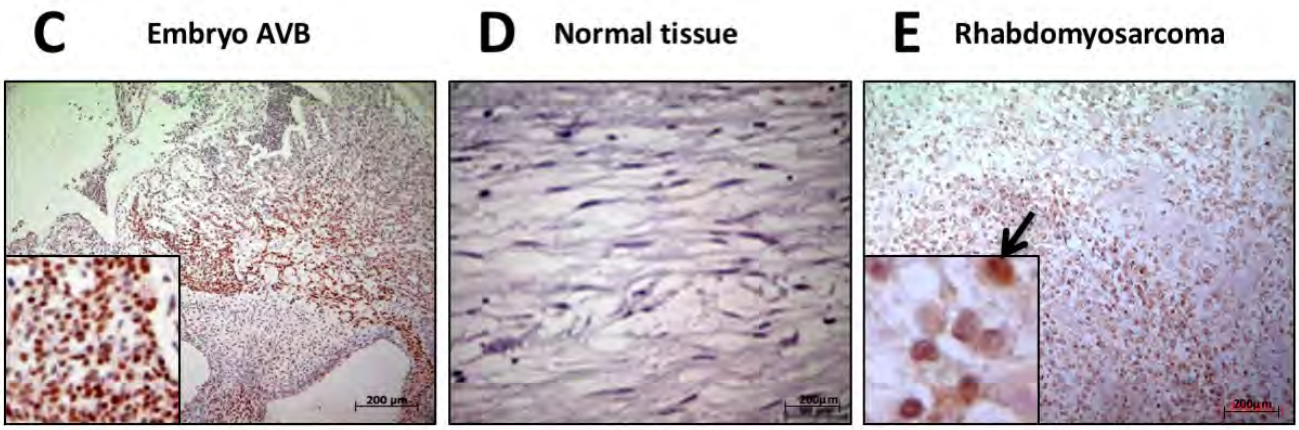

Figure 3.1: **Screening TBX3 status in a panel of sarcoma cell lines and tumour tissue.** ***(A)*** Protein extracts (30 µg) from DMB and FG0 human fibroblast, immortalised CT-1 fibroblast, HT1080 fibrosarcoma, ATDC5 and SW1353 chondrosarcoma, SW982 synovial sarcoma, SW872 liposarcoma and RD rhabdomyosarcoma cell lines were analysed by SDS-PAGE (8%) and western blotting using a rabbit polyclonal anti-TBX3 (1:1000) antibody. p38 was used as a loading control. (Taken from Wilmer *et al.*, 2016). ***(B)*** mRNA from the indicated cell lines were analysed by quantitative real-time PCR (qRT-PCR). qRT-PCR was performed on reverse transcribed RNA using primers specific to TBX3 and mRNA levels were normalised to GUSB relative to DMB cells (lowest expression of TBX3 mRNA levels). Two-way ANOVA was used to measure statistical significance, *p<0.05; **p<0.001; ***p<0.0001; error bars represent standard error of the mean. (Taken from Wilmer *et al.*, 2016). ***(C-E)*** Archival patient-derived rhabdomyosarcoma (N=3) tissue sections were immunohistochemically stained using an antibody specific to TBX3. ***(C)*** Tissue sections from a 6 week old embryo were included as a positive control, positive TBX3 staining is shown in the atrioventricular bundle (ABV). ***(D)*** Normal tissue with no TBX3 expression. ***(E)*** Brown nuclear TBX3 staining in RMS tumour tissue (indicated by black arrow). Representative images are shown (scale bars 200 µm; Insets are magnified images from selected areas).

clones were isolated and expanded into cell lines. The efficacy of the shRNA-mediated inhibition of TBX3 expression was monitored by western blotting and qRT-PCR and **Figures 3.2A & B** show the RD cell lines SHTBX3 (1) and SHTBX3 (2) in which TBX3 was effectively knocked down compared to the SHCTRL cells and which were used for further analyses.

3.2.1.1 Knocking down TBX3 has no effect on cell morphology in RD cells

Cell morphology can give clues to the cellular state of a cell line. For example, are the cells stressed or optimally growing, are the cells undergoing mitosis, apoptosis or autophagy or are the cells undergoing epithelial-to-mesenchymal transition? The microscopic images shown in **Figure 3.3** indicate that there were no notable differences in cell morphology seen across any of the cell lines when TBX3 was depleted. Indeed, throughout all experimental analyses, they displayed an elongated, bipolar and multipolar, spindle-shaped cell morphology characteristic of RD cells.

3.2.1.2 Knocking down TBX3 decreases proliferation in RD cells *in vitro*

One of the defining characteristics of cancer cells is their ability to bypass senescence and proliferate in a chronic, uncontrolled fashion. Therefore the next set of experiments investigated the effect of knocking down TBX3 on cell proliferation. Short-term cell proliferation was measured by the methylthiazol tetrazolium (MTT) assay, using mitochondrial activity as a proxy for cell viability and proliferation. In this assay the number of living cells present is related to their ability to reduce yellow tetrazolium salt into purple formazan crystal that is then measured by spectrophotometric absorbance. **Figure 3.4A** shows that over a 48-hour time period the proliferative ability of the SHCTRL and SHTBX3 cells was comparable.

The possibility was considered that while TBX3 may have no significant effect on cell proliferation over a 48-hour time course it may impact long-term cell proliferation. Growth curves were therefore performed in which cells were allowed to proliferate in medium supplemented with 10% fetal bovine serum (FBS) over a period of 9 days and counted every 2-3 days using a haemocytometer. **Figure 3.4B** shows a significant decrease in proliferative rates on days 7 and 9 for both SHTBX3 (1) and SHTBX3 (2) cell lines relative to SHCTRL cells. These results indicate that TBX3 expression contributes to the proliferative capacity of RD cells. The next set of experiments therefore determined the impact of TBX3 on the cell cycle profile of SHCTRL and SHTBX3 cell lines cultured in standard 10% FBS using fluorescence assisted cell sorting (FACS). The results show that the SHCTRL and SHTBX3 (1) cells exhibited a profile typical of dividing cells (**Fig.3.4C & D**). Interestingly, the SHTBX3 (2) cell line displayed an increased percentage of apoptotic and S-phase cells (**Fig.3.4E**) which provides support for previous studies showing that TBX3 promotes cancer cell survival through its ability to evade apoptosis (Renard *et al.*, 2007). In addition, the Prince laboratory has also recently reported that TBX3 may be required for cells to transit through S-phase and that this function may be linked to its role as a pro-proliferative factor (Willmer *et al*., 2015). It is worth noting that compared to the SHTBX3 (1) cell line the levels of TBX3 was always lower in the SHTBX3 (2) cell line and that it proliferated slower, albeit not statistically significant, suggesting that the impact of TBX3 on apoptosis and the cell cycle may be dose dependent but due to time constraints this was not further investigated.

Cancer cells often have reduced dependence on the levels of growth factors present in their environment. Therefore the ability of SHCTRL and SHTBX3 cells to proliferate in low serum (2% FBS) medium, compared to 10% FBS medium, was investigated. **Figure 3.4F** shows a significant decrease in proliferative rates of both SHTBX3 (1) and SHTBX3 (2) cell lines relative to SHCTRL on day 9. It is worth noting when comparing the graphs in **Figure 3.4B & F** that both the control and knock-down cells had decreased proliferative rates in the 2% versus the 10% FBS containing medium. These results suggest that the growth of RD cells is proportional to the levels of growth factors in their environment and that TBX3 does not contribute to growth factor independence. The western blots in **Figure 3.4A, B & F** confirmed that relative to the SHCTRL cells, TBX3 was knocked down in the SHTBX3 cell lines.

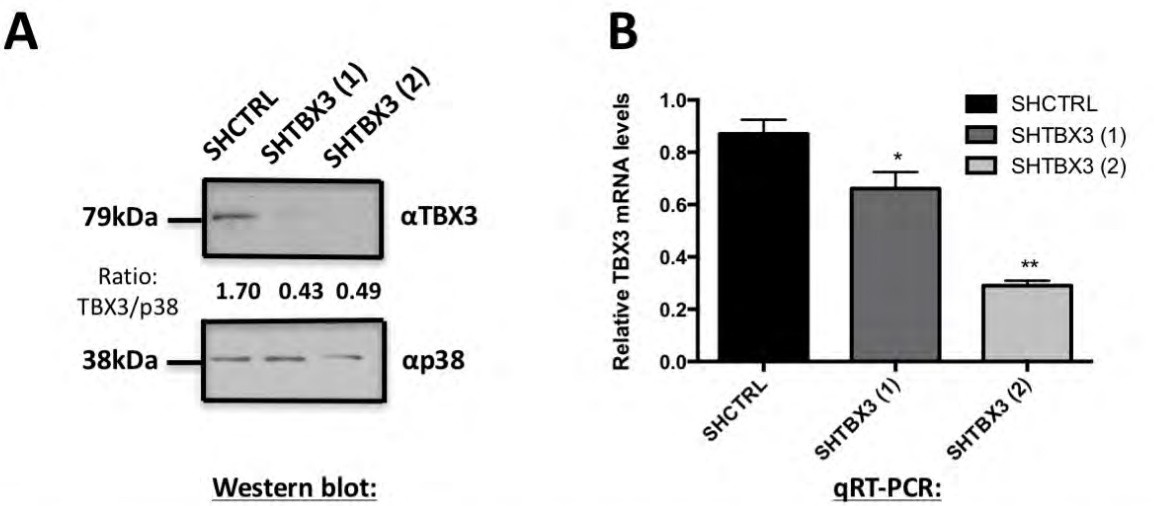

Figure 3.2. Establishment of ERMS cells in which TBX3 expression was stably knocked down. RD Cells were stably transfected with the pSuper.neo/GFP (Oligoengine) expression vector containing either a TBX3 specific shRNA sequence (SHTBX3) or a non-specific, scrambled control sequence (SHCTRL). ***(A)*** Western blot analysis of stable transfected RD cells showing TBX3 protein levels in SHCTRL, SHTBX3 (1) and SHTBX3 (2) cell lines. Protein was harvested from the indicated cell lines, analysed by SDS-PAGE (8%) and TBX3 was detected using rabbit polyclonal anti-TBX3 (Zymed or Abcam) antibody (1:500 or 1:1000) and a goat anti-rabbit secondary antibody (1:5000). p38 was used as a loading control. Densitometric values represent the expression of each protein band quantified using the UN-SCANT-IT gel 6.1 software and normalized to p38 levels. ***(B)*** Quantitative real-time PCR was performed on reverse transcribed RNA using primers specific to TBX3, mRNA levels were normalised to GUSB. Microsoft Excel student t-test was performed to calculate statistical significance *p<0.05; **p<0.001; ***p<0.0001. This figure shows pooled data from three independent experiments performed in duplicate and the error bars represent standard error of the mean.

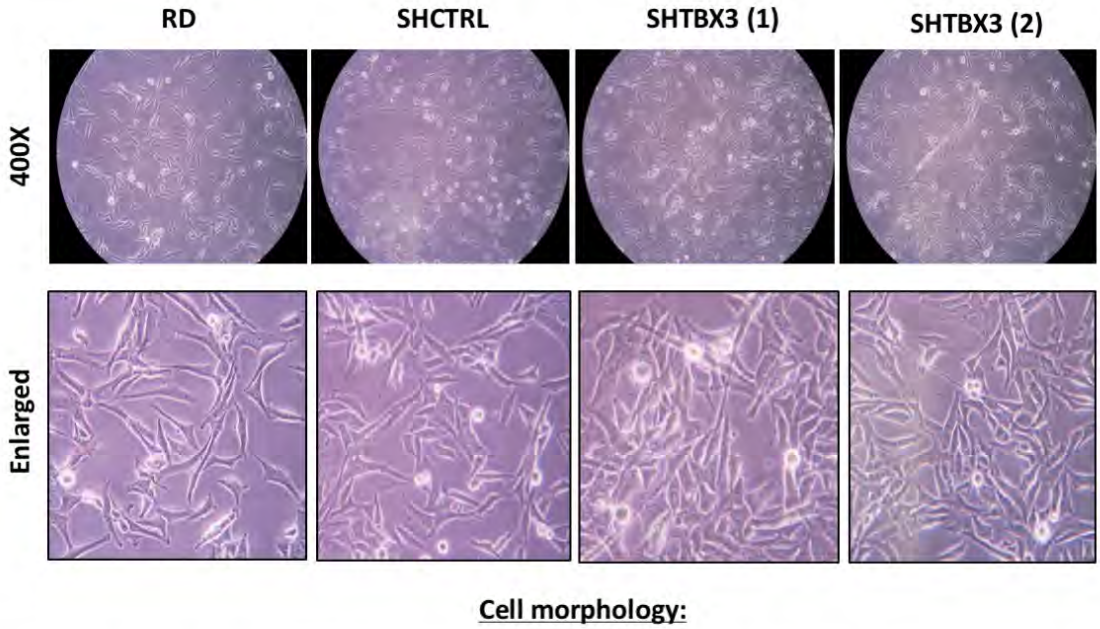

Figure 3.3: **Knocking down TBX3 has no effect on cell morphology in RD cells**. Representative phase contrast light microscopic images of the indicated cell lines photographed using a Canon camera (PowerShot S50). Microscopic images of cells were taken at 400X magnification ***(top panels)*** and further enlargements ***(bottom panels)*** of the above microscopic images are shown.

A

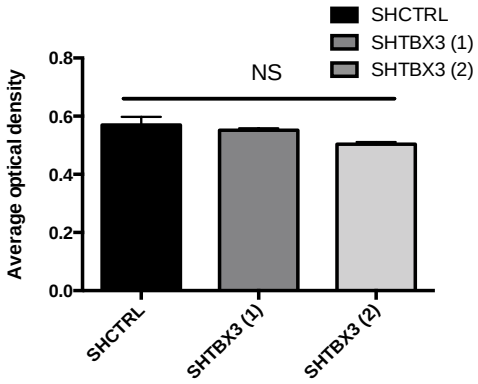

MTT assay:

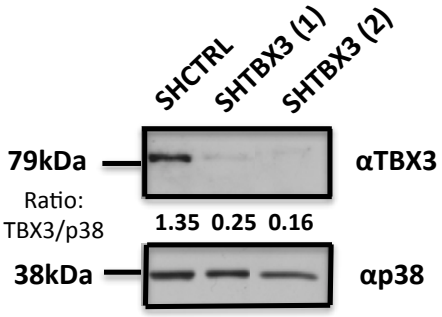

Western blot:

B

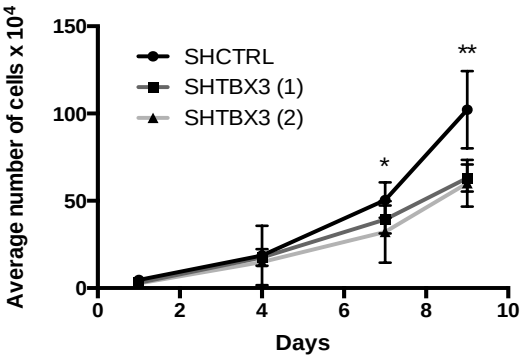

10% FBS Growth curve:

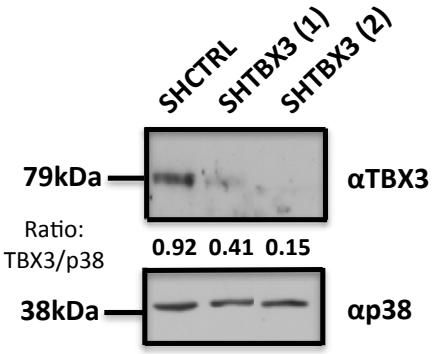

Western blot:

C

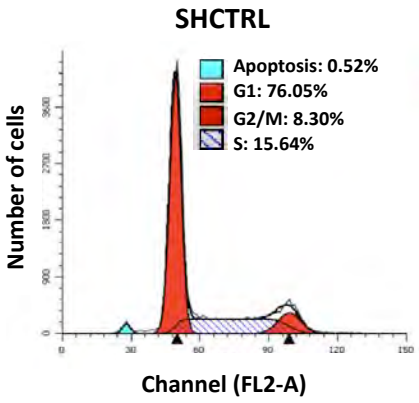

D

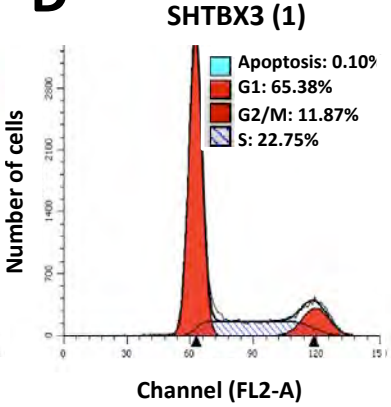

E

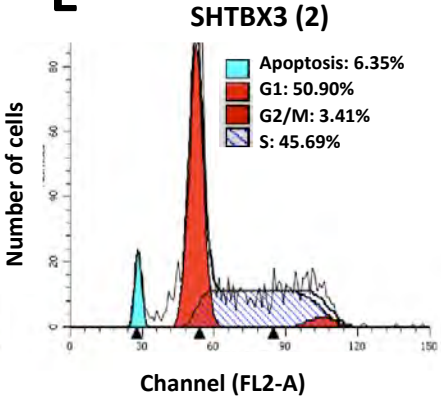

Fluorescence assisted cell sorting (FACS):

F

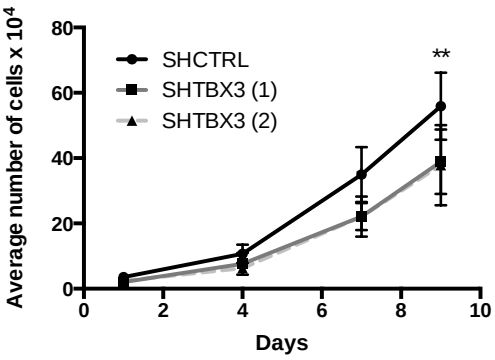

2% FBS Growth curve:

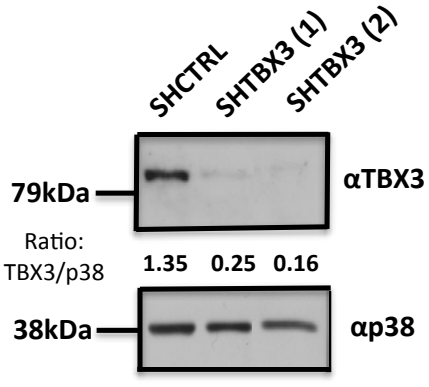

Western blot:

Figure 3.4: Knocking down TBX3 decreases the proliferation of RD cells *in vitro*. *(A) Left panel:* Short term cell viability was assessed by a methylthiazol tetrazolium (MTT) assay by plating RD SHTBX3 and SHCTRL cells in quadruplicate at a density of 6 x 10^3 cells per well of a 96-well plate and grown in media supplemented with 10% fetal bovine serum (FBS) for 48 hours. Following the addition of the MTT solution and solubilization buffer, absorbance (585 nm) was then determined by spectrophotometry. This figure shows pooled data from six independent experiments performed in quadruplicate and the error bars represent standard error of the mean. Microsoft Excel student t-test was performed to calculate statistical significance. ***(B & F) Left panels:*** Long term cell proliferation, and the effect of growth factors, was assessed by growing cells in 10% versus 2% FBS growth factor containing medium. Cells were plated in triplicate at a density of 1 x 10^4 cells per well of a 12-well plate and were grown in medium supplemented with either ***(B)*** 10% or ***(F)*** 2% FBS. Growth curve assays were performed over a 9-day period and cells were harvested by trypsinisation and counted on a haemocytometer. These figures show pooled data from three independent experiments performed in triplicate and the error bars represent standard error of the mean. Microsoft Excel student t-test was performed to calculate statistical significance *p<0.05; **p<0.001; ***p<0.0001). (***A, B & F) Right panels:*** Accompanying western blot analyses of protein prepared from indicated cells used to plate a MTT assay or from cells on day 9 day of the growth curves. Protein was analysed by SDS-PAGE (8%) and TBX3 was detected using rabbit polyclonal anti-TBX3 (Zymed or Abcam) antibody (1:500 or 1:1000) and a goat anti-rabbit secondary antibody (1:5000). p38 was used as a loading control. Densitometric values represent the expression of each protein band quantified using the UN-SCANT-IT gel 6.1 software and normalized to p38 levels. ***(C-E)*** Cell cycle distribution was determined by staining cells with propidium iodide and measuring their DNA content by fluorescence assisted cell sorting (FACS) analysis. Percentage of cells in each phase of the cell cycle are indicated.

3.2.1.3 Knocking down TBX3 decreases anchorage independent growth of RD cells *in vitro*

A key characteristic of cancer cells is the ability to proliferate independently of a substrate (anchor), which enables them to form tumours. To assess whether TBX3 impacts on this characteristic of RD cells, soft agar assays were performed. In this assay, anchorage independent cells will proliferate and form colonies in the soft agar, whereas anchorage dependent cells fail to do so. Briefly, RD cells were suspended in lower percentage soft agar/media slurry on top of a higher percentage agar/media base, and after 30 days the plates were stained with p-iodinitrotetrazolium chloride and the colonies visualized by microscopy. **Figure 3.5A (top panel)** shows microscopic images of stained SHCTRL and SHTBX3 cells at day 1 after plating. This was done to confirm that a comparable number of cells were plated at the start of the experiment. **Figure 3.5A (bottom panel) and B** show that when TBX3 was depleted, fewer RD cells were able to proliferate in the absence of a substrate and hence fewer colonies were observed for the SHTBX3 cells. **Figure 3.5C** shows a western blot confirming TBX3 knock-down in the cells plated for the soft agar assay shown

in **Figure 3.5A**. These results demonstrate that TBX3 promotes anchorage-independent growth of ERMS cells.

3.2.1.4 Knocking down TBX3 decreases migration of RD cells *in vitro*

In order for cancer cells to metastasize they must gain the ability to invade adjacent tissues and establish colonies at new locations (Hanahan & Weinberg, 2011). To investigate whether TBX3 impacts these later stages of tumourigenesis the migratory ability of the SHCTRL and SHTBX3 knock-down cell lines were compared using a two-dimensional *in vitro* cell motility assay. Briefly, cells were grown to confluence and then, using a pipette tip, a linear scratch was made through the cell monolayer. Mitomycin C, which prevents *de novo* cell proliferation, was added to exclude effects of cell proliferation on the results. Light microscopy images were taken at three-hour intervals from the time the scratch was made until the ninth hour. The area of the scratch was measured at each time point, thus the change in area over time indicated the area migrated. **Figure 3.6A** shows that the average area migrated was significantly reduced in both SHTBX3 (1) and SHTBX3 (2) knock-down cell lines at the 3, 6 and 9 hour time points tested. **Figure 3.6B** shows a representative western blot from the cells used in one of the cell motility assays, indicating knock-down of TBX3 in SHTBX3 (1) and SHTBX3 (2) cell lines. It is important to note that, as seen in the proliferation assays, the SHTBX3 (2) cells migrated significantly more slowly than the SHTBX3 (1) cells. This again suggests that the impact of TBX3 on the cancer phenotype is directly proportional to the levels of the protein because as mentioned earlier, TBX3 was consistently seen to be more effectively depleted in the SHTBX3 (2) cells. These results demonstrate that TBX3 promotes cell migration of ERMS cells.

3.2.1.5 The effect of knocking down TBX3 on tumour forming ability *in vivo*

While results from the above *in vitro* assays suggested that TBX3 promotes rhabdomyosarcomagenesis they are not necessarily reflective of what might occur *in vivo* because they do not recapitulate the tumour environment. The oncogenic role of TBX3 in

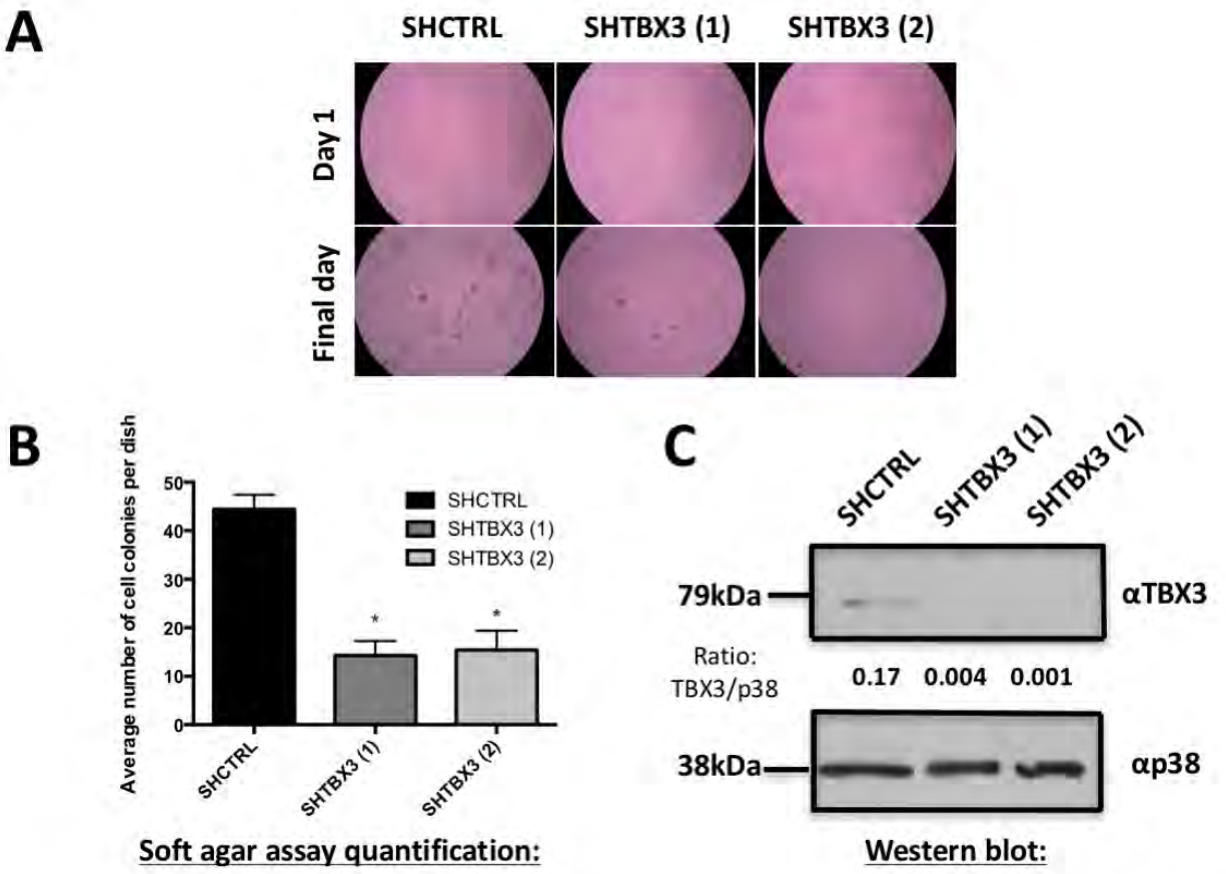

Figure 3.5: Knocking down TBX3 decreases anchorage independent growth of RD cells *in vitro*. *(A)* 3 x 10^5 cells were resuspended in 0.35% agar-medium slurry and plated on top of a 0.5% agar-medium layer and allowed to proliferate for 30 days. Cell growth was assessed by staining with p-iodinitrotetrazolium chloride to indicate viable populations. ***(Top panels)*** Microscopic images taken at 200X magnification shows plating of the indicated cell lines at day 1, ***(Bottom panels)*** microscopic images taken at 200X magnification on the final day of staining. ***(B)*** Quantification of soft agar assays with the average number of stained colonies counted per sample. This figure shows pooled results of three independent experiments each performed in triplicate, *p<0.05; **p<0.001; ***p<0.0001. ***(C)*** Western blot analysis of protein prepared from indicated cell lines used to plate the assays was analysed by SDS-PAGE (8%) and TBX3 was detected using rabbit polyclonal anti-TBX3 (Zymed) antibody (1:500) and a goat anti-rabbit secondary antibody (1:5000). p38 was used as a loading control. Densitometric values represent the expression of each protein band quantified using the UN-SCANT-IT gel 6.1 software and normalized to p38 levels.

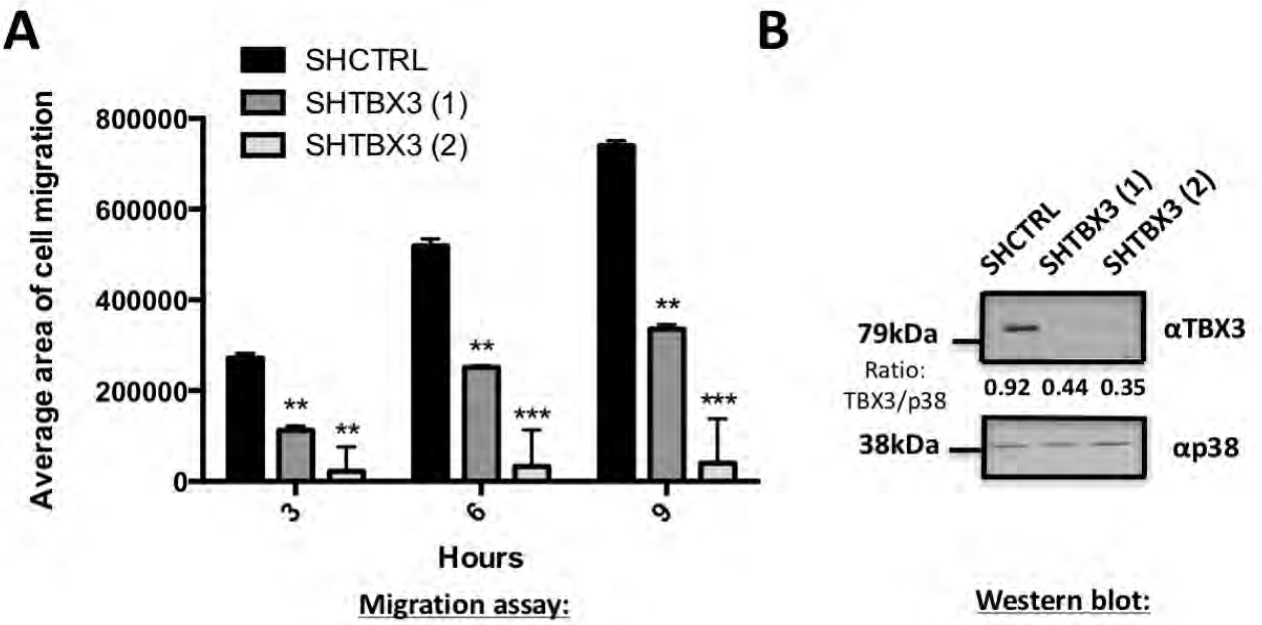

Figure 3.6. Knocking down TBX3 decreases migration of RD cells *in vitro*. *(A)* Migration was measured using a two-dimensional *in vitro* scratch motility assay. Cells were grown to confluence and a linear wound was made by scratching through the cell monolayer using a sterile 20 µl pipette tip. Mitomycin C (5 µg/ml) was added to prevent *de novo* cell proliferation and migration was measured at 3 hour intervals for 9 hours. Results are plotted as the average area migrated over time. A Microsoft Excel student t-test was performed to calculate statistical significance (*p<0.05; **p<0.001; ***p<0.0001). This figure shows pooled results of six independent experiments each performed in triplicate and the error bars represent standard error of the mean. ***(B)*** Western blot analysis of TBX3 protein levels in the indicated cell lines. Protein was harvested from migration assays and analysed by SDS-PAGE (8%). TBX3 levels were detected using rabbit polyclonal anti-TBX3 (Zymed) antibody (1:500) and a goat anti-rabbit secondary antibody (1:5000). p38 was used as a loading control. Densitometric values represent the expression of each protein band quantified using the UN-SCANT-IT gel 6.1 software and normalized to p38 levels.

ERMS was therefore tested in an *in vivo* mouse model involving MF-1 nude mice (nu/nu BALB/c, Charles River strain). These mice were used because they have a deteriorated or absent thymus making them immunocompromised and hence useful for homo- and hetero-transplants (xenografts) in cancer research (Pantelouris, 1968). Based on the conditions described in published reports where the tumour forming ability of RD cells were described, a pilot study was conducted using 3 x 10^6 RD cells injected subcutaneously into the right flank of 4-6 week old mice and tumour growth monitored *in situ* (Kourkalis *et al.*, 1999; Faggi *et al.,* 2014; Czifra *et al.*, 2015). However, after our experimental endpoint of 6 weeks

no tumours were observed and thus the SHTBX3 cells were not tested in these experiments. Reasons for why no tumours were observed are discussed in Chapter 4.

3.2.2 Establishment and characterisation of the ERMS cell culture model in which TBX3 was overexpressed

The TBX3 knock-down cell culture model established and characterised in this study suggests that TBX3 may promote rhabdomyosarcomagenesis when it is overexpressed. It was therefore hypothesised that further increasing the levels of TBX3 in RD cells would result in a more aggressive cancer phenotype. As there is some controversy in the literature as to whether the TBX3 and TBX3+2a isoforms have distinct or redundant functions, this study also aimed to determine if both isoforms could promote the oncogenic phenotype of RD cells. To this end, Flag-tagged mouse (m)tbx3 and mtbx3+2a isoforms, that share 98% amino acid sequence identity with their human counterparts (Bamshad *et al*., 1997), were stably transfected in the RD cells. Transfectants were selected for with G-418 (0.8 mg/ml) and successful overexpression of Flag-mtbx3 and Flag-mtbx3+2a protein and mRNA, compared to the control cell line, was confirmed using western blotting and qRT-PCR respectively (**Fig.3.7**).

3.2.2.1 Overexpression of Flag-mtbx3 and Flag-mtbx3+2a has no effect on cell morphology but promotes cell proliferation of RD cells *in vitro*

The next experiments explored the impact of Flag-mtbx3 and Flag-mtbx3+2a on the morphology and proliferative ability of RD cells. In support of the knock-down data, while overexpressing either TBX3 isoforms has no effect on RD cell morphology (**Fig.3.8A**), overexpression of either Flag-mtbx3 or Flag-mtbx3+2a significantly increased the proliferative ability of RD cells at days 4 and 7 (**Fig.3.8B**). The accompanying western blot confirms overexpression of Flag-mtbx3 and Flag-mtbx3+2a (**Fig.3.8B**). Interestingly, the

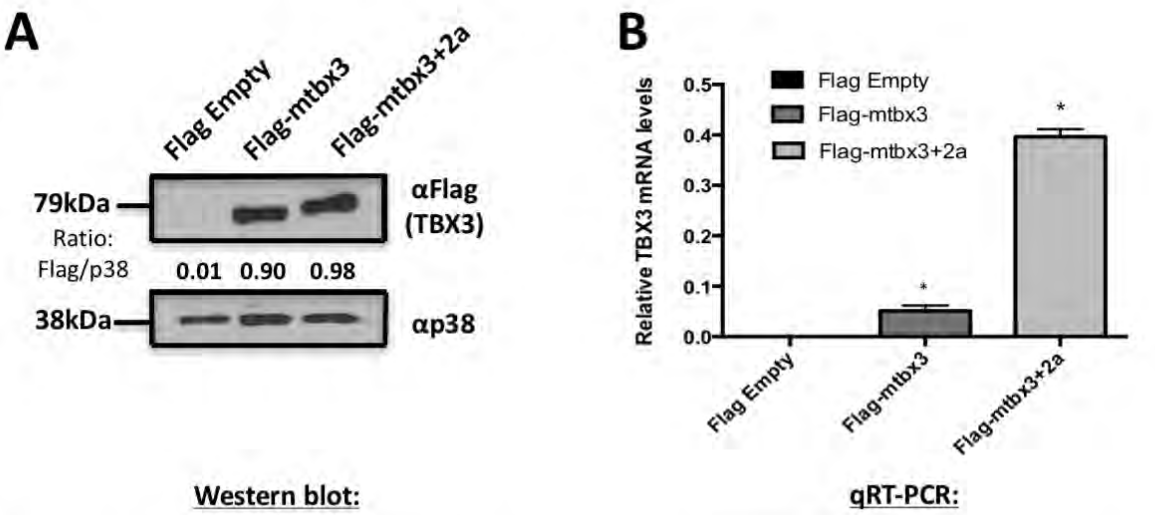

Figure 3.7. Establishment of the ERMS cell culture model in which Flag-mtbx3 and Flag-mtbx3+2a was overexpressed. RD cells were stably transfected with either 3XFLAGpCMV-Empty, 3XFLAGpCMV-mtbx3 or 3XFLAGpCMV-mtbx3+2a. ***(A)*** Protein was harvested from the indicated cell lines, analysed by SDS-PAGE (8%) and Flag-tagged TBX3 was detected using a mouse monoclonal Flag M2 (Sigma) (1:1000) antibody and a a goat anti-mouse secondary antibody (1:5000). p38 was used as a loading control. Densitometric values represent the expression of each protein band quantified using the UN-SCANT-IT gel 6.1 software and normalized to p38 levels. ***(B)*** Quantitative real-time PCR was performed on reverse transcribed RNA using primers specific to mtbx3, mRNA levels were normalised to GUSB relative to the Flag Empty mRNA. Microsoft Excel student t-test was performed to calculate statistical significance (*p<0.05; **p<0.001; ***p<0.0001). This figure shows three independent experiments each in duplicate and the error bars represent standard error of the mean.

mtbx3+2a cells always appeared to be proliferating faster than the mtbx3 cells, albeit not statistically significant. Whether this is a dose effect, because the mtbx3+2a isoform was consistently expressed at higher levels, or whether it is related to structural differences in the two proteins is unclear. Together these results demonstrate that Flag-mtbx3 and Flag-mtbx3+2a promotes cell proliferation in RD cells.

3.2.2.2 Overexpression of Flag-mtbx3 and Flag-mtbx3+2a promotes anchorage independent growth and migration of RD cells *in vitro*

To determine whether Flag-mtbx3 and Flag-mtbx3+2a are able to promote anchorage-independent growth and migration of RD cells, soft agar and cell motility assays were performed respectively. Interestingly, the overexpression of both isoforms enhanced the

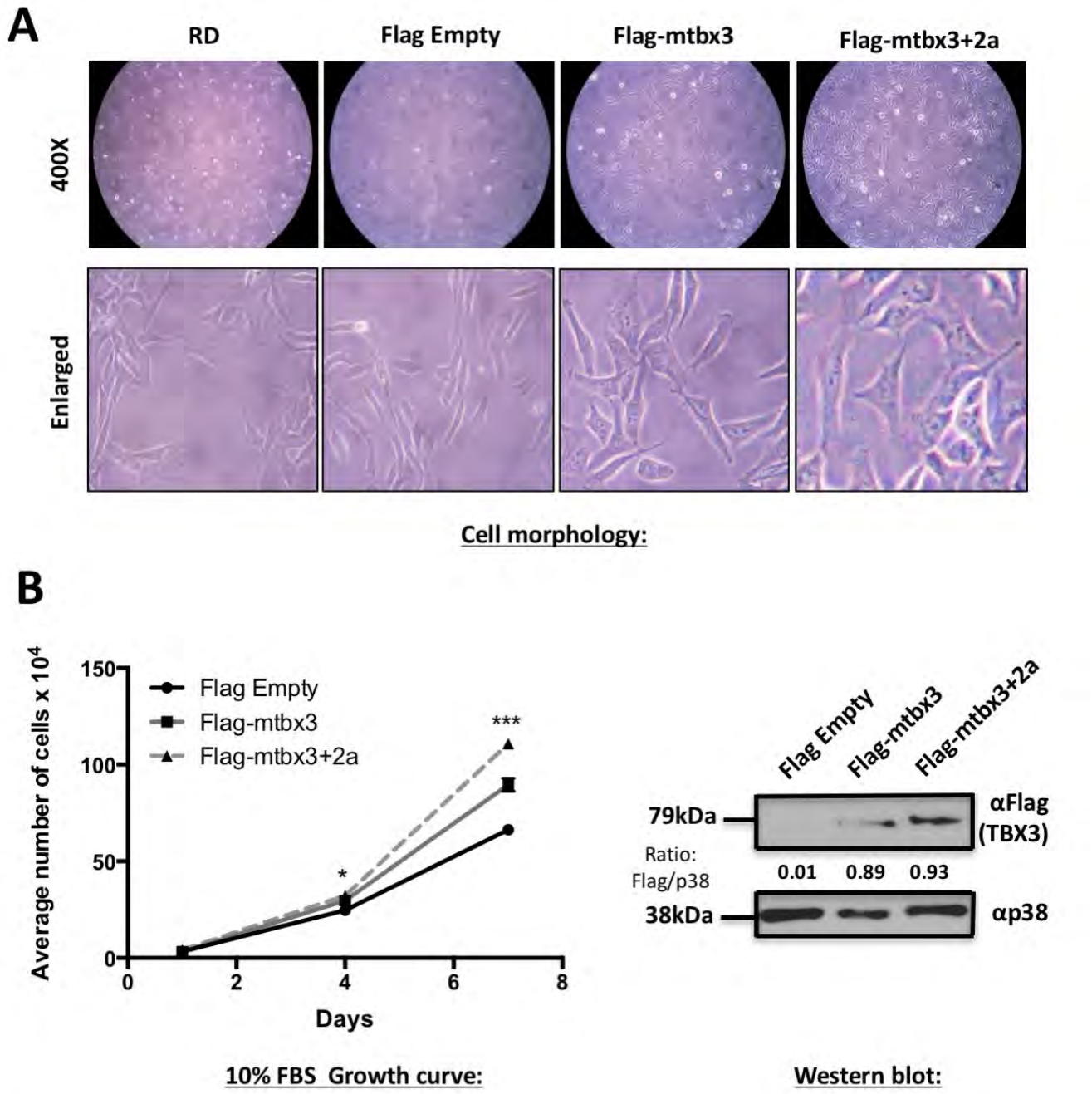

Figure 3.8: **Overexpression of Flag-mtbx3 and Flag-mtbx3+2a has no effect on cell morphology but promotes cell proliferation of RD cells *in vitro*. *(A)*** Representative phase contrast light microscopic images of the indicated cell lines using a Canon camera (PowerShot S50). Microscopic images of cells at 400X magnification ***(top panels)*** and ***(bottom panels)*** further enlargement of the above microscopic images are shown. ***(B)*** Long term cell proliferation was assessed by growing cells in 10% FBS growth factor containing medium (***left panel***). Cells were plated in triplicate at a density of 1 x 10^4 cells per well of a 12-well plate. Growth curve assays were performed over a 7-day period. Cells were harvested by trypsinisation and counted on a haemocytometer. This figure shows pooled results of two independent experiments each performed in triplicate and the error bars represent standard error of the mean. Microsoft Excel student t-test was performed to calculate statistical significance (*p<0.05; **p<0.001; ***p<0.0001). Accompanying western blot analyses ***(right panel)*** of protein prepared from on day 9 day of the growth curves. Protein was analysed by SDS-PAGE (8%) and Flag-tagged TBX3 was detected using mouse monoclonal M2 Flag antibody (1:1000) and a goat anti-mouse secondary antibody (1:5000). Densitometric values represent the expression of each protein band quantified using the UN-SCANT-IT gel 6.1 software and normalized to p38 levels.

ability of RD cells to proliferate independent of a substrate (**Fig.3.9A & B**) and migrate (**Fig.3.9C**) but only the results obtained for the Flag-mtbx3+2a were significant. As mentioned earlier, this may be as a result of a dosage sensitivity response since the Flag-mtbx3+2a cell line consistently expressed slightly higher levels of TBX3, as shown in the accompanying western blots (**Fig.3.9B & C**).

3.2.2.3 The effect of Flag-mtbx3+2a overexpression on tumour formation of RD cells *in vivo*

The above results suggested that, statistically, Flag-mtbx3+2a had a greater impact on rhabdomyosarcomagenesis and therefore the effect of overexpressing this isoform on RD tumour forming ability in nude mice was tested. Based on the results from our pilot study described in the knock-down cell culture model (see section 3.2.1.5), 1 x 10^7 (instead of 3 x 10^6) Flag Empty and Flag-mtbx3+2a RD cells were injected subcutaneously into the right flanks of 4-6 week old MF-1 nude mice and tumour growth monitored over a period of 6 weeks. Whereas the mice injected with Flag-mtbx3+2a cells developed tumours as early as 4 weeks (**Fig.3.10A**), tumours were only visible after 5 weeks in mice injected with the RD Flag Empty tumour cells (**Fig.3.10B**). These results suggested that, consistent with the *in vitro* assays, TBX3 promotes the cancer phenotype of RD cells. Quite unexpectedly, when the tumours were excised and weighed at the 6 week end point, the Flag Empty tumours weighed significantly more than the Flag-mtbx3+2a tumours (**Fig.3.10C**). Furthermore, it was noted that whereas tumours from mice injected with the Flag Empty cells had a long and flattened appearance, tumours from mice injected with the Flag-mtbx3+2a cells were more spherical or rod shaped in appearance (**Fig.3.10D**). Tumours were then processed for histopathological analysis and tumour sections stained with haematoxylin and eosin (H&E) and examined by a pathologist, Professor Dhiren Govender (**Fig.3.11**). All tumour sections displayed general pleomorphic morphology, with cells differing in shape and size. Importantly, morphological distinctions were observed between the Flag Empty and Flag-mtbx3+2a tumour sections: the Flag Empty tumour tissue sections displayed cells with

A

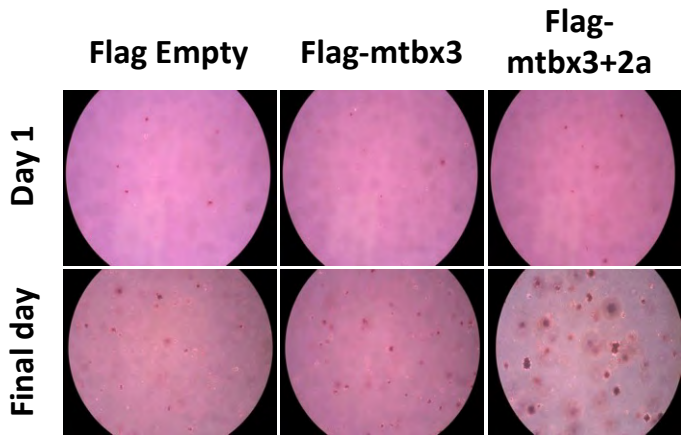

B

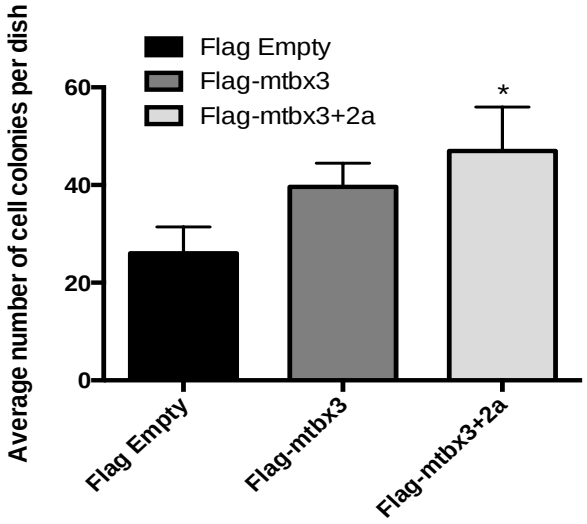

Soft agar assay quantification:

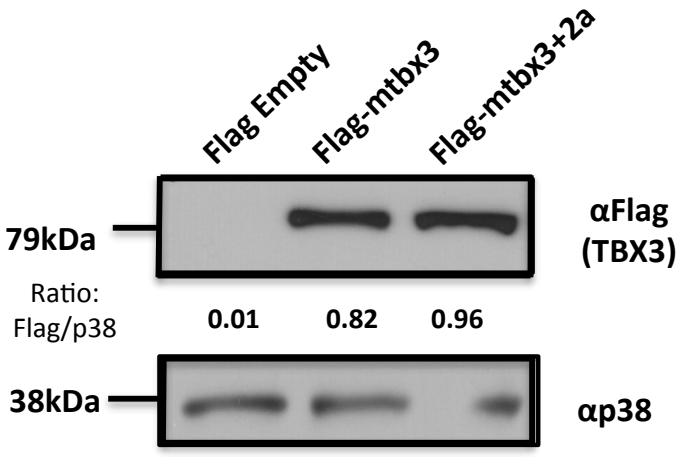

Western blot:

C

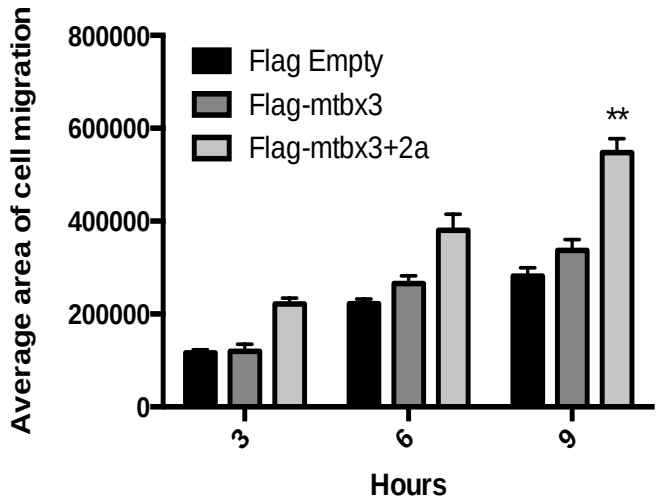

Migration assay:

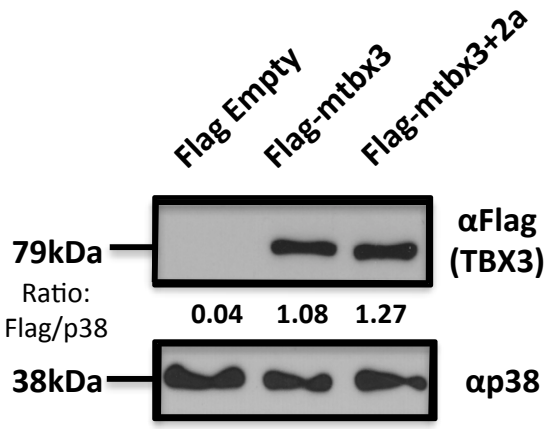

Western blot:

Figure 3.9: Overexpression of Flag-mtbx3 and Flag-mtbx3+2a promotes anchorage independent growth and migration of RD cells *in vitro*. *(A)* 3 x 10^5 cells were resuspended in 0.35% agar-medium slurry and plated on top of a 0.5% agar-medium layer and allowed to proliferate for 14 days. Cell growth was assessed by staining with p-iodinitrotetrazolium chloride to indicate viable populations. Microscopic images taken at 200X magnification shows plating in the Flag Empty, Flag-mtbx3 and Flag-mtbx3+2a cell lines at day 1 and microscopic images taken at 200X magnification on the final day of staining. ***(B)*** Quantification of soft agar assays with the average number of stained colonies counted per sample. This figure shows pooled results of three independent experiments each performed in triplicate and the error bars represent standard error of the mean. A Microsoft Excel student t-test was performed to calculate statistical significance (*p<0.05; **p<0.001; ***p<0.0001). ***(C)*** Migration was measured using a two-dimensional *in vitro* scratch motility assay (***left panel***). Cells were grown to confluence and a linear wound was made by scratching through the cell monolayer using a sterile 20 µl pipette tip. Mitomycin C (5 µg/ml) was added to prevent *de novo* cell proliferation and migration measured at 3 hour intervals for 9 hours. A Microsoft Excel student t-test was performed to calculate statistical significance (*p<0.05; **p<0.001; ***p<0.0001). This figure shows pooled results of six independent experiments each performed in triplicate and the error bars represent standard error of the mean. Western blot analyses of protein prepared from indicated cell lines used to plate the assays was analysed by SDS-PAGE (8%) and Flag-tagged TBX3 was detected using mouse monoclonal Flag M2 (Sigma) (1:1000) and a goat anti-mouse secondary antibody (1:5000). p38 was used as a loading control. Densitometric values represent the expression of each protein band quantified using the UN-SCANT-IT gel 6.1 software and normalized to p38 levels.

a classic diffuse round polygonal shape arranged in a sheet (**Fig.3.11A-D**) whereas the Flag-mtbx3+2a tumour tissue sections displayed predominant fascicular cell growth, in which round and spindle-shaped cells appear to grow in cords of differing polarities (**Fig.3.11E-H**). In brief, the Flag-mtbx3+2a cells had morphology more typical of migratory cells. Interestingly, sections of the Flag Empty tumours displayed more mitotic cells (8-12 counts compared to 2-3 counts per high powered field of view, data not shown). While both Flag Empty and Flag-mtbx3+2a tumour cells appeared capable of invading surrounding skeletal muscle, the Flag-mtbx3+2a cells appeared to do this more aggressively (**Fig.3.11C-F**). This was deduced by observations that whereas the Flag Empty cells had only just begun to invade skeletal muscle (found at the edge of the tumour), Flag-mtbx3+2a cells had moved through skeletal muscle (found inside the tumour) and adipose tissue (**Fig.3.11G & H**). Please note that the histopathology described above was as reported by the pathologist, Professor Dhiren Govender.

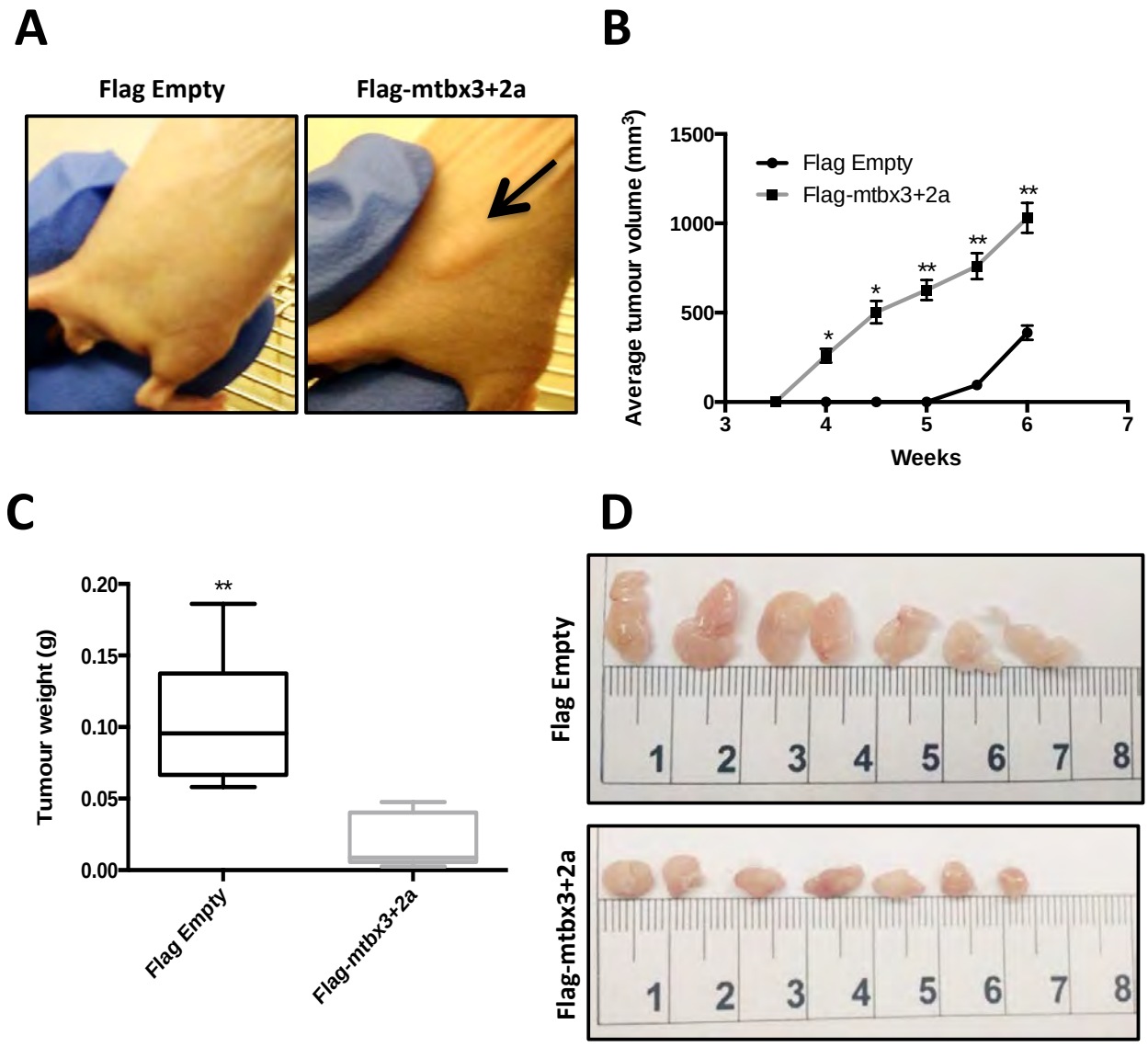

Figure 3.10. The effect of Flag-mtbx3+2a overexpression on tumour formation of RD cells *in vivo*. *(A)* *In vivo* tumour formation was assayed by subcutaneously injecting $1x10^7$ RD Flag Empty and Flag-mbx3+2a cells into 4-6 week-old athymic nude mice (N=7 each). Mice were photographed at week 4 once visible tumour formation occurred (indicated by the black arrow). ***(B)*** *In situ* tumour volume (mm^3) was measured over the 6 week period using callipers, average tumour volume plotted per group, error bars represent standard deviation. ***(C & D)*** Mice were euthanised after 6 weeks and the tumours removed and ***(C)*** average tumour weight (g) was measured, error bars represent standard deviation, and ***(D)*** tumours photographed. ***(B & C)*** A Microsoft Excel student t-test was performed to calculate statistical significance (*p<0.05, **p<0.001).

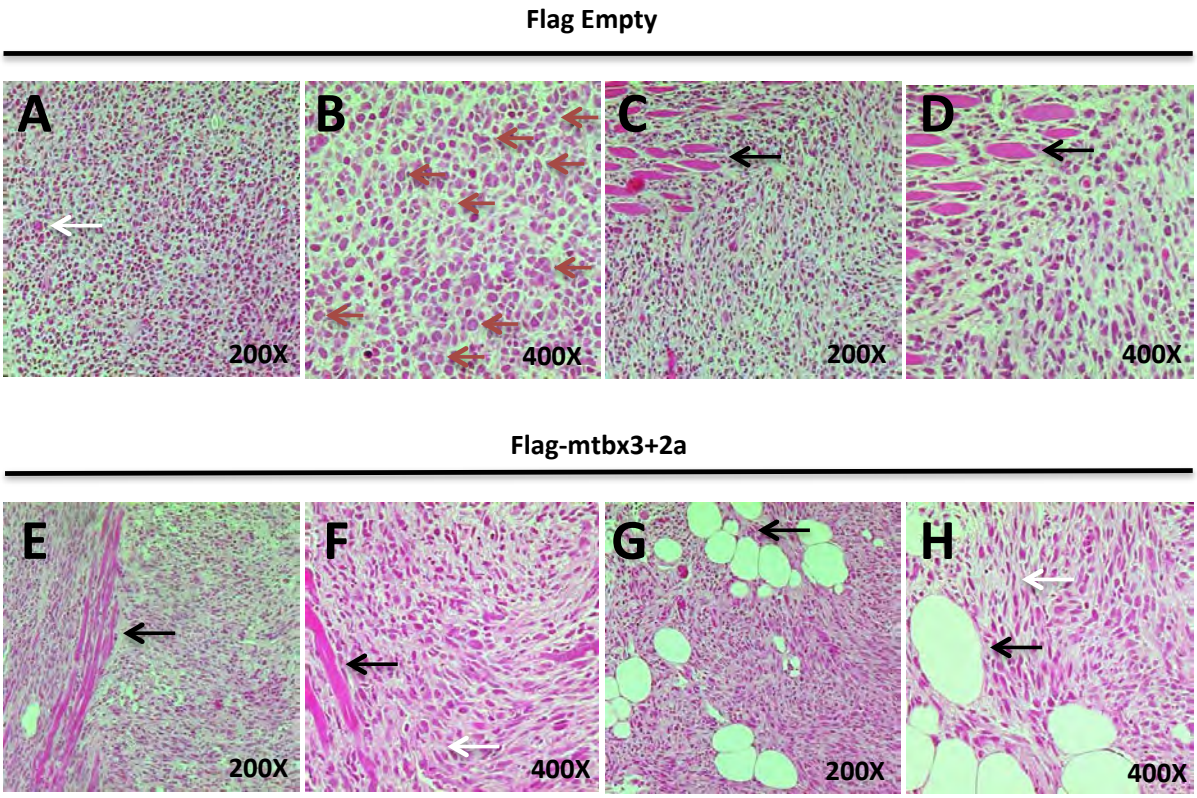

Figure 3.11. H&E histopathology of RD Flag Empty and Flag-mtbx3+2a tumour tissues. *In vivo* tumour formation was assayed by subcutaneously injecting 1x10^7 RD Flag Empty and Flag-mtbx3+2a cells into 4-6 week-old nude mice (N=7 each). Mice were euthanised after 6 weeks and the tumours removed and processed with haematoxylin and eosin (H&E) staining for histopathological analysis. Representative phase contrast light microscopic images of the indicated cell lines photographed using a Canon camera (PowerShot S50). Microscopic images of cells were taken at 200X and 400X magnification. ***(A-D)*** Flag Empty tumour tissue sections with classic diffuse round polygonal cells, tumour giant cells (***A***, white arrow), mitotic cells (***B***, red arrows) and invasion into skeletal muscle (***C & D***, black arrows). ***(E-H)*** Flag-mtbx3+2a tumour tissue sections with predominant fascicular growth of round and spindle-shaped cells (***F & H***, white arrows) and invasion into skeletal muscle (***E & F***, black arrows) and adipose tissue (***G & H***, black arrows).

3.3 Characterization of TBX3 protein partners in RD cells

In order to gain a better mechanistic understanding of the role of TBX3 in sarcomagenesis, a previous PhD student in the Prince laboratory, Dr Willmer, performed mass spectrometry and identified several putative TBX3 co-factors in chondrosarcoma. Of these she went on to validate Hsc70 and nucleolin as *bona fide* TBX3 co-factors and further demonstrated that whereas Hsc70 plays a critical role in stabilizing the TBX3 protein, nucleolin was required for TBX3's ability to promote proliferation and migration (unpublished data). Importantly, western blot analyses performed by Dr Willmer revealed that the diverse panel of sarcoma

cell lines, including the RD cell line, shown to overexpress TBX3 also overexpressed nucleolin and Hsc70 (unpublished data). It was therefore of interest to determine if TBX3 also interacts with Hsc70 and nucleolin in ERMS with similar effects as seen in chondrosarcomas.

3.3.1 Nucleolin binds and co-localises with TBX3 in RD cells *in vivo*

Nucleolin is a ubiquitous, highly conserved, multifunctional phosphoprotein that is traditionally known for its roles in ribosome biogenesis (Srivastava *et al*., 1989; Tuteja & Tuteja, 1998; Ginisty *et al.*, 1999). While it is most abundant in the nucleolus, it is also present in other nuclear regions as well as in the cytoplasm and on the cell membrane (Borer *et al*., 1989; Ginisty *et al.*, 1999; Tuteja & Tuteja, 1998). It is therefore not surprising that nucleolin has also been implicated in DNA metabolism, DNA replication, recombination and repair, apoptosis, telomere maintenance, chromatin remodeling, histone chaperoning, nucleo-cytoplasmic transport and shuttling, mRNA stability, centriole and microtubule organization, cytokinesis, cell adhesion and cell signaling (reviewed in Abdelmohsen & Gorospe, 2012). Aberrant expression of nucleolin has been associated with a wide range of cancers including breast, lung, gastric, cervical and colorectal cancers, chronic lymphocytic leukaemia, hepatocellular carcinoma, renal cell carcinoma, non-small cell lung carcinoma, melanoma and paediatric intracranial ependymoma, and it has been connected with cancer initiation, progression, tumour aggressiveness, drug resistance and poor prognosis (Pichiorri *et al.*, 2013; Bates *et al*., 2009; Fu *et al*., 2005; Grinstein *et al*., 2006; Hovanessian *et al*., 2010; Guo *et al.*, 2014; Qiu *et al*., 2013; Tulchin *et al*., 2010; Zhao *et al*., 2013; Li *et al.*, 2014; Ridley *et al.*, 2008; Fujiki *et al*., 2014; Palmieria *et al*., 2015).

It was hypothesized that, similar to the data obtained in chondrosarcomas, TBX3 and nucleolin may interact and co-operate to promote the proliferation and migration of RD cells. To test this, immunoprecipitation assays were firstly performed to establish whether TBX3 and nucleolin do indeed interact. Briefly, Flag-mtbx3 or Flag-mtbx3+2a was immunoprecipitated from RD cells stably overexpressing either one of these isoforms using anti-Flag agarose beads. Immune complexes were then analysed by western blotting using antibodies against Flag, TBX3 and nucleolin. Results with antibodies to either Flag or TBX3

confirmed that TBX3 was only in the immune complexes from cells overexpressing either Flag-mtbx3 or Flag-mtbx3+2a and not Flag Empty cells (**Fig.3.12A)**. Importantly, results from the western blots probed with an antibody to nucleolin confirmed that nucleolin was in the immune complexes with TBX3 (**Fig.3.12A)**. These results confirm that TBX3 and nucleolin do indeed interact in RD cells.

To further validate the TBX3-nucleolin interaction, RD cells were processed for immunocytochemistry with antibodies to nucleolin and TBX3 and the cells visualized by confocal microscopy. **Figure 3.12B & C** show co-localisation as indicated by white pixels in the merged image of nucleolin (green channel) and TBX3 (red channel) within nuclei of cells and in particular within structures assumed to be nucleoli. Hoechst staining was performed to visualize nuclei (blue channel) and, as negative controls, the primary antibodies were excluded and cells were incubated with only secondary antibodies used to detect TBX3 and nucleolin (data not shown). The co-localisation between TBX3 and nucleolin was quantified using Zen (Carl Zeiss) imaging software. **Figure 3.12D** shows a representative two-dimensional scatter plot of the staining intensities of nucleolin (quadrant 1, bottom right), TBX3 (quadrant 2, top left) and the overlap between the TBX3 and nucleolin (quadrant 3, top right). The coincidence of nucleolin and TBX3 co-localising was quantified with Pearson's (PCC) and Manders' (MCC) correlation coefficients, as well as weighted co-localisation coefficients (WCC). The PCC value defines the overall correlation between two channels as a value between -1 and 1, where a value of 1 represents perfect co-localisation and a value of -1 represents perfect exclusion. MCC values range between 0 and 1, where a value of 1 represents high co-localisation and 0 represents low co-localisation. Importantly, these values are determined independently for each channel thereby measuring the proportion of TBX3 co-localising with nucleolin and visa versa. WCC values range from 0 to 1 where a value of 0 indicates random staining and a value of 1 indicates dependent staining. **Figure 3.13E** summarises the results of PCC, MCC and WCC calculated from 20 random fields of view. The MCC values report low co-localisation of total TBX3 with nucleolin (MCC = 0.04), which is expected as the area and subcellular locations of TBX3 expression is more widespread/ubiquitous than that of nucleolin, and high co-localisation of total nucleolin with TBX3 (MCC = 0.99) in what appears to be the nucleolus. Similarly the WCC values for TBX3 and nucleolin, 0.06 and 0.93 respectively, show that low levels of TBX3 expression co-

localise with very high levels of nucleolin expression. Importantly, the PCC value is 0.65 which is close to 1 and therefore suggests co-localisation between TBX3 and nucleolin indicating possible interaction between these two proteins. In the future, co-localisation should be measured within the nucleus only, as opposed to the whole cell, as we expect the TBX3/nucleolin interaction to occur largely within the nucleus, and this may therefore improve the co-localisation co-efficient values for TBX3.

3.3.2 Nucleolin and TBX3 co-operate to promote cell proliferation and migration in RD cells

To investigate the functional significance of the TBX3 and nucleolin interaction, the impact of nucleolin on RD cell proliferation and migration was first established. **Figure 3.13A (left panel)** and **3.13B (left panel)** show that transiently knocking down nucleolin inhibits RD cell proliferation and migration respectively. Western blots confirm that nucleolin was successfully knocked down in these experiments **(Fig.3.13A & B)**. Consistent with the above data, results from experiments where nucleolin was transiently overexpressed show that like TBX3, nucleolin also promotes RD cell proliferation and migration (**Fig. 3.13C & D**). The next set of experiments was performed to investigate whether knocking down or overexpressing nucleolin could influence the ability of TBX3 to promote proliferation or migration. Firstly, nucleolin was transiently silenced in Flag Empty and Flag-mtbx3+2a cells using siRNA and the effect on cell proliferation measured using a growth curve assay. Please note that, instead of the Flag-mtbx3 cells, the Flag-mtbx3+2a cells were used for these experiments because they proliferated and migrated significantly faster than control cells. **Figure 3.14A** confirms the overexpression of Flag-mtbx3+2a and the efficacy of the siRNA to nucleolin in this experiment. Consistent with previous observations in this study, compared with Flag Empty + siCTRL cells, Flag-mtbx3+2a + siCTRL cells had enhanced proliferative ability and Flag Empty + siNucleolin cells proliferated significantly slower (**Fig.3.14B**). Importantly, depleting nucleolin in Flag-mtbx3+2a overexpressing cells (Flag-mtbx3+2a + siNucleolin) significantly abrogated the positive effect of TBX3 on proliferation. These results suggested that TBX3 promotes proliferation in part by co-operating with nucleolin.

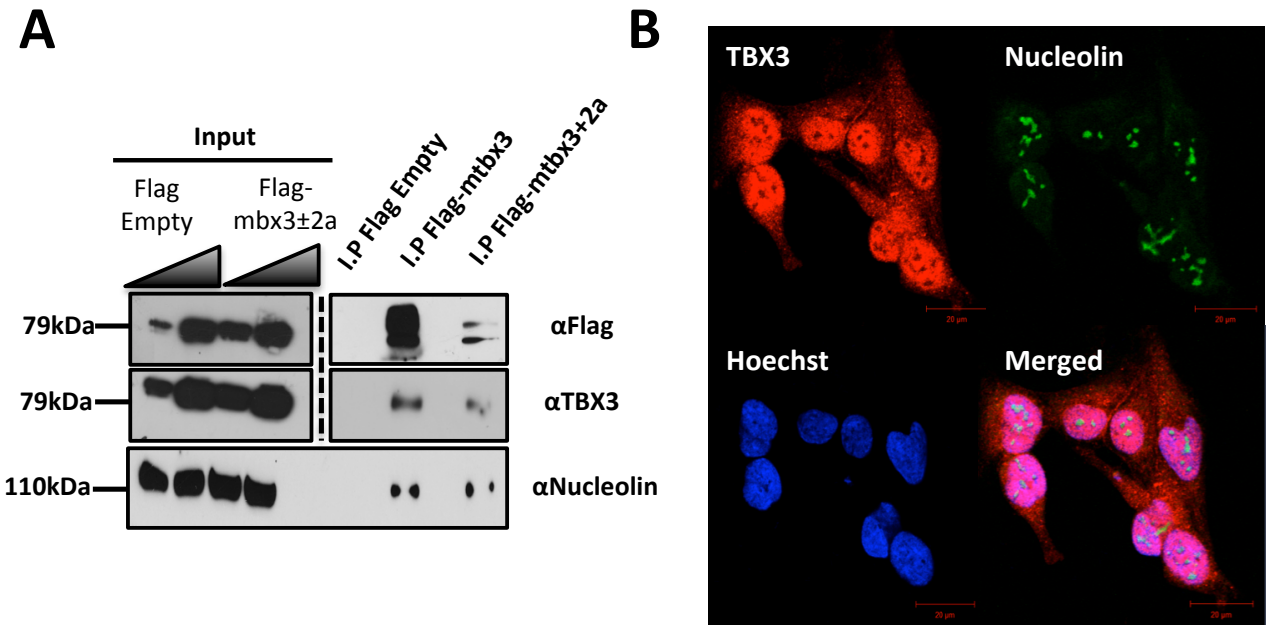

Immunoprecipitation: Flag (TBX3) **immunocytochemistry:**

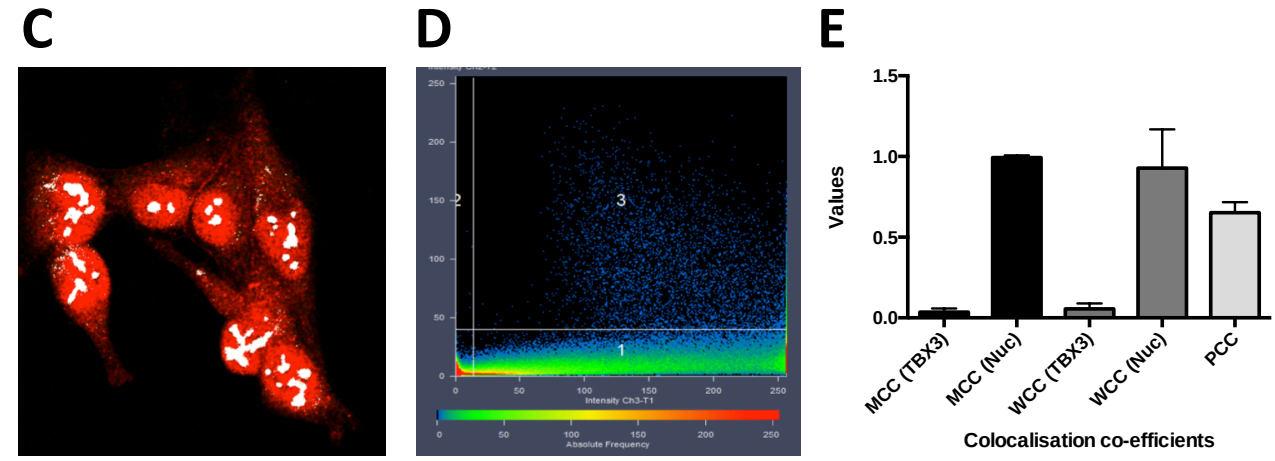

Co-localization analysis:

Figure 3.12. Nucleolin binds and co-localises with TBX3 in RD cells *in vivo*. ***(A)*** Protein extracts from RD cells were immunoprecipitated using an anti-Flag antibody, pulling down Flag-tagged TBX3 and protein partners bound to it. Purified immune complexes were subjected to western blot analysis with antibodies to mouse monoclonal Flag M2 (Sigma) (1:1000), rabbit polyclonal TBX3 (1:1000), mouse polyclonal nucleolin (1:1000) and secondary A/G protein (1:5000). ***(B)*** RD cells were plated on coverslips and processed for immunofluorescence with antibodies specific to TBX3 (Cy3; red channel) and nucleolin (Alexa 488; green channel) and visualised by confocal microscopy. Representative images are shown at 400X magnification. All cells were co-stained with Hoechst to determine the location of the nuclei. ***(C)*** Merged image from co-localisation analysis with white pixels indicating TBX3 and nucleolin co-localisation. ***(D)*** Representative scatter plot of TBX3 and nucleolin co-localisation in RD cells. Images from ***(C)*** were analysed by Zeiss software where the signal intensity of each channel is shown as a 2D graph. ***(E)*** Co-localisation of TBX3 and nucleolin was quantified using Mander's, Weighted and Pearson's coefficients using Zeiss software. Data is presented as the mean ± SEM of 20 fields of view.

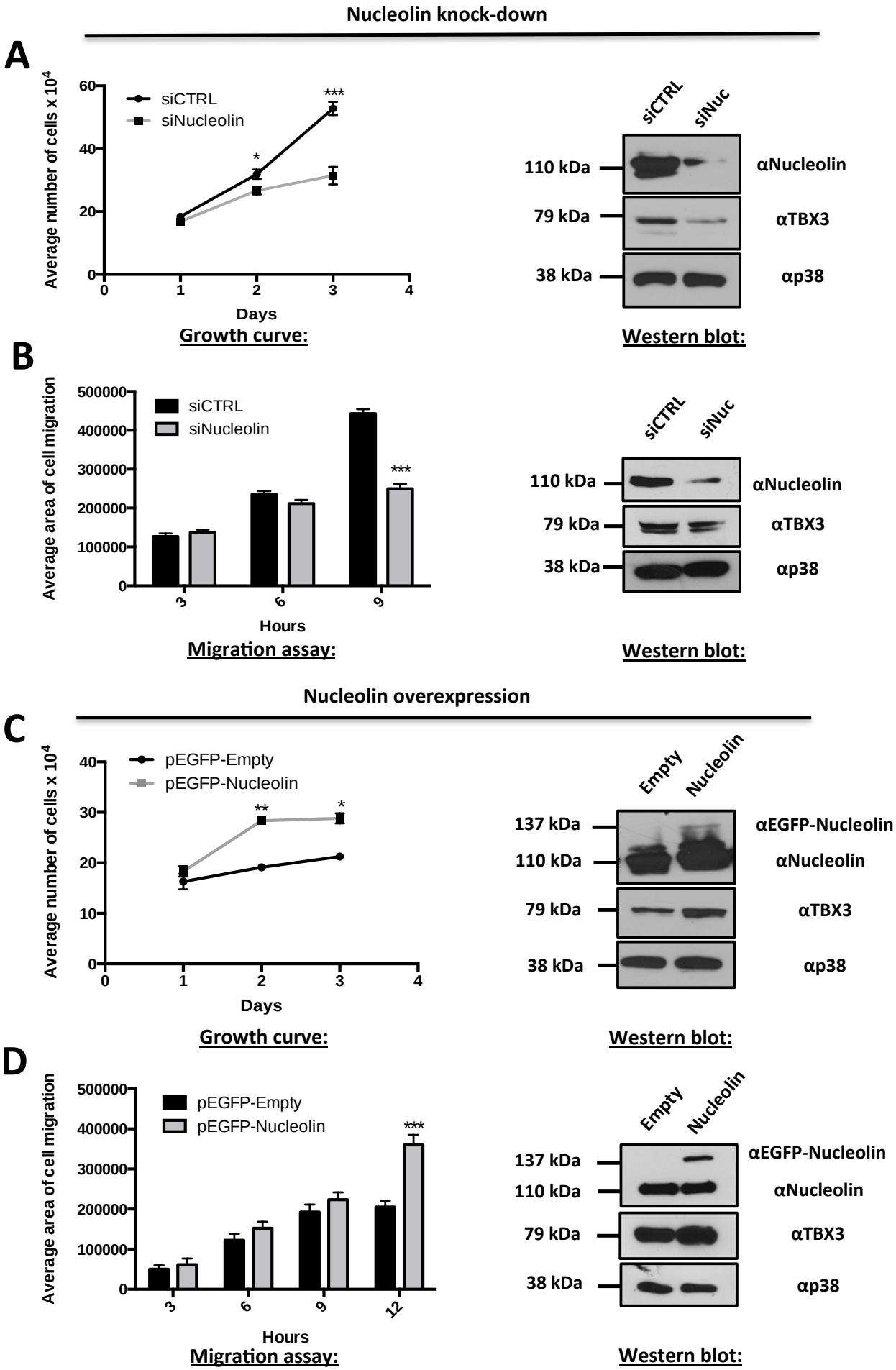
Nucleolin knock-down
A
Average number of cells x 10^4
siCTRL
siNucleolin
Days
Growth curve:
siCTRL
siNuc
110 kDa
79 kDa
38 kDa
αNucleolin
αTBX3
αp38
Western blot:
B
Average area of cell migration
siCTRL
siNucleolin
Hours
Migration assay:
Western blot:
Nucleolin overexpression
C
Average number of cells x 10^4
pEGFP-Empty
pEGFP-Nucleolin
Days
Growth curve:
Empty
Nucleolin
137 kDa
110 kDa
79 kDa
38 kDa
αEGFP-Nucleolin
αNucleolin
αTBX3
αp38
Western blot:
D
Average area of cell migration
pEGFP-Empty
pEGFP-Nucleolin
Hours
Migration assay:
Western blot:

Figure 3.13. Nucleolin promotes proliferative and migratory ability of RD cells *in vitro*. Nucleolin was transiently knocked down ***(A & B)*** or overexpressed ***(C & D)*** in RD cells. ***(A & C)*** Cell proliferation was assessed by growing cells in 10% fetal bovine serum (FBS) growth factor containing medium. Cells were plated in triplicate at a density of 3 x 10^4 cells per well of a 12-well plate. Growth curve assays were performed over a 3-day period. Cells were harvested by trypsinisation and counted on a haemocytometer. ***(B & D)*** Migration was measured using a *in vitro* two-dimensional cell motility assay. Cells were grown to confluence and a linear wound was made by scratching through the cell monolayer using a sterile 20 µl pipette tip. Mitomycin C (5 µg/ml) was added to prevent *de novo* cell proliferation. Migration measured at 3 hour intervals for 9 or 12 hours. A Microsoft Excel student t-test was performed to calculate statistical significance (*p<0.05, **p<0.001, ***p<0.0001); error bar represent standard error of the mean. Pooled results representative of two independent experiments each performed in triplicate. ***(A-D, right panels)*** Western blot analyses of Nucleolin and TBX3 protein levels in indicated transiently transfected RD cells. Protein was harvested from growth curve and migration assays and analysed via SDS-PAGE (8%). Protein levels were quantified using antibodies to rabbit polyclonal TBX3 (1:500), mouse polyclonal Nucleolin (1:1000), rabbit polyclonal p38 (1:2000) and a goat anti-rabbit or goat-anti-mouse secondary antibody (1:5000). p38 was used as a loading control.

To confirm these findings, nucleolin was ectopically overexpressed using a pEGFP-nucleolin construct in RD SHCTRL and SHTBX3 cells and growth curve assays performed. Western blotting confirmed the overexpression of nucleolin and the knock-down of TBX3 in these experiments (**Fig. 3.14C**). As anticipated, overexpressing nucleolin could not rescue the effect of silencing TBX3 on cell proliferation (**Fig. 3.14D**). If anything, in the absence of TBX3, the overexpression of nucleolin appeared to be cytotoxic and killed the cells from day 3 (data not shown). To determine whether TBX3 and nucleolin co-operate to promote cell migration, the same experimental conditions as described above were used and scratch motility assays were performed. Results showed that TBX3 and nucleolin both positively impact on cell migration and partly require each other to do this (**Fig. 3.14E & F**).

3.3.3 Heat shock cognate 70 (Hsc70) binds and co-localises with TBX3 in RD cells *in vivo*

Hsc70 belongs to the heat shock protein (Hsp) 70 family of molecular chaperones which plays an important role in maintaining protein homeostasis through (1) protecting the folding of proteins during translation, refolding misfolded or denatured proteins and keeping them in an unfolded or folding-competent state if needed, (2) transporting proteins

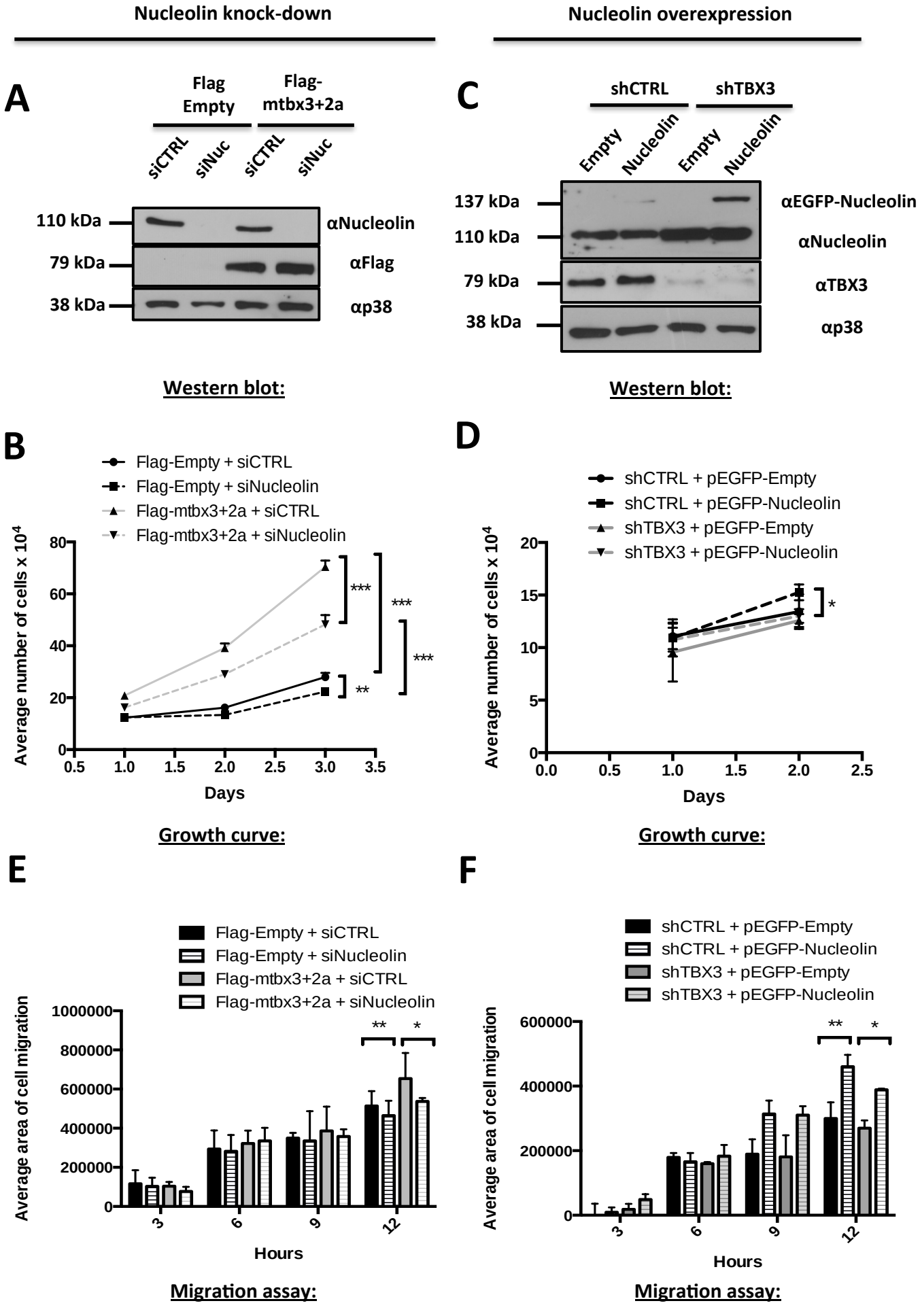
Nucleolin knock-down
Nucleolin overexpression
A
Flag Empty
Flag-mtbx3+2a
siCTRL
siNuc
siCTRL
siNuc
110 kDa
79 kDa
38 kDa
αNucleolin
αFlag
αp38
Western blot:
C
shCTRL
shTBX3
Empty
Nucleolin
Empty
Nucleolin
137 kDa
110 kDa
79 kDa
38 kDa
αEGFP-Nucleolin
αNucleolin
αTBX3
αp38
Western blot:
B
Flag-Empty + siCTRL
Flag-Empty + siNucleolin
Flag-mtbx3+2a + siCTRL
Flag-mtbx3+2a + siNucleolin
Average number of cells x 10^4
Days
***
***
***
**
Growth curve:
D
shCTRL + pEGFP-Empty
shCTRL + pEGFP-Nucleolin
shTBX3 + pEGFP-Empty
shTBX3 + pEGFP-Nucleolin
Average number of cells x 10^4
Days
*
Growth curve:
E
Flag-Empty + siCTRL
Flag-Empty + siNucleolin
Flag-mtbx3+2a + siCTRL
Flag-mtbx3+2a + siNucleolin
Average area of cell migration
Hours
**
*
Migration assay:
F
shCTRL + pEGFP-Empty
shCTRL + pEGFP-Nucleolin
shTBX3 + pEGFP-Empty
shTBX3 + pEGFP-Nucleolin
Average area of cell migration
Hours
**
*
Migration assay:

Figure 3.14. Nucleolin and TBX3 co-operate to promote RD cell proliferation and migration *in vitro.* ***(A, B, E)*** RD Flag-Empty and Flag-mtbx3+2a were plated in triplicate in 24-well plates and left to adhere overnight. Cells were transiently transfected with 50nM siCTRL or siNucleolin. Overexpression of Flag-tagged TBX3 and knock-down of nucleolin was confirmed via western blotting. ***(C, D, F)*** RD shCTRL and shTBX3 cells were plated in triplicate in 24-well plates and left to adhere overnight. Cells were transiently transfected with pEGFP-Nucleolin or pEGFP-Empty. TBX3 knock-down and nucleolin overexpression were confirmed via western blotting. ***(A & C)*** Protein was harvested from the indicated cell lines and analyzed by SDS-PAGE (8%) using antibodies to mouse monoclonal M2 Flag (1:1000), rabbit polyclonal TBX3 (1:1000), mouse polyclonal Nucleolin (1:1000), rabbit polyclonal p38 (1:2000) and a goat anti-rabbit or goat-anti-mouse secondary antibody (1:5000). p38 was used as a loading control. ***(B & D)*** Growth curve assays were performed over a 3-day period and cells harvested by trypsinisation and counted using a haemocytometer. ***(E & F)*** Migration assays were performed 48 hours after the transfection in which a linear wound was made by scratching through the monolayer using a sterile 20 µl pipette tip. Mitomycin C (5 µg/ml) was added to prevent *de novo* cell proliferation. Migration was measured at 3 hour intervals for 12 hours. ***(B - F)*** A Microsoft Excel student t-test was performed to calculate statistical significance (*p<0.05, **p<0.001, ***p<0.0001). This figure represents pooled results representative of two independent experiments each performed in triplicate, error bar represent standard error of the mean.

within cells and organelles, (3) chaperone-mediated autophagy, (4) preventing an accumulation of proteotoxic protein aggregates and (5) uncoating clathrin-coated vesicles (reviewed in Mayer & Bukau, 2005; Murphy, 2013; Lui *et al.*, 2012 and Liao & Tang, 2014). Members of the Hsp70 family have also been implicated in oncogenesis and of importance to this study are observations that Hsc70 is overexpressed in several cancers and was recently shown to stabilize oncoproteins (Tanaka *et al.*, 2014). Importantly, the Prince laboratory recently found that Hsc70 stabilises TBX3 in chondrosarcomas (unpublished data) and this study was interested to determine if Hsc70 interacts with TBX3 in a similar manner in ERMS. To this end, immunoprecipitation assays were performed using both Flag-mtbx3 and Flag-mtbx3+2a overexpressing cells and anti-Flag agarose beads. Immune complexes were then analysed by western blotting using antibodies against Flag, TBX3 and Hsc70. **Figure 3.15A** shows that the Flag agarose beads did indeed immunoprecipitate the Flag-mtbx3 and Flag-mtbx3+2a proteins and that Hsc70 is in complex with both these TBX3 isoforms.

In light of the above results, immunocytochemistry and confocal microscopy were performed to determine if TBX3 (red channel) and Hsc70 (green channel) co-localise and therefore possibly interact in RD cells. It is important to note that both TBX3 and Hsc70 expression levels and nuclear localization peak in S-phase (Willmer *et al.*, 2015; Milarski &

Morimoto, 1987) and that initial findings in asynchronous cells revealed weak cytoplasmic staining for Hsc70. Therefore to enrich for possible TBX3:Hsc70 co-localisation and interaction, RD cells were subjected to a double-thymidine S-phase block as described by Willmer *et al*. (2015), prior to being processed for immunocytochemistry. The merged images in **Figure 3.15B & C** suggest that TBX3 and Hsc70 do indeed co-localise in the nuclei of S-phase cells. Importantly, MCC, WCC and PCC values for TBX3/Hsc70 range from 0.69-0.81 i.e. are close to 1 indicating strong co-localisation (**Fig. 3.15D & E**). Importantly, as we expect the TBX3/Hsc70 interaction to occur within the nucleus, measuring co-localisation in the nucleus only, and not the entire cell as reported here, could improve the co-localisation co-efficient values.

3.4 Signaling molecules that upregulate TBX3 expression in RD cells

Given the above data showing that the overexpression of TBX3 is a key driver of ERMS, the impact of c-Myc and AKT on TBX3 levels was next explored. These signaling molecules were selected because they have been implicated in promoting sarcomagenesis (Wan & Helman, 2003; Ridzewski, 2015) and reported to be active in RMS (Kouraklis *et al.*, 1999; Marampon *et al.*, 2006; Wan & Helman, 2003; Ridzewski, 2015). In addition, work done in the Prince laboratory found that the diverse panel of sarcoma cell lines, including the RD cell line, shown to overexpress TBX3 also overexpressed c-Myc and had activated AKT (unpublished data).

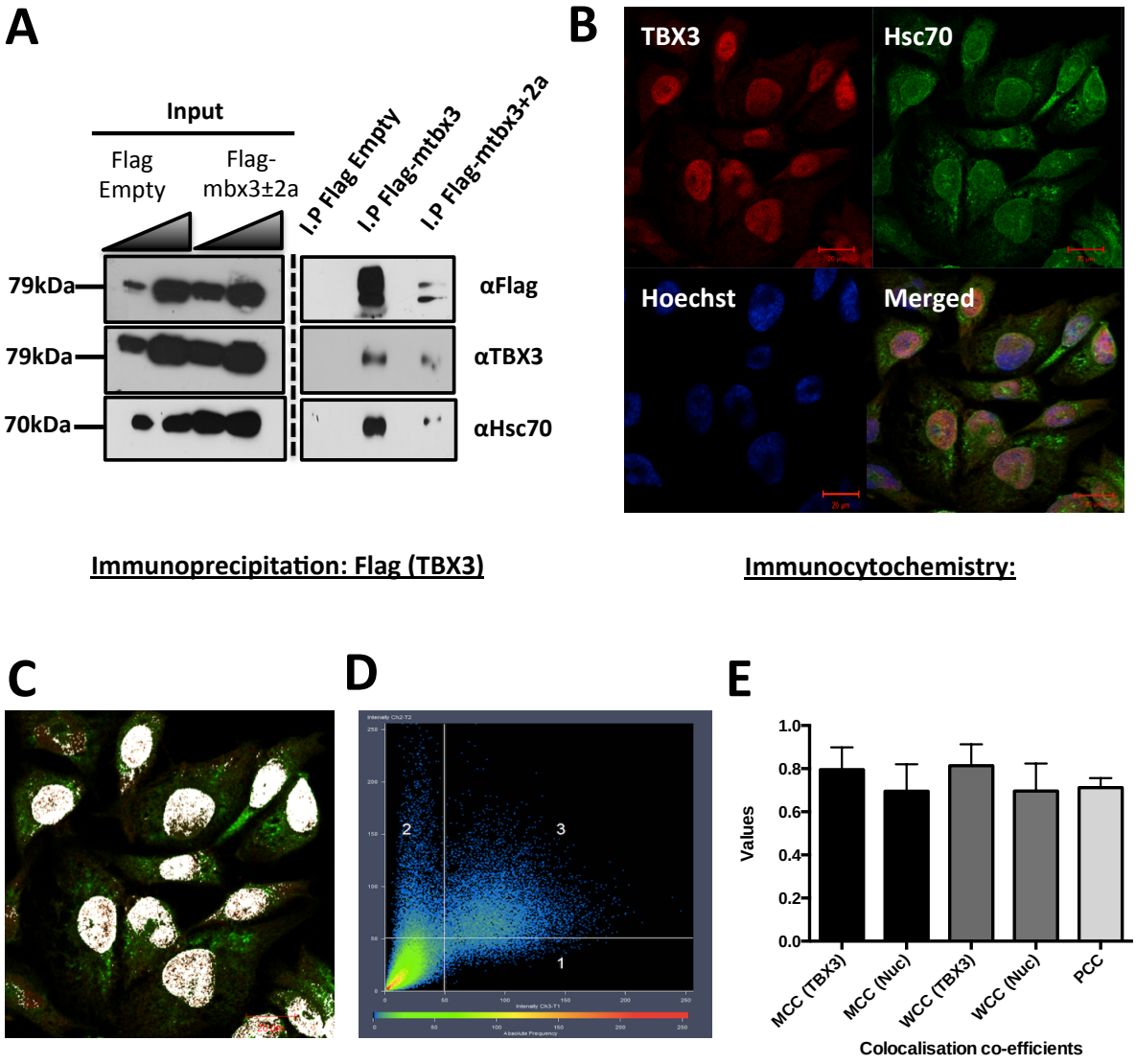

Figure 3.15. Hsc70 binds and co-localises with TBX3 in RD cells *in vivo*. ***(A)*** Protein extracts from RD cells were immunoprecipitated using an anti-Flag antibody, pulling down Flag-tagged TBX3 and protein partners bound to it. Purified immune complexes were subjected to western blot analysis using mouse monoclonal M2 Flag (1:1000), rabbit polyclonal TBX3 (1:1000) and mouse monoclonal Hsc70 (1:1000). ***(B)*** RD cells were plated on coverslips and processed for immunofluorescence with antibodies specific to TBX3 (Cy3; red channel) and nucleolin (Alexa 488; green channel) and visualised by confocal microscopy. Representative images are shown at 400X magnification. All cells were co-stained with Hoechst to determine the location of the nuclei. TBX3 and nucleolin co-localize in the nucleus (merged image). ***(C)*** Merged image from co-localisation analysis with white pixels indicating TBX3 and Hsc70 co-localisation. ***(D)*** Representative scatter plot of TBX3 and nucleolin colocalisation in RD cells. Images from ***(C)*** were analysed by Zeiss software where the signal intensity of each channel is shown as a 2D graph. ***(E)*** Colocalisation of TBX3 and nucleolin was quantified using Mander's, Weighted and Pearson's coefficients using Zeiss software. Error bars represent standard deviation.

3.4.1 Depleting c-Myc results in decreased TBX3 protein and mRNA levels in RD cells

The constitutive expression of c-Myc is oncogenic in a wide variety of cancers as well as a number of sarcomas, including liposarcoma, fibrosarcoma, synovial sarcoma, chondrosarcoma, osteosarcoma, Ewing's sarcoma and Kaposi's sarcoma (Barrios *et al*., 1994; Barrios *et al*., 1993; Castresana *et al*., 1992; Demir *et al*., 2014; Sollazzo *et al*., 1999). Importantly, c-Myc is overexpressed in the RD cell line (Kouraklis *et al.*, 1999; Marampon *et al.*, 2006; unpublished data from our laboratory) and repression of c-Myc in these cells caused cell cycle arrest and a decrease in anchorage independent growth (Marampon *et al.*, 2006). Lastly, our laboratory has revealed that there are four highly conserved E-Box motifs in the TBX3 promoter and that c-Myc transcriptionally activates the TBX3 gene through two of these sites (Wilmer *et al.*, 2015). The possibility was therefore considered that TBX3 may also be upregulated by c-Myc in RD cells. To this end the impact of transiently knocking down c-Myc on TBX3 levels in RD cells was explored using a siRNA approach. Western blot analyses with antibodies to c-Myc confirmed the efficacy of the two siRNA to c-Myc used in this study and antibodies to TBX3 show that there is a corresponding decrease in TBX3 protein levels when c-Myc is depleted (**Fig.3.16A**). These results suggest that c-Myc may indeed act upstream of TBX3 to increase its expression. To confirm this qRT-PCR was performed, and indeed, knocking down c-Myc led to a decrease in TBX3 mRNA levels (**Fig.3.16B**).

3.4.2 Inhibiting AKT decreases TBX3 protein levels in RD cells

The AKT/PKB (Protein Kinase B) family of threonine/serine-specific kinases consists of AKT1, AKT2 and AKT3 which are activated by phosphorylation (p-AKT). AKT overexpression and hyperactivity have been implicated in a number of sarcomas including RMS (Wan & Helman, 2003; Ridzewski, 2015). Additionally, Peres *et al.* (2015) recently reported that AKT3 upregulates TBX3 protein levels in a subset of melanoma cell lines by increasing its stabilization through phosphorylation. The possibility that AKT may also upregulate TBX3 in RD cells was therefore next investigated. Briefly, to inhibit the AKT signaling pathway RD

cells were treated with 10 μM of the commercially available AKT VIII inhibitor which inhibits AKT 1, 2 and 3 activities by preventing phosphorylation at Thr 308 and Ser 473 (Barnett *et al*., 2005). The concentration and duration of treatment with this inhibitor was based on optimization experiments. Western blot analyses with an antibody to phosphorylated AKT i.e. the active form of the kinase show that the AKT pathway is constitutively active in RD cells and that the pathway was effectively blocked at 2h and 4h of AKT VIII treatment (**Fig.3.16C**). Importantly, as seen in **Figure 3.16C**, TBX3 protein levels were reduced at 2h and 4h of AKT VIII treatment suggesting that TBX3 was indeed activated by the AKT pathway in RD cells. Furthermore, our laboratory has unpublished data implicating AKT1 in regulating TBX3 levels in fibrosarcomas. Therefore to identify which AKT isoform may be responsible for upregulating TBX3 in RD cells, the cells were transiently transfected with a siRNA to AKT1 and western blotting performed to determine the impact on TBX3 levels. **Figure 3.16D** shows that when AKT1 is depleting there is a corresponding decrease in TBX3 protein levels. Interestingly, a decrease in p-AKT also caused a decrease in c-Myc protein expression at 4h of AKT VIII treatment (data not shown). These results suggest that AKT may upregulate TBX3 directly by phosphorylation as well as indirectly through upregulating c-Myc.

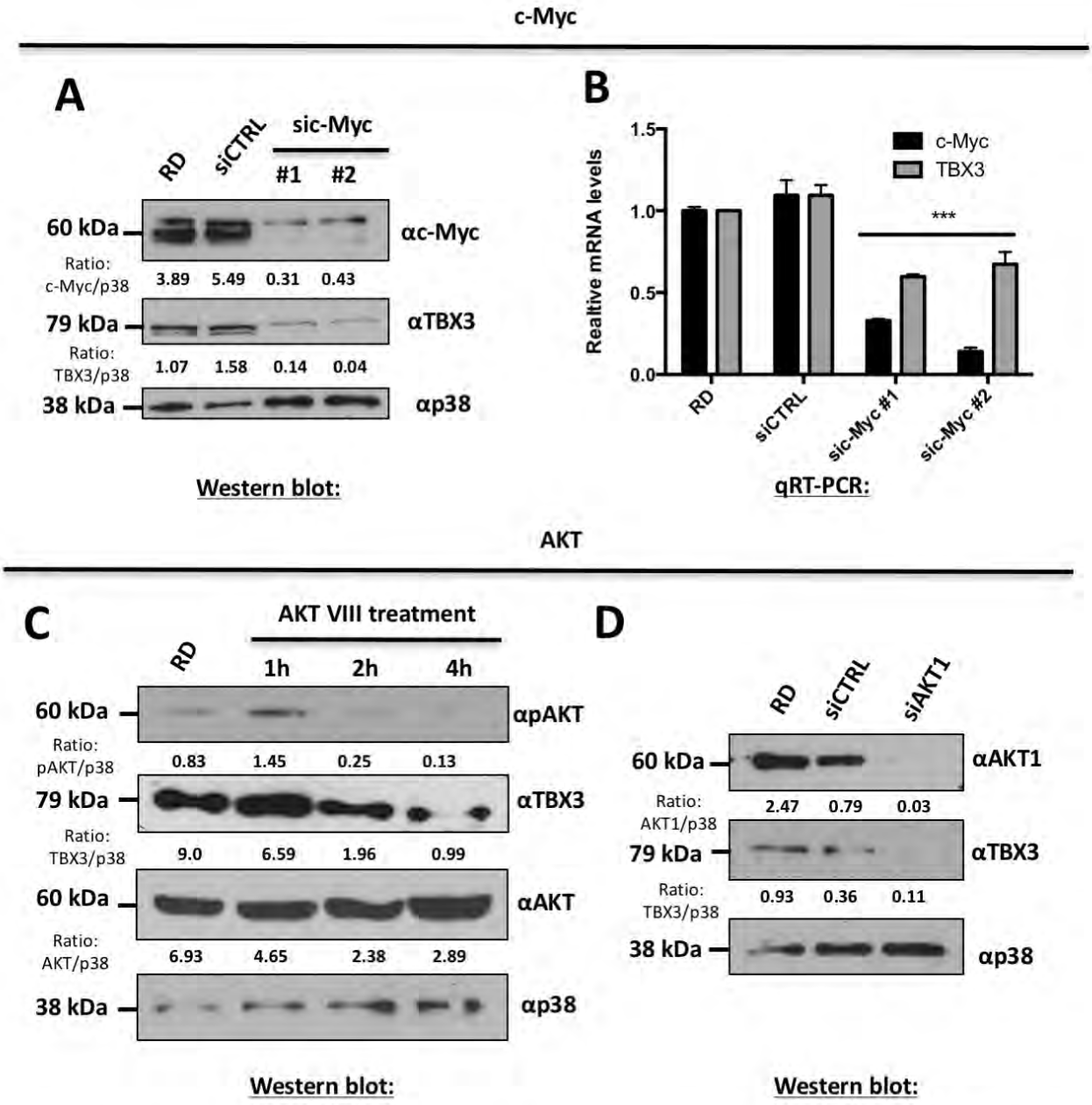

Figure 3.16. Depleting c-Myc and AKT results in decreased TBX3 levels in RD cells. ***(A)*** RD cells were transiently transfected with 50nM siRNAs to c-Myc (sic-Myc#1 and sic-Myc#2) or the equivalent concentration of control siRNA (siCTRL) for 48 hours. Protein extracts were subjected to western blot analyses with antibodies to rabbit c-Myc (1:1000), rabbit polyclonal TBX3 (1:1000) and rabbit polyclonal p38 (1:2000). ***(B)*** Quantitative real-time PCR was performed on reverse transcribed RNA using primers specific to c-Myc and TBX3, mRNA levels were normalised to GUSB. Microsoft Excel student t-test was performed to calculate statistical significance (*p<0.05; **p<0.001; ***p<0.0001). This figure shows two independent experiments each in duplicate and the error bars represent standard error of the mean. ***(C)*** RD cells were treated with 10μM of AKT inhibitor AKT VIII for 1, 2 and 4 hours or ***(D)*** were transiently transfected with 50nM siRNAs to AKT1, or the equivalent concentration of control siRNA (siCTRL), for 48 hours. Protein extracts were subjected to western blot analyses with antibodies to rabbit AKT (1:1000), rabbit pAKT (1:1000), rabbit AKT1 (1:1000), rabbit polyclonal TBX3 (1:1000) and rabbit polyclonal p38 (1:2000)**. *(A, C & D)*** Western blot analyses of protein prepared from indicated cell lines used in these experiments were analysed by SDS-PAGE (8%) and the above mentioned antibodies and goat anti-rabbit secondary antibodies (1:5000). p38 was used as a loading control. Densitometric values represent the expression of each protein band quantified using the UN-SCANT-IT gel 6.1 software and normalized to p38 levels.

Chapter 4. Discussion and Conclusion

Rhabdomyosarcoma (RMS) is a deadly cancer of the skeletal muscle and the most common soft tissue sarcoma in children (Ries *et al.*, 1999). Decreased mortality and increased life expectancy may be achieved by early detection, accurate diagnosis and more effective chemotherapeutic treatments. There is therefore an urgent need to elucidate the molecular mechanisms underpinning RMS formation because it will reveal novel diagnostic markers and targets for therapeutics. There is a large body of evidence implicating T-box transcription factor TBX3 as an oncogene in several cancers of epithelial origin, yet until recently little was known about the status, role and regulation of TBX3 in sarcomas (Fan *et al*., 2004; Rowley *et al*., 2004; Ito *et al*., 2005; Renard *et al*., 2007; Rodriguez *et al*., 2008). Our laboratory has however shown that TBX3 is upregulated in several sarcoma subtypes including human embryonal RMS cells (ERMS), and provided compelling data showing that whereas TBX3 promotes oncogenesis in chondrosarcomas it functions as a tumour suppressor in fibrosarcomas (Willmer *et al*., 2016). The focus of the current study was to determine the impact of TBX3 overexpression on the ERMS cancer phenotype and to begin to explore molecules responsible for upregulating TBX3 in this cancer as well as to carry out preliminary studies to identify TBX3 proteins partners in ERMS.

The role of TBX3 in ERMS

To determine the significance of TBX3 overexpression in ERMS, cell culture models in which TBX3 was stably knocked down or overexpressed in RD cells were first established and the resulting cells subjected to a number of assays to determine the consequence of altering TBX3 levels on the cancer phenotype. The results showed that TBX3 does indeed impact directly on the ERMS phenotype because when it is knocked down several features of transformation including substrate-dependent and -independent proliferation and cell migration are inhibited. Importantly, overexpression of TBX3 enhanced RD cell proliferation, anchorage independence, migration and tumour forming abilities. Together the results from the knock-down and overexpression models generated in this study provided compelling evidence that TBX3 was a key driver of the ERMS phenotype. These results are consistent

with TBX3 playing an oncogenic role in carcinomas and chondrosarcomas where it is overexpressed (Wansleben *et al*., 2014; Wilmer *et al.*, 2016). It is however important to note that only a single ERMS cell line was analysed in this study and to strengthen the data future work should include more ERMS cell lines. Furthermore, based on recent data from Dr Judy Davie's laboratory at Southern Illinois University School of Medicine in the USA, showing that TBX3 is expressed in samples of patients with ARMS and ERMS, and indeed this study showed TBX3 to be exclusively expressed in RMS patient tumour samples and not healthy adjacent tissue, it will be interesting to investigate whether TBX3 also contributes to ARMS (Zhu *et al*., 2015b). Future studies should include screening an RMS tissue array for TBX3 overexpression. This will provide valuable information as to whether the upregulation of TBX3 is a general feature of specific or all RMS subtypes. Taken together, this study extends our understanding of a novel role that we have recently described for TBX3 in sarcomas and in particular it contributes to an understanding of the molecular mechanisms underpinning ERMS which has potential implications for the diagnosis and treatment of this childhood cancer.

Results from both the knock-down and overexpression cell culture models show that TBX3 promotes cell proliferation of ERMS cells. This is consistent with results from studies in other cancers including liver cancer, bladder cancer, head and neck squamous cell carcinoma and chondrosarcoma (Renard, 2007; Burgucu *et al*., 2012; Humtsoe *et al.*, 2012; Wilmer *et al.*, 2016). While the current study did not explore the mechanism by which TBX3 promotes RD cell proliferation it has previously been shown to function as a pro-proliferative factor by bypassing senescence and/or inhibiting apoptosis through its ability to repress p14/p19 and p21 (Brummelkamp *et al*., 2002; Carlson *et al*., 2002; Lingbeek *et al*., 2002; Hoogaars *et al*., 2008). Of special interest to this study, our laboratory has recently shown that TBX3 can promote chondrosarcoma cell proliferation by directly inhibiting p21 (Willmer *et al*., 2016b). It would therefore be interesting to determine if p14/p19 and p21 levels correlate inversely with TBX3 levels in the ERMS cell culture models established in this study and whether their repression is the mechanism through which TBX3 promotes proliferation of RD cells. Interestingly, work from the Davie's group has shown that TBX2, a homologue of TBX3, promotes RMS by recruiting HDACs to the promoters of p14 and p21, as well as the myogenic transcription factors MyoD and myogenin (Zhu *et al*., 2015; Zhu *et*

al., 2015b). The authors show that this results in the loss of terminal myogenic differentiation and the maintenance of cell proliferation. It is worth noting that while this group has reported that RD cells have high levels of TBX2 and almost undetectable levels of TBX3, our laboratory has shown the opposite for the levels for the two proteins in RD cells. We speculate that the difference may be due to the different antibodies used for TBX2 and TBX3 which will be essential to resolve in the future. Nevertheless, it will be important to investigate whether TBX3 can promote the ERMS phenotype by similarly disrupting p14/p19, p21 and the myogenic transcription factors. This will be particularly interesting in light of reports that TBX3 is highly expressed in undifferentiated mouse skeletal muscle cells and tissues and that the overexpression of TBX3 prevents skeletal muscle differentiation (Carlson *et al.*, 2002). Furthermore, Nanni *et al*. (2009) showed that cell proliferation and migration of RMS cells ceased upon terminal muscle differentiation. Importantly, they observed that the overexpression of myogenin inhibited RMS migration and halted metastasis and tumour growth.

Results from this study also show that stably knocking down TBX3 in the SHTBX3 (2) RD cell line caused no change in cell morphology but triggered an S-phase arrest and increased apoptosis. This is consistent with other reports that TBX3 may also promote cancer cell proliferation by inhibiting apoptosis (Brummelkamp *et al*., 2002; Carlson *et al*., 2002). Furthermore, this effect has also been seen in the Prince laboratory in chondrosarcoma cell lines in which TBX3 has been knocked down (Willmer *et al*., 2015). It is important to note however that the SHTBX3 (1) RD cell line did not exhibit an S-phase arrest or apoptosis. A possible explanation for this difference between the SHTBX3 (1) and SHTBX3 (2) cell lines could be the degree to which TBX3 is knocked down in these two cell lines i.e. a dose-dependent effect. This is a real possibility because T-box factors are known to display dosage sensitivity (Wansleben *et al*., 2014) and hence the TBX3 expression levels could relate to the degree of its ability to transcriptionally repress p14/p19 and p21. Indeed, qRT-PCR screening of TBX3 mRNA levels showed that TBX3 was expressed significantly lower in SHTBX3 (2) than in SHTBX3 (1) cells (see **Fig.3.2B**). It would therefore be worth following up on the impact of different levels of TBX3 on the cell cycle profile and apoptosis in RD cells.

Quite unexpectedly, while mice injected with Flag-mtbx3+2a overexpressing cells initially formed tumours earlier than mice injected with Flag Empty cells, upon dissection of the tumours the Flag Empty tumours were larger and weighed significantly more than the Flag-mtbx3+2a tumours. To gain insight into this observation, histopathological analyses were performed with H&E staining. The pathologist's report indicates that Flag Empty tumours have a greater mitotic count which indicates that these tumour cells had a greater proliferative rate than the Flag-mtbx3+2a tumour cells. To confirm this finding Ki-67 staining of tumour sections could be performed to quantify the proliferative indices of the tumour cells. It is interesting to note, however, that the Flag-mtbx3+2a tumour cells displayed a more migratory morphology and appeared to be more invasive that the Flag Empty tumour cells. It is therefore tempting to speculate that while not seen *in vitro*, *in vivo*, the proliferation/migration dichotomy may apply with TBX3 overexpressing cells favouring cell migration/invasion over proliferation. It must also be mentioned that in carcinoma cells undergoing epithelial-to-mesenchymal transition (EMT) cell morphology often changes to become more spindle-shaped allowing the cell to become more migratory and invasive. To further investigate this possibility it would be essential to perform immunohistochemistry on the tumour sections with antibodies to EMT markers as well as to carry out trans-well invasion assays with Flag Empty and Flag-mtbx3+2a cells.

This study did not explore the mechanism(s) by which TBX3 may promote anchorage independent growth, migration, *in vivo* tumour forming ability and invasion of RD cells. To address this, future experiments will need to perform chromatin immunoprecipitation (ChIP) sequencing, microarrays and/or pathway focused PCR arrays to identify putative TBX3 target genes and subsequent work should fully characterize those that may mediate these oncogenic functions.

Identification and characterization of TBX3 co-factors in ERMS

The molecular mechanisms that regulate the diverse roles of TBX3 in development and cancer are still largely unknown but there is a widely held view that it will involve protein co-factors. To date, very few TBX3 co-factors have however been identified. A previous PhD

student in the Prince laboratory, Dr Willmer, therefore performed affinity purifications coupled with mass spectrometry analyses (AP-MS) to identify TBX3 interaction protein partners that may mediate its oncogenic roles in chondrosarcomas. From the 37 candidate proteins identified nucleolin and Hsc70 were further validated as co-factors of TBX3. Importantly, nucleolin was shown to co-operate with TBX3 to promote chondrosarcoma cell proliferation and migration and Hsc70 stabilised the TBX3 protein leading to, in part, its upregulation in chondrosarcomas (unpublished data). This study was therefore interested to determine if nucleolin and Hsc70 also interacted with TBX3 in ERMS and indeed, using immunoprecipitation assays and co-localisation experiments shows this to be the case.

Based on the data obtained in chondrosarcomas it was hypothesized that nucleolin co-operated with TBX3 to promote cell proliferation and migration in RD cells. There is overlap between the roles, upstream activators and some targets of TBX3 and nucleolin and both are involved in cancer pathogenesis. For example, similar to TBX3, the levels of nucleolin peak in S-phase and it is well characterized for its roles in stimulating proliferation, suppressing apoptosis through targeting p21 and p53, promoting migration and EMT through MMP-9 when activated by AKT and contributing to metastasis when upregulated by VEGF (Bates *et al*., 2009; Hovanessian *et al*., 2010; Abdelmohsen & Gorospe, 2012; Takagi *et al*., 2005; Bhatt *et al*., 2012; Wu *et al.*, 2014; Willmer et al., 2015). This study confirmed that, like TBX3, nucleolin also promotes RD cell proliferation and migration. Importantly, reciprocal rescue growth curves and migration assays revealed that TBX3 and nucleolin also co-operate to promote both cell proliferation and migration of RD cells. It will be important for future studies to further characterize the domains of the TBX3 and nucleolin proteins required for their interaction because it could reveal additional ways of interrupting the oncogenic functions of TBX3 and nucleolin. This can be done using GST-pull-down experiments. For the same reason it will be useful to identify TBX3/nucleolin target genes that mediate their pro-proliferative and pro-migratory roles in RD cells. Of interest to their pro-proliferative role would be p21 because it has already been identified as a TBX3 and nucleolin target (Carlson *et al.*, 2002; Rodriguez *et al.*, 2008; Wilmer *et al.*, 2015). This possibility could be examined through the following experiments: (1) western blotting and qRT-PCR to determine the impact of TBX3 and nucleolin on *de novo* p21 transcription, (2) luciferase reporter assays to determine whether TBX3 and nucleolin can synergistically

repress the p21 promoter and (3) ChIP assays to determine whether TBX3 and nucleolin co-occupy the p21 promoter *in vivo*. It is also possible that TBX3 and nucleolin could co-operate to regulate p21 gene expression at a post-transcriptional level, as both have been implicated in RNA binding and are key components of the spliceosome (Ginisty *et al*., 1998; Kumar *et al*., 2014b).

It was speculated that the interaction between TBX3 and Hsc70 was to maintain TBX3's stability and therefore contributing to TBX3's oncogenic function through prolonging its active period. This would be consistent with a reported function of Hsc70 in oncogenesis being through its ability to bind and stabilize oncoproteins (Finlay *et al.*, 1989; Shiota *et al.*, 2009; Koren *et al.*, 2009; Ding *et al.*, 2012; Tanaka *et al.*, 2014; Prince laboratory, unpublished data). Furthermore, bioinformatics analysis reveals that the TBX3 protein is highly disordered and unstable (PSIPRED) which suggests that TBX3 may require a chaperone protein to fold it correctly and optimally in cancers in which it is overexpressed. To test this western blot analysis of RD cells transfected with a siRNA to Hsc70 could first be performed to investigate if a decrease in TBX3 protein levels correspond to a decrease in Hsc70. Confirmation would require experiments with the proteasome inhibitor MG132 to determine if TBX3 protein levels can be rescued after Hsc70 knock-down.

Identification of TBX3 upstream regulators in ERMS

Wilmer *et al.* (2016) found TBX3 to be overexpressed in a range of sarcoma cell lines, including the RDs, at both the protein and mRNA levels. This suggests that TBX3 may be transcriptionally and/or post-transcriptionally upregulated in RD cells. This study performed preliminary experiments which identified the oncogenic transcription factor, c-Myc, and the pro-survival kinase, AKT, to be upstream of TBX3 expression in the RD cell line. Indeed, preliminary qRT-PCR and western blotting data show that when c-Myc was effectively knocked down by two different siRNAs there was a corresponding decrease in TBX3 mRNA and protein levels. While this data do not conclusively show that c-Myc directly activates TBX3 transcriptionally in RDs, it is speculated that this will be true because our laboratory recently reported this to be the case in chondrosarcomas (Wilmer *et al.*, 2015). This raises

the exciting possibility that c-Myc may be one of the common mechanisms by which TBX3 is upregulated in a wide range of sarcoma subtypes.

Lastly, constitutive activation of AKT has been linked to sarcomagenesis (Tomita *et al*., 2006; Hernando *et al*., 2007; Zhu *et al*., 2008; Friedrichs *et al*., 2011; Valkov *et al*., 2011; Ahmed *et al*., 2015) and our laboratory recently showed that TBX3 is a key substrate and mediator of AKT3 in melanomagenesis (Peres *et al*., 2015). It was therefore hypothesized that AKT may also phosphorylate TBX3 in ERMS. Using a chemical inhibitor of AKT1, 2 and 3, this study shows that TBX3 protein levels are dependent on the presence of active AKT. It was speculated that AKT1 may be the isoform responsible for positively regulating TBX3 levels in RD cells because it appears to be the active isoform in sarcomas (Goldstein *et al.*, 2007). To test this a siRNA to AKT1 was transiently transfected into RD cells and the results show that depleting AKT1 leads to a decrease in TBX3 levels. This provides preliminary evidence that TBX3 may be a *bona fide* substrate of AKT1. Further work is required to determine if AKT1, like AKT3 in melanomas, phosphorylates TBX3 in rhabdomyosarcomas to enhance it protein stability, nuclear localisation and downstream oncogenic activities.

Technical considerations

A disappointing result in this study was the failure to determine the impact of knocking down TBX3 on the tumour forming ability of RD cells in immunocompromised nude mice. Indeed a pilot study, using published conditions, showed that parental RD cells were unable to form tumours in these mice and therefore the experiment with TBX3 knock-down cells could not proceed. After the overexpression cell culture was established it was speculated that compared with the Empty control cells, the TBX3-overexpressing RD cells may have enhanced tumour forming ability. To improve the likelihood of this occurring mice were injected with 1 x 10^7 cells compared to 3 x 10^6 cells which were used in the pilot study. Interestingly, mice injected with both Empty control cells and TBX3-overexpressing cells formed tumours. Since, technically, the Empty control cells should have the same tumour forming ability as the parental cells it will be important to repeat the pilot study using 1 x 10^7 cells. Based on the data obtained, the impact of knocking down TBX3 on tumour

forming ability in nude mice can be investigated. In addition, nude mice could be replaced with NOD Scid Gamma (NSG) mice because they lack a functional IL-2 receptor γ-chain and are deficient in B cells and natural killer cells and therefore more immunocompromised (Rongvaux *et al*., 2013; Shultz *et al*., 2005). These features translate into an improved tolerance of the engraftment of human cells (Iorns *et al*., 2012; Shultz *et al*., 2005) suggesting that perhaps in the NOD Scid mouse model RD cells may be able to form tumours more easily.

Concluding remarks

Based on the results generated in this study and the current literature the following model is proposed for the role and regulation of TBX3 in ERMS where it is overexpressed (see **Fig.4**). Briefly, c-Myc and AKT1 were found to be upstream of TBX3 and both nucleolin and Hsc70 were observed to interact with TBX3. Therefore, we propose that c-Myc transcriptionally upregulates TBX3 mRNA and that phosphorylation of the TBX3 protein by AKT1 results in an increase in TBX3 protein stability and levels. Interaction with Hsc70 leads to correct protein folding and further stabilization of the TBX3 protein. TBX3 then interacts and co-operates with nucleolin to promote proliferation and migration in ERMS.

While a criticism of this work is that it was performed in a single ERMS cell line, and future investigations will expand into more ERMS and ARMS cell lines and patient tumour tissues, it is important to note that this study formed part of a larger study investigating the status, role and regulation of TBX3 in a diverse range of sarcoma cell lines and tissue samples (Wilmer *et al.*, 2016). In conclusion, this study shows that TBX3 may be considered as a diagnostic biomarker of ERMS and a possible diagnostic marker and target, along with nucleolin, Hsc70, c-Myc and AKT1, in more effectively treating ERMS.

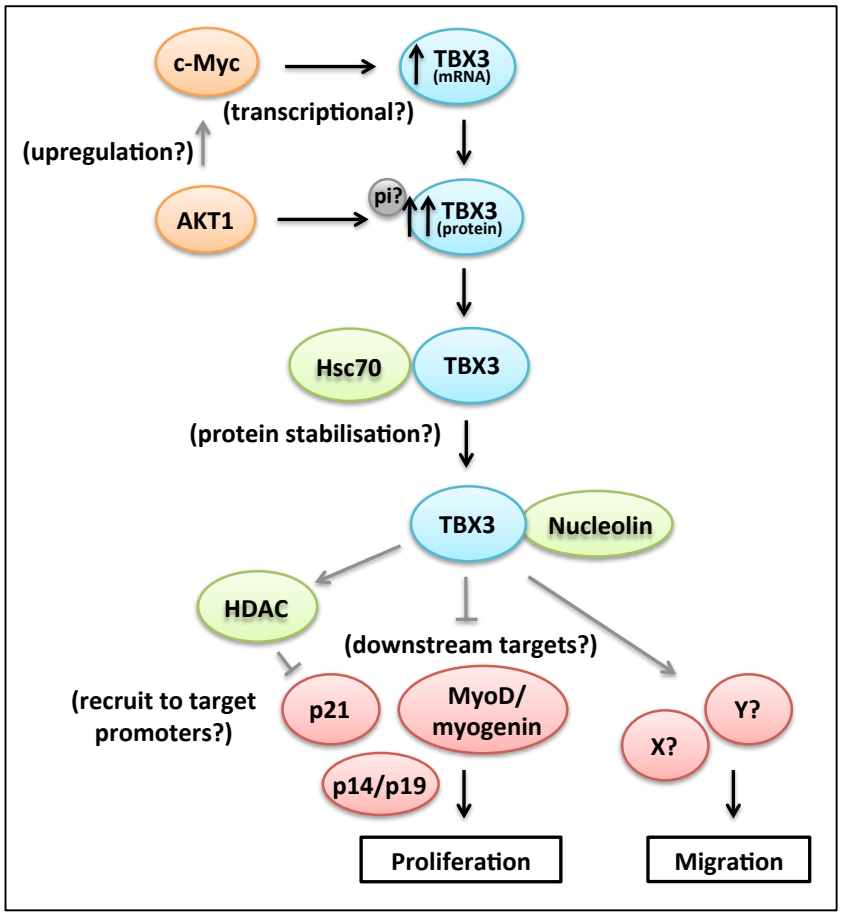

Figure 4: A proposed model of TBX3 role and regulation in ERMS.

Chapter 5. References

K., Abdelmohsen, M., Gorospe, RNA-binding protein nucleolin in disease, RNA Biol 9 (6) (2012) 799-808.

S.I. Agulnik, N. Garvey, S. Hancock, I. Ruvinsky, D.L. Chapman, I. Agulnik, R. Bollag R, V. Papaioannou, L.M. Silver, Evolution of mouse T-box genes by tandem duplication and cluster dispersion, Genet 144 (1996) 249-254.

S.I. Agulnik, V.E. Papaioannou, L.M. Silver, Cloning, mapping, and expression analysis of TBX15, a new member of the T-box gene family, Genomics 51 (1998) 68-75.

A.A. Ahmed, M. Abedalthagafi, A.E. Anwar, M.M. Bui, Akt and Hippo Pathways in Ewing's Sarcoma Tumors and Their Prognostic Significance, J Can 6 (10) (2015) 1005-1010.

E., Akinwunmi, S., Xiao, Y., Guo, X., Li, A.D., Saxena, Nucleolin phosphorylation by CK2 is important for its role in regulating apoptosis, Cancer Res 75 (14) (2015)

D.A Altomare, J.R Testa, Perturbations of the AKT signaling pathway in human cancer, Oncogene 24 (2005) 7455–7464.

E.K. Amankwah, A.P. Conley, D.R. Reed, Epidemiology and therapies for metastatic sarcoma, Clin Epidem 5 (2013) 147–162.

A.M. Andreou *et al*., TBX22 Missense Mutations Found in Patients with X-Linked Cleft Palate Affect DNA Binding, Sumoylation and Transcriptional Repression, Am J Hum Genet 81 (2007) 700–712.

S.R. Annavarapu, S. Cialfi, C. Dominici, G.K. Kokai, S. Uccini, S. Ceccarelli *et al*., Characterization of Wnt/beta-catenin signaling in rhabdomyosarcoma, Lab Invest 93 (2013) 1090–1099.

L.M. Arendt, J. St. Laurent, A. Wronski, S. Caballero, S.R. Lyle, S.P. Naber, C. Kuperwasser, Human Breast Progenitor Cell Numbers Are Regulated by WNT and TBX3, PLoS one 9 (10) (2014)

P. Ataliotis *et al*., XTbx1 is a Transcriptional Activator Involved in Head and Pharyngeal Arch Development in Xenopus laevis, Dev dynamics, 232 (2005) 979–991.

I. Atreya, *et al*., The T-box transcription factor eomesodermin controls CD8 T cell activity and lymph node metastasis in human colorectal cancer, Gut 56 (2007) 1572–1578.

M.L. Bakker, B.J. Boukens, M.T.M. Mommersteeg, J.F. Brons, V. Wakker, A.F.M. Moorman, V.M. Christoffels, Transcription Factor Tbx3 Is Required for the Specification of the Atrioventricular Conduction System, Circ Res 102 (2008) 1340-1349.

B.C. Ballif, A. Theisen, J. Rosenfeld, R.N. Traylor, J. Gastier-Foster, D.L. Thrush, C. Astbury, D. Bartholomew, K.L. McBride, R.E. Pyatt, *et al.*, Identification of a recurrent microdeletion at 17q23.1q23.2 flanked by segmental duplications associated with heart defects and limb abnormalities, Am J Hum Genet 86 (2010) 454–461.

M. Bamshad, T. Le, W.S. Watkins, M.E. Dixon, B.E. Kramer, A.D. Roeder, J.C. Carey, S. Root, A. Schinzel, L. Van Maldergem, R.J. Gardner, R.C. Lin, C.E. Seidman, J.G. Seidman, R. Wallerstein, E. Moran, R. Sutphen, C.E. Campbell, L.B. Jorde, The spectrum of mutations in TBX3: Genotype/Phenotype relationship in ulnar-mammary syndrome. Am J Hum Genet 64 (1999) 1550-1562.

S.F. Barnett, D. Defeo-Jones, S. Fu, P.J. Hancock, K.M. Haskell, R.E. Jones, J.A. Kahana, A.M. Kral, K. Leander, L.L. Lee, J. Malinowski, E.M. McAvoy, D.D. Nahas, R.G. Robinson, H.E. Huber, Identification and characterization of pleckstrin-homology-domain-dependent and isoenzyme-specific Akt inhibitors, Biochem J (385) (2005) 399–408.

S. Bar-Nun *et al*., G-418, an elongation inhibitor of 80 S ribosomes, Biochim Biophys Acta 741 (1983) 123-127.

C. Barrios, J. Castresana J. Ruiz, A. Kreicbergs, Amplification of the c-myc proto-oncogene in soft tissue sarcomas, Oncology 51 (1) (1994) 13-17.

C. Barrios, J.S. Castresana, J.A. Ruiz, A. Kreicbergs, Amplification of c-myc oncogene and absence of c-Ha-ras point mutation in human bone sarcoma, J Orthopaedic Res 11 (4) (1993) 556-563.

P.J. Bates, D.A. Laber, D.M. Miller, S.D. Thomas, J.O. Trent, Discovery and Development of the G-rich Oligonucleotide AS1411 as a Novel Treatment for Cancer, Exp Mol Pathol 86 (3) (2009) 151–164.

E. Beck *et al*., Nucleotide sequence and exact localization of the neomycin phosphotransferase gene from transposon Tn5, Gene 19 (1982) 327-336.

T.B. Beckingsale, C. Shaw, Epidemiology of bone & soft tissue sarcomas, Orthopaedics Trauma 29 (3) (2015) 182-188.

A. Bellacosa, C.C. Kumar, A. Di Cristofano, J.R. Testa, Activation of AKT Kinases in Cancer: Implications for Therapeutic Targeting, Advances Cancer Res 94 (2005) 29-86.

E. Bernstein *et al*., Role for a bidentate ribonuclease in the initiation step of RNA interference, Nature 409 (2001) 363-366.

M. Bertolessi, L. Linta, T. Seufferlein, A. Kleger, S. Liebau, Stem Cells Dev 24 (16) (2015) 1833-1851.

B. Belyea, J.G. Kephart, J. Blum, D.G. Kirsch, C.M. Linardic, Embryonic signaling pathways and rhabdomyosarcoma: contributions to cancer development and opportunities for therapeutic targeting, Sarcoma (2012)

P., Bhatt, C., d'Avout, N.S., Kane, J.A., Borowiec, A., Saxena, Specific domains of nucleolin interact with Hdm2 and antagonize Hdm2-mediated p53-ubiquitination, FEBS J 279 (3) (2012) 370–383.

C. Birchmeier, W. Birchmeier, E. Gherardi *et al*., Met, metastasis, motility, and more, Nat Rev Mol Cell Biol 4 (2003) 915–925.

K. Bjornlan, K. Flatmark, S. Pettersen *et al*., Matrix metalloproteinases participate in osteosarcoma invasion, J Surg Res 127 (2005) 151–156.

T.K. Blackwell, J. Huang, A. Ma, L. Kretzner, F.W. Alt, R.N. Eisenman, H. Weintraub, Binding of Myc Proteins to Canonical and Noncanonical DNA Sequences, Mol Cel Biol 13 (9) (1993) 5216-5224.

E.M. Bongers *et al*., Mutations in the human TBX4 gene cause small patella syndrome, Am J Hum Genet 74 (2004) 1239-1248.

C.J., Boogerd, L.Y., Wong, M., van den Boogaard, M.L., Bakker, F., Tessadori, J.T., Bakkers, P.A., Hoen,
A.F., Moorman, V.M., Christoffels & P., Barnett, Sox4 mediates Tbx3 transcriptional regulation of the
gap junction protein Cx43. Cellular and molecular life sciences, 68(23) (2011), 3949-3961.

C.J., Boogerd, L.Y., Wong, V.M., Christoffels, M., Klarenbeek, J.M., Ruijter, A.F., Moorman & P., Barnett,

Msx1 and Msx2 are functional interacting partners of T- box factors in the regulation of Connexin43.
Cardiovasc Research, 78(3) (2008), 485-493.

R.A., Borer, C.F., Lehner, H.M., Eppenberger, E.A., Nigg, Major nucleolar proteins shuttle between
nucleus and cytoplasm, Cell 56 (3) (1989) 379-390.

H.M., Bourbon & F., Amalric, Nucleolin gene organization in rodents: highly conserved sequences
within three of the 13 introns, Gene 88(2) (1990) 187-196.

C. Braybrook *et al*., The T-box transcription factor gene TBX22 is mutated in X- linked cleft palate and
ankyloglossia, Nature Genet 29 (2002) 179-183.

T.R. Brummelkamp *et al*., A System for Stable Expression of Short Interfering RNAs in Mammalian Cells, Science, 296 (2002b) 550–553.

T.R. Brummelkamp, R.M. Kortlever, M. Lingbeek, F. Trettel, M.E. MacDonald, M. van Lohuizen, R. Bernards, TBX-3, the Gene Mutated in Ulnar-Mammary Syndrome, Is a Negative Regulator of p19ARF and Inhibits Senescence, J Biol Chem 277 (2002) 6567-6572.

D.W.A. Buchan, F. Minneci, T.C.O. Nugent, K. Bryson, D.T. Jones, Scalable web services for the PSIPRED Protein Analysis Workbench, Nucleic Acids Res 41 (W1) (2013) W340-W348.

D. Burgucu *et al*., Tbx3 represses PTEN and is over-expressed in head and neck squamous cell carcinoma, BMC Cancer 12 (2012) 481.

Cancer facts and figures, American Cancer Society, 2014.

Z. Burningham, M. Hashibe, L. Spector, J.D. Schiffman, The Epidemiology of Sarcoma, Clin Sarcoma Res 2 14 (2012)

J. Campsi, Aging, Cellular Senescence and Cancer, Annu Rev Physiol 75 (2013) 685–705.

H. Carlson, S. Ota, C.E. Campbell, P.J. Hurlin, A dominant repression domain in Tbx3 mediates transcriptional repression and cell immortalization: relevance to mutations in Tbx3 that cause ulnar-mammary syndrome, Hum Mol Genet 10 (2001) 2403-2413.

H. Carlson, S. Ota, Y. Song, Y. Chen, P.J. Hurlin, Tbx3 impinges on the p53 pathway to suppress apoptosis, facilitate cell transformation and block myogenic differentiation, Oncogene 21 (2002) 3827- 3835.

S. Carreira *et al*., Brachyury-related transcription factor Tbx2 and repression of the melanocyte-specific TRP-1 promoter, Mol Cell Biol 18 (1998) 5099–5108.

E.S. Casey *et al*., The T-box transcription factor Brachyury regulates expression of eFGF through binding to a non-palindromic response element, Dev 125 (1998) 3887–3894.

J.S. Castresana, C. Barrios, L. Gómez, A. Kreicbergs, Amplification of the c-myc Proto-oncogene in Human Chondrosarcoma, Diag Mol Patho 1 (4) (1992) 235-238.

X. Chen, E. Stewart, A.A. Shelat, C. Qu, A. Bahrami, M. Hatley *et al.*, Targeting oxidative stress in embryonal rhabdomyosarcoma, Cancer Cell 24 (2013) 710–724.

E.Y. Chena, M.T. De Ran, M.S. Ignatius, K.B. Grandinettid, R. Clagg, K.M. McCarthy, R.M. Lobbardia, J. Brockmanna , C. Kellere , X. Wub, D.M. Langenaua, Glycogen synthase kinase 3 inhibitors induce the canonical WNT/β-catenin pathway to suppress growth and self-renewal in embryonal rhabdomyosarcoma, PNAS 111 (14) (2014) 5349–5354.

D.D., Cheng, H.G., Zhao, Y.S., Yang, T. Hu, Q.C., Yang, GSK3b negatively regulates HIF1a mRNA stability via nucleolin in the MG63 osteosarcoma cell line, Biochem Biophys Res Comm 443 (2014) 598–603.

Y.N. Choi, S.K. Lee, T.W. Seo, J.S. Lee, S.J. Yoo, C-terminus of Hsc70-interacting protein regulates profilin1 and breast cancer cell migration, Biochem BiophysRes Com 446 (2014) 1060–1066.

S., Christian, J., Pilch, M.E., Akerman K., Porkka, L., Laakkonen, E., Ruoslahti, Nucleolin expressed at the cell surface is a marker of endothelial cells in angiogenic blood vessels. J Cell Biol 163 (2003) 871 – 878.

C. Ciccarelli, F. Marampon, A. Scoglio, A. Mauro, C. Giacinti, P. De Cesaris, B.M. Zani, p21WAF1 expression induced by MEK/ERK pathway activation or inhibition correlates with growth arrest, myogenic differentiation and onco-phenotype reversal in rhabdomyosarcoma cells, Mol Cancer 4 (2005) 41.

M.F. Clarke, *et al.*, Cancer stem cells - Perspectives on current status and future directions: AACR Workshop on Cancer Stem Cells. Cancer Res 66 (2006) 9339–9344.

M. Coll, J.D. Seidman, C.W. Müller, Structure of the DNA-bound T-box domain of human TBX3, a transcription factor responsible for ulnar-mammary syndrome, Structure, 10 (3) (2002) 343-356.

K.D. Courtney, R.B. Corcoran, J.A. Engelman, The PI3K Pathway As Drug Target in Human Cancer, J Clin Oncol 28 (6) (2010) 1075-1080.

S. Courtois-Cox, S.M. Genther-Williams, E.E. Reczek, B.W. Johnson, L.T. McGillicuddy, C.M. Johannessen, P.E. Hollstein, M. MacCollin, K. Cichowski, A negative feedback signaling network underlies oncogene-induced senescence, Cancer Cell 10 (2006) 459-472.

L., Cui, Y., Deng, Y., Rong, W., Lou, Z., Mao, Y., Feng Y *et al*., IRF-2 is overexpressed in pancreatic cancer
and promotes the growth of pancreatic cancer cells, Tumour Biol 33 (2012) 247-255.

Czifra, G., *et al.*, Protein kinase Cd promotes proliferation and induces malignant transformation in
skeletal muscle, J Cel Mol Med 19 (2) (2015) 396-407.

C.V. Dang, MYC on the Path to Cancer, Cell, 149 (1) (2012) 22–35.

C.V. Dang, A. Le, P. Gao, MYC-induced Cancer Cell Energy Metabolism and Therapeutic Opportunities, Clin Cancer Res 15 (21) (2009) 6479–6483.

C.V. Dang, L.M. S. Resar, E. Emison, S. Kim, Q. Li, J.E. Prescott, D. Wonsey, K. Zeller, Function of the c-
Myc Oncogenic Transcription Factor, Experimental Cel Res 253 (1999) 63–77.

T.G. Davenport, L.A. Jerome-Majewska, V.E. Papaioannou, Mammary gland,
limb and yolk sac defects in mice lacking Tbx3, the gene mutated in human ulnar
mammary syndrome, Dev 130 (2003) 2263-2273.

J. Davies, A. Jimenez A, A new selective agent for eukaryotic cloning vectors, Am J Trop Med Hyg 29 (1980) 1089-1092.

P. De Benedittis, K. Jiao, Alternative splicing of T-box transcription factor genes, iochem Biophys Res Commun 412 (4) (2011) 513–517.

C. De Giovanni, C. Melani, P. Nanni *et al*., Redundancy of autocrine loops in human rhabdomyosarcoma cells: induction of differentiation by suramin, Br J Cancer 72 (1995) 1224–1229.

T.F. De Laney, D.G. Kirsch, Pathogenetic factors in soft tissue and bone sarcomas, UpToDate (2015)

F. Demay, B. Bilican, M. Rodriguez, S. Carreira, M. Pontecorvi, L. Ling, C.R. Goding, T-box factors: targeting to chromatin and interaction with the histone H3 N-terminal tail, Pigment Cell Res 20 (4) (2007) 279-287.

D. Demir, B. Yaman Y. Anacak, B. Kececi, G. Kandiloglu, T. Akalin, Prognostic significance of bcl-1 c-myc, survivin and tumor grade in synovial sarcoma, Turkish J Patho 30 (1) (2014) 55-65.

M. De Salvo, L. Raimondi, S. Vella, L. Adesso, R. Ciarapica, F. Verginelli, A. Pannuti, A. Citti, R. Boldrini, G.M. Milano, A. Cacchione, A. Ferrari, P. Collini, A. Rosolen, G. Bisogno, R. Alaggio, A. Inserra, M Locatelli, S. Stifani, I. Screpanti, L. Miele, F. Locatelli, R. Rota, Hyper-Activation of Notch3 Amplifies the Proliferative Potential of Rhabdomyosarcoma Cells, PLoS ONE 9 (5) (2014)

J.A. Diehl, W. Yang, R.A. Rimerman, H. Xiao, A. Emili, Hsc70 Regulates Accumulation of Cyclin D1 and Cyclin D1-Dependent Protein Kinase, Mol Cel Biol 23 (5) (2003) 1764–1774.

R. Dienstmann, J. Rodon, V. Serra, J. Tabernero, Picking the Point of Inhibition: A Comparative Review of PI3K/AKT/mTOR Pathway Inhibitors, AACR Mol Cancer Review (2014) 1021-1031.

Y. Ding, N. Song, C. Liu, T. He, W. Zhuo, X. He, Y. Chen, X. Song, Y. Fu, Y. Luo, Heat Shock Cognate 70 Regulates the Translocation and Angiogenic Function of Nucleolin, Arterioscler Thromb Vasc Biol (32) (2012) 126-134.

Y. Dobashi, S. Suzuki, E. Sato, Y. Hamada, T. Yanagawa, A. Ooi, EGFR-dependent and independent activation of Akt/mTOR cascade in bone and soft tissue tumors, Modern Pathol 22 (2009) 1328–1340.

N.C. Douglas, V.E. Papaioannou, The T-box Transcription Factors TBX2 and TBX3 in Mammary Gland Development and Breast Cancer, J Mammary Gland Biol Neoplasia 18 (2013) 143–147.

L.A. Doyle, Sarcoma classification: An update based on the 2013 World Health Organization Classification of Tumors of Soft Tissue and Bone, Cancer 120 (12) (2014) 1763-1774.

H.F. Du, L.P. Ou, X. Yang, X.D. Song, Y.R. Fan, B. Tan, C.L. Luo, X.H. Wu, A new PKCα/β/TBX3/E-cadherin pathway is involved in PLCε-regulated invasion and migration in human bladder cancer cells, Cell Signal 26 (3) (2014) 580-593.

F. Ducimetiere, A. Lurkin, D. Ranchere-Vince, A.V. Decouvelaere, M. Peoch, L. Istier, P. Chalabreysse, C. Muller, L. Alberti, P.P. Bringuier, J.Y. Scoazec, A.M. Schott, C. Bergeron, Do. Cellier, J.Y. Blay, I. Ray-Coquard, Incidence of Sarcoma Histotypes and Molecular Subtypes in a Prospective Epidemiological Study with Central Pathology Review and Molecular Testing, PLoS ONE 6 (8) (2011) 1-14.

M.C. Eblaghie *et al.*, Interactions between FGF and Wnt signals and Tbx3 gene expression in mammary gland initiation in mouse embryos, J Anat 205 (1) (2004) 1-13.

O.M. El-Badry, C. Minniti, E.C. Kohn, P.J. Houghton, W.H. Daughaday, L.J. Helman, Insulin-like growth factor II acts as an autocrine growth and motility factor in human rhabdomyosarcoma tumors, Cell Growth Differ 1 (1990) 325–331.

F. Faggi *et al.*, Phosphocaveolin-1 Enforces Tumor Growth and Chemoresistance in Rhabdomyosarcoma, PLoS ONE 9 (1) (2014)

T. Faial, A.S. Bernardo, S. Mendjan, E. Diamanti, D. Ortmann, G.E. Gentsch, R.A. Pedersen, Brachyury and SMAD signalling collaboratively orchestrate distinct mesoderm and endoderm gene regulatory networks in differentiating human embryonic stem cells, Dev 142 (12) (2015) 2121–2135.

W. Fan, X. Huang, C. Chen, J, Gray, T. Huang, TBX3 and Its Isoform TBX3+2a Are Functionally Distinctive in Inhibition of Senescence and Are Overexpressed in a Subset of Breast Cancer Cell Lines, Cancer Res 64 (2004) 5132–5139.

H.F. Farin *et al*., Transcriptional Repression by the T-box Proteins Tbx18 and Tbx15 Depends on Groucho Corepressors, J Biol Chem 282 (2007) 25748–25759.

S. Fedotov, A. Iomin, Migration and Proliferation Dichotomy in Tumor-Cell Invasion, Physical Letter Rev, 98 (11) (2007) 118101-118104.

C.A. Felix *et al.*, Frequency and diversity of p53 mutations in childhood rhabdomyosarcoma, Cancer Res 52 (1992) 2243-2247.

R.I. Fernando *et al*., The T-box transcription factor Brachyury promotes epithelial-mesenchymal transition in human tumor cells, In Vitro 120 (2010) 533–545.

R. Ferracini, M.F. Di Renzo, K. Scotlandi *et al*., The Met/HGF receptor is over-expressed in human osteosarcomas and is activated by either a paracrine or an autocrine circuit, Oncogene 10 (1995) 739–749.

R. Ferracini, M. Olivero, M.F. Di Renzo *et al*., Retrogenic expression of the MET proto-oncogene correlates with the invasive phenotype of human rhabdomyosarcomas, Oncogene 12 (1996) 1697–1705.

C.M. Fillmore *et al*., Estrogen expands breast cancer stem-like cells through paracrine FGF/Tbx3 signaling, PNAS USA 107 (2010) 21737–21742.

C.A. Finlay, P.W. Hinds, A.J. Levine, The p53 Proto-Oncogene Can Act as a Suppressor of Transformation, Cell 57 (1989) 1083–1093.

N. Friedrichs, M. Trautmann, E.Endl, E. Sievers, D. Kindler, P. Wurst, J. Czerwitzki, S. Steiner, M. Renner, R. Penzel, A. Koch, O. Larsson, S. Tanaka, A. Kawai, P. Schirmacher, G. Mechtersheimer, E. Wardelmann, R. Buettner, W. Hartmann, Phosphatidylinositol-30 - kinase/AKT signaling is essential in synovial sarcoma, Int J Cancer 129 (2011) 1564–1575.

D.A. Fruman, C. Rommel, PI3K and cancer: lessons, challenges and opportunities, Nat Rev Drug Discovery 13 (2014) 140-156.

Z. Fu & C. Fenselau, Proteomic Evidence for Roles for Nucleolin and Poly[ADP-ribosyl] Transferase in Drug Resistance, J Proteome Res 4 (2005) 1583-1591.

H. Fujiki, T. Watanabe, M. Suganuma, Cell-surface nucleolin acts as a central mediator for carcinogenic, anti-carcinogenic, and disease-related ligands, J Cancer Res Clin Oncol 140 (2014) 689–699.

K.N. Ganjoo, New Developments in Targeted Therapy for Soft Tissue Sarcoma, Curr Oncol Rep 12 (2010) 261–265.

N. Gaspar, A. Di Giannatale, B. Geoerger, F. Redini, N. Corradini, N. Enz-Werle, F. Tirode, P. Marec-Berard, J.C. Gentet, V. Laurence, S. Piperno-Neumann, O. Oberlin, L. Brugieres, Bone Sarcomas: From Biology to Targeted Therapies, Sarcoma (2012) 1-18.

S. George, Systemic treatment of metastatic soft tissue sarcoma, UpToDate (2016)

H., Ginisty, H., Sicard, B., Roger, P., Bouvet, Structure and functions of nucleolin, J Cell Sci 112 (1999) 761-772.

E. Grinstein, P. Wernet, P.J.F. Snijders, F. Rösl, I. Weinert, W. Jia, R. Kraft, C. Schewe, M. Schwabe, S. Hauptmann, M. Dietel, C.J.L.M. Meijer, H.D. Royer, Nucleolin as Activator of Human Papillomavirus Type 18 Oncogene Transcription in Cervical Cancer, J Exp Med 196 (8) (2002) 1067-1078.

E., Grinstein, Y., Shan, L., Karawajew, P.J.F., Snijders, C.J.L.M., Meijer, H.D., Royer, P., Wernet, Cell Cycle-controlled Interaction of Nucleolin with the Retinoblastoma Protein and Cancerous Cell Transformation, J Biol Chem 281 (31) (2006) 22223–22235.

P. Greasley et al., cDNA sequences of chicken nucleolin/C23 and N038/B23, two major nucleolar proteins, Nucleic Acids Research, 28(2) (2000) 446-453.

S.C. Grifoni, S.E. McKey, H.A. Drummond, Hsc70 regulates cell surface ASIC2 expression and vascular smooth muscle cell migration, Am J Physiol Heart Circ Physiol 294 (2008).

M. Goldstein, I. Meller, A. Orr-Urtreger, FGFR1 over-expression in primary rhabdomyosarcoma tumors is associated with hypomethylation of a 5' CpG island and abnormal expression of the AKT1, NOG, and BMP4 genes, Gen Chromo Cancer 46 (11) (2007) 1028-1038.

A. Gonzalez *et al*., Control of Hes7 Expression by Tbx6, the Wnt Pathway and the Chemical Gsk3 Inhibitor LiCl in the Mouse Segmentation Clock, PloS one 8 (2013).

V. Gonzalez, K. Guo, L. Hurley, D. Sun, Identification and Characterization of Nucleolin as a c-myc G-quadruplex-binding Protein, J Biol Chem, 284 (35) (2009) 23622–23635.

Y. Guo, J. Xie, E. Rubin, Y.X. Tang, F. Lin, X. Zi *et al*., Frzb, a secreted Wnt antagonist, decreases growth and invasiveness of fibrosarcoma cells associated with inhibition of Met signaling, Cancer Res 68 (2008) 3350–3356.

P.E. Habets, A.F. Moorman, D.E. Clout, M.A. van Roon, M. Lingbeek, M. van Lohuizen, M. Campione, V.M. Christoffels, Cooperative action of Tbx2 and Nkx2.5 inhibits ANF expression in the atrioventricular canal: implications for cardiac chamber formation, Genes Dev 16 (10) (2002) 1234-1246.

S.M. Hammond *et al*., An RNA-directed nuclease mediates post-transcriptional gene silencing in Drosophila cells, Nature 404 (2000) 293-296.

K.D. Hanson, M. Shichiri, M.R. Follansbee, J.M. Sedivy, Effects of c-myc Expression on Cell Cycle Progression, Mol Cel Biol 14 (9) (1994) 5748-5755.

S. Hare, S. Prince, Regulation of the Cyclin-Dependent Kinase Inhibitor p21 by TBX3, Masters dissertation for Cell biology (2013) 1-96.

M. Harris, V. Hartley Al-Blair, J.M. Birch, S.S. Banerjee, A.J. Freemont, J. McClure, L.J. McWilliam, Sarcomas in north west England: I. Histopathological peer review, British J Cancer 64 (2) (1991) 315-320.

D.S. Hawkins, A.A. Gupta, E.R. Rudzinski, What is new in the biology and treatment of pediatric rhabdomyosarcoma? Curr Opin Pediatr 26 (2014) 50–56.

M.L. He *et al*., Induction of apoptosis and inhibition of cell growth by developmental regulator hTBX5, Biochem Biophys Res Comm 297 (2002) 185–192.

K. Helmbrecht, L. Rensing, Different constitutive heat shock protein 70 expression during proliferation and differentiation of rat C6 glioma cells, Neurochem Res 24 (10) (1999) 1293-1299.

J.G. Herman, S.B. Baylin, Gene silencing in cancer in association with promoter hypermethylation, N Engl J Med 349 (2003) 2042-2054.

B.G. Herrmann, S. Labeit, A. Poustka, T.R. King, H. Lehrach, Cloning of the T gene required in mesoderm formation in the mouse, Nature 343 (1990) 617-622.

E. Hernando, E. Charytonowicz, M.E. Dudas, S. Menendez, I. Matushansky, J. Mills, N.D. Socci, N. Behrendt, L. Ma, R.G. Maki, P.P. Pandolfi, C. Cordon-Cardo, The AKT-mTOR pathway plays a critical role in the development of leiomyosarcomas, Nat Med 13 (6) (2007) 748-753.

Y. Hiroi, S. Kudoh, K. Monzen, Y. Ikeda, Y. Yazaki, R. Nagai, I. Komuro, Tbx5 associates with Nkx2-5 and synergistically promotes cardiomyocyte differentiation, Nat Genet 28 (3) (2001) 276-280.

W.M. Hoogaars, P. Barnett, M. Rodriguez, D.E. Clout, A.F. Moorman, C.R. Goding, V.M. Christoffels, TBX3 and its splice variant TBX3 + exon 2a are functionally similar, Pigment Cell Melanoma Res 21 (2008) 379–387.

A.G., Hovanessian, F., Puvion-Dutilleul, S., Nisole *et al*., The cell-surfaceexpressed nucleolin is associated with the actin cytoskeleton, Exp Cell Res 261 (2000) 312 – 328.

A. G., Hovanessian, C., Soundaramourty, D., El Khoury, I., Nondier, J., Svab, B., Krust, Surface Expressed Nucleolin Is Constantly Induced in Tumor Cells to Mediate Calcium-Dependent Ligand Internalization, PLoS ONE 5 (12) (2010) 1-13.

T.I. Hsu, S.C Lin, P.S. Lu, W.C. Chang, C.Y. Hung, Y.M. Yeh, W.C. Su, P.C. Liao, J.J. Hung, MMP7-mediated cleavage of nucleolin at Asp255 induces MMP9 expression to promote tumor malignancy, Oncogene34 (2015) 826–837.

Y.P. Hsueh, T.F. Wang, F.C. Yang, M. Sheng, Nuclear translocation and transcription regulation by the membrane-associated guanylate kinase CASK/LIN-2, Nature 404 (2000) 298-302.

Y., Huang, H., Shi, H., Zhou, X., Song, S., Yuan, Y., Luo, The angiogenesis function of nucleolin is mediated by vascular endothelial growth factor and nonmuscle myosin, Blood 107 (2006) 3564 – 3571.

C.Y. Hung, W.B. Yang, S.A. Wang, T.I Hsu, W.C. Chang, J.J. Hung, Nucleolin enhances internal ribosomal entry site (IRES)-mediated translation of Sp1 in tumorigenesis, Biochimica et Biophysica Acta 1843 (2014) 2843–2854.

P.J. Hurlin *et al*., Mga, a dual-specificity transcription factor that interacts with Max and contains a T-domain DNA-binding motif, EMBO J 18 (1999) 7019–7028.

J.Koren Ill, U.K. Jinwal, Y. Jin, J. O'Leary, J.R. Jones, A.G. Johnson, L.J. Blair, J.F. Abisambra, L. Chang, Y. Miyata, A.M. Cheng, J. Guo, J.Q. Cheng, J.E. Gestwicki, C.A. Dickey, Facilitating Akt Clearance via Manipulation of Hsp70 Activity and Levels, J Biolchem 285 (4) (2010) 2498 – 2505.

E. Iorns, K. Drews-Elger, T.M. Ward, S. Dean, J. Clarke, D. Berry, D. El Ashry, M. Lippman, A new mouse model for the study of human breast cancer metastasis, PLoS One 7 (10) (2012)

C.R. Ireson, L.R. Kelland, Discovery and development of anticancer aptamers, Mol Cancer Ther 5 (12) (2006) 2957-2962.

A. Ismail, A. Bateman, Expression of TBX2 promotes anchorage-independent growth and survival in the p53-negative SW13 adrenocortical carcinoma, Cancer Letters 278 (2009) 230–240.

A. Italiano, S. Mathoulin-Pelissier, A. Le Cesne, P. Terrier, S. Bonvalot, F. Collin, J.J. Michels, J.Y. J.M. Coindre, B. Bui, Trends in Survival for Patients With Metastatic Soft-Tissue Sarcoma, Cancer (2011) 1049-1054.

N. Ivanova, R. Dobrin, R. Lu, I. Kotenko, J. Levorse, C. DeCoste, X. Schafer, Y. Lun, I.R. Lemischka, Dissecting self-renewal in stem cells with RNA interference, Nature 442 (2006)

K. Iwao, Y. Miyoshi, G. Nawa *et al*., Frequent h-catenin abnormalities in bone and soft tissue tumors, Jpn J Cancer Res 90 (1999) 205–209.

M. Jäättelä, Over-expression of hsp70 confers tumorigenicity to mouse fibrosarcoma cells, Int J Cancer 60 (1995) 689–693.

J.J. Jacobs *et al*., Senescence bypass screen identifies TBX2, which represses Cdkn2a (p19(ARF)) and is amplified in a subset of human breast cancers, Nature genet 26 (2000) 291–299.

A.J. Jacobs, R. Michels, J. Stein, A.S. Levin, Improvement in Overall Survival from Extremity Soft Tissue Sarcoma over Twenty Years, Sarcoma (2015) 1-9.

S. Jain, G. Kapoor, Chemotherapy in Ewing's sarcoma, Indian J Orthop 44 (2010) 369-377.

L.A. Jerome, V.E. Papaioannou, DiGeorge syndrome phenotype in mice mutant for the T-box gene, Tbx1, Nature Genet 27 (2001) 286–291.

D.T. Jones, Protein secondary structure prediction based on position-specific scoring matrices, J Mol Biol 292 (1999) 195-202.

I. Judson, Targeted therapies in soft tissue sarcomas, Annals Oncol 21 (7) (2010) vii277–vii280.

K. Juhasz, A.M. Lipp, B. Nimmervoll, A. Sonnleitner, J. Hesse, T. Haselgruebler, Z. Balogi, The Complex Function of Hsp70 in Metastatic Cancer, Cancers 6 (2014) 42-66.

R. Kandimalla, A.A.G. van Tilborg, L.C. Kompier, D.J.P.M. Stumpel, R.W. Stam, C.H. Bangma, E.C. Zwarthoff, Genome-wide Analysis of CpG Island Methylation in Bladder Cancer Identified TBX2, TBX3, GATA2, and ZIC4 as pTa-Specific Prognostic Markers, European Urology 61 (2012) 1245-1256.

A.R. Karpf, S. Matsui, Genetic disruption of cytosine DNA methyltransferase enzymes induces chromosomal instability in human cancer cells, Cancer Res 65 (2005) 8635-8639.

V.P. Kashi, M.E. Hatley, R.L. Galindo, Probing for a deeper understanding of rhabdomyosarcoma: insights from complementary model systems, Nat Rev Cancer 15 (2015) 426–439.

A. Kavka, J. Green, Tales of tails: Brachyury and the T-box genes, Biochem Biophys Acts, 1333 (1997) 73-84.

A. Kawamura, S. Koshida, S. Takada, Activator-to-repressor conversion of T-box transcription factors by the Ripply family of Groucho/TLE-associated mediators, Mol Cell Biol 28 (2008) 3236–3244.

C. Keller, D.C. Guttridge, Mechanisms of impaired differentiation in rhabdomyosarcoma, FEBS J 280 (2013) 4323–4334.

K.H. Khan, T.A. Yap, L. Yan, D. Cunningham, Targeting the PI3K-AKT-mTOR signaling network in cancer, Chinese J Can 35 (5) (2013) 253-265.

K. Kikuchi, S. Hettmer, M.I. Aslam, J.E. Michalek, W. Laub, B.A. Wilky, D.M. Loeb, B.P. Rubin, A.J. Wagers, C. Keller, Cell-cycle dependent expression of a translocation-mediated fusion oncogene mediates checkpoint adaptation in rhabdomyosarcoma, PLoS Genet 10 (2014).

A. Kispert, B.G. Herrmann, The Brachyury gene encodes a novel DNA binding protein, EMBO J 12 (1993) 3211-3220.

E. Klopocki, L.M. Neumann, H. Tonnies, H.H. Ropers, S. Mundlos, R. Ullmann, Ulnar–mammary syndrome with dysmorphic facies and mental retardation caused by a novel 1.28 Mb deletion encompassing the TBX3 gene, Euro J Hum Genet 14 (2006) 1274-1279.

B.B. Koch, L.H. Karnell, H.T. Hoffman *et al.*, National cancer database report on chondrosarcoma of the head and neck, Head Neck 22 (2000) 408-425.

G. Kourkalis, *et al.*, Myc oncogene expression and nude mice tumourigenicity and metastasis formation are higher in alveolar than emrbyonal rhabdomyosarcoma cells, Pediatric Res 45 (1999) 552-558.

M. Koutsioumpa, C. Polytarchou, J. Courty, Y. Zhang, N. Kieffer, C. Mikelis, S.S. Skandalis, U. Hellman, D. Iliopoulos, E. Papadimitriou, Interplay between αvβ3 Integrin and Nucleolin Regulates Human Endothelial and Glioma Cell Migration, J Biol Chem 288 (1) (2013) 343-354.

H. Kubota, S. Yamamoto, E. Itoh, Y. Abe, A. Nakamura, Y. Izumi, H. Okada, M. Iida, H. Nanjo, H. Itoh, Y. Yamamoto, Increased expression of co-chaperone HOP with HSP90 and HSC70 and complex formation in human colonic carcinoma, Cell Stress Chaperones 15 (2010) 1003–1011.

T. Kuilman, C. Michaloglou, W.J. Mooi, D.S. Peeper, The essence of senescence, Genes Devel 24 (2010) 2463–2479.

P. Kumar, S. Franklin, U. Emechebe, H. Hu, B. Moore, C. Lehman, M. Yandell, A.M. Moon, TBX3 Regulates Splicing In Vivo: A Novel Molecular Mechanism for Ulnar-Mammary Syndrome, PLoS ONE Genet 10 (3) (2014)

P. Kumar, U. Emechebe, R. Smith, S. Franklin, B. Moore, M. Yandell, S.L. Lessnick, A.M. Moon, Coordinated control of senescence by lncRNA and a novel T-box3 co-repressor complex, eLIFE (2014b)

R.T. Kurmasheva, F.C. Harwood, P.J. Houghton, Differential regulation of vascular endothelial growth factor by Akt and mammalian target of rapa- mycin inhibitors in cell lines derived from childhood solid tumors, Mol Cancer Ther 6 (2007) 1620–1628.

W.Y. Lai, W.Y. Wang, Y.C. Chang, C.J. Chang, P.C. Yang, K. Peck, Synergistic inhibition of lung cancer cell invasion, tumor growth and angiogenesis using aptamer-siRNA chimeras, Biomaterials 35 (2014) 2905-2914.

B. Lamolet, A.M. Pulichino, T. Lamonerie, Y. Gauthier, T. Brue, A. Enjalbert, J. Drouin, A Pituitary Cell-Restricted T Box Factor, Tpit, Activates POMC Transcription in Cooperation with Pitx Homeoproteins, Cell 104 (2001) 849-859.

D.M. Langenau, M.D. Keefe, N.Y. Storer, J.R. Guyon, J.L. Kutok, X. Le, W. Goessling, D.S. Neuberg, L.M. Kunkel, L.I. Zon, Effects of RAS on the genesis of embryonal rhabdomyosarcoma, Genes Dev 21 (2007) 1382-1395.

J.H. Lee, P. Meltzer, Mechanisms of Sarcoma Development, Nature Rev 3 (2003) 685-693.

P.C. Leow, Q. Tian, Z.Y. Ong, Z. Yang, P.L. Rachel, Antitumor activity of natural compounds, curcumin and PKF118-310, as Wnt/β-catenin antagonists against human osteosarcoma cells, Invest New Drugs 28 (2010) 766–782.

M.T. Lewis, Homeobox genes in mammary gland development and neoplasia, Breast Cancer Res 2 (2000) 158–169.

J. Li, S.M. Weinberg, L. Zerbini, S. Prince, The oncogenic TBX3 is a downstream target and mediator of the TGF-1 signaling pathway, Mol Biol Cell 24 (2013) 3569–3576.

J. Li, D. Ballim, M. Rodriguez, R. Cui, C.R. Goding, H. Teng, S. Prince, The Anti-proliferative Function of the TGF-1 Signaling Pathway Involves the Repression of the Oncogenic TBX2 by Its Homologue TBX3, J Biol Chem 289 (51) (2014) 35633–35643.

Q.Y. Li *et al*., Holt-Oram syndrome is caused by mutations in TBX5, a member of the Brachyury (T) gene family, Nature Genet 15 (1997) 21 - 29.

L., Li, J., Hou, X., Liu, Y., Guo, Y., Wu, L., Zhang, Z., Yang, Nucleolin-targeting liposomes guided by aptamer AS1411 for the delivery of siRNA for the treatment of malignant melanomas, Biomaterials 35 (2014) 3840–3850

Y. Liao, L. Tang, The Critical Roles of HSC70 in Physiological and Pathological Processes, Curr Pharma Des 20 (1) (2014) 101-107.

J.M. Liberal, L. Lagares-Tena, M. Sainz-Jaspeado, S. Mateo-Lozano, X. Garcıa del Muro, O.M. Tirado, Targeted Therapies in Sarcomas: Challenging the Challenge, Sarcoma (2012) 1-13.

T.A. Libermann, L.F. Zerbini, Targeting transcription factors for cancer gene therapy. Current Gene Therapy, 6 (2006) 17-33.

M.E. Lingbeek, J.J.L. Jacobs, M.V. Lohuizen, The T-box Repressors TBX2 and TBX3 Specifically Regulate the Tumor Suppressor Genep14ARF via a Variant T-site in the Initiator, J Biol Chem 277 (2002) 26120-26127.

J. Liu, C. Lin, A. Gleiberman, K.A. Ohgi, T. Herman, H.P. Huang, M.J. Tsai, M.G. Rosenfeld, Tbx19, a tissue-selective regulator of POMC gene expression. PNAS 98 (2001) 8674-8679.

T. Liu, C.K. Daniels, S. Cao, Comprehensive review on the HSC70 functions, interactions with related molecules and involvement in clinical diseases and therapeutic potential, Pharmacol Therapeutics 136 (2012) 354–374.

C.Y. Logan, R. Nusse, The Wnt signaling pathway in development and disease, Ann Rev Cell Dev Biol 20 (2004) 781–810.

R. Lu, A. Yang, Y. Jin, Dual Functions of T-Box 3 (Tbx3) in the Control of Self-renewal and Extraembryonic Endoderm Differentiation in Mouse Embryonic Stem Cells, J Biol Chem 286 (2011) 8425–8436.

C.L. Mackall, P.S. Meltzer, L.J. Helma, Focus on sarcomas, Cancer Cell 2 (2002) 175-178.

A. MacMurray, H.S. Shin, The antimorphic nature of the Tc allele at the mouse T locus, Genet 120 (1988) 2545-2550.

S. Malempati, D.S. Hawkins, Rhabdomyosarcoma: Review of the Children's Oncology Group (COG) Soft-Tissue Sarcoma Committee Experience and Rationale for Current COG Studies, Pediatr Blood Cancer 59 (1) (2012) 5–10.

F. Marampon, C. Ciccarelli, B.M. Zani, Down-regulation of c-Myc following MEK/ERK inhibition halts the expression of malignant phenotype in rhabdomyosarcoma and in non muscle-derived human tumors, Mol Cancer 5 (31) (2006)

G.N. Marchenko, N.D. Marchenko, J. Leng, A.Y. Strongin, Promoter characterization of the novel human matrix metalloproteinase-26 gene: regulation by the T-cell factor-4 implies specific expression of the gene in cancer cells of epithelial origin, Biochem J 363 (2002) 253–562.

M. Maira *et al*., The T-box Factor Tpit Recruits SRC / p160 Co-activators and Mediates Hormone Action, J Biol Chem 278 (2003) 46523–46532.

G., Maridor and E.A., Nigg, cDNA sequences of chicken nucleolin/C23 and N038/B23, two major nucleolar proteins, Nucleic Acids Research, 18(5) (1990) 1286.

A.D. Marshall, G.C. Grosveld, Alveolar rhabdomyosarcoma—the molecular drivers of PAX3/7-FOXO1-induced tumorigenesis, Skelet Muscle 2 (2012) 25.

S. Martinelli, H.P. McDowell, S. Delle Vigne, G. Kokai, S. Uccini, M. Tartaglia, C. Dominici, RAS Signaling Dysregulation in Human Embryonal Rhabdomyosarcoma, Genes Chromo Cancer, 48 (2009) 975–982.

M. Martini, M.C. De Santis, L. Braccini, F. Gulluni, E. Hirsch, PI3K/AKT signaling pathway and cancer: an updated review, Ann Med (6) (2014) 372-383.

G.A. Maston, S.K. Evans, M.R. Green, Transcriptional regulatory elements in the human genome, Annu Rev Genomics Hum Genet 7 (2006) 29–59.

A., Masumi, H., Fukazawa, T., Shimazu, M., Yoshida, K., Ozato, K., Komuro *et al*., Nucleolin is involved in interferon regulatory factor-2-dependent transcriptional activation, Oncogene 25 (2006) 5113-5124.

I. Matushansky, E. Charytonowicz, J. Mills, S. Siddiqi, T. Hricik, C. Cordon-Cardo, MFH classification: differentiating undifferentiated pleomorphic sarcoma in the 21st century, Expert Rev Anticancer Ther 9 (8) (2009) 1135–1144.

M.P. Mayer, B. Bukau, Hsp70 chaperones: Cellular functions and molecular mechanism, Cell Mol Life Sci 62 (2005) 670–684.

K. McCune *et al*., Prognosis of hormone-dependent breast cancers: implications of the presence of dysfunctional transcriptional networks activated by insulin via the immune transcription factor T-bet, Cancer Res 70 (2011) 685–696.

C. Mees, J. Nemunaitis, Senzer, N. Transcription factors: their potential as targets for an individualized therapeutic approach to cancer, Cancer Gene Therapy 16 (2009) 103-112.

G. Merlino, L.J. Helman, Rhabdomyosarcoma—working out the pathways, Oncogene 18 (1999) 5340–5348.

S. Merscher *et al*., TBX1 is responsible for cardiovascular defects in velo-cardio facial/DiGeorge syndrome, Cell 104 (2001) 619–629.

N.J. Messenger, C. Kabitschke, R. Andrews, D. Grimmer, R. Núñez Miguel, T.L. Blundell, J.C. Smith, F.C. Wardle, Functional specificity of the Xenopus T-domain protein Brachyury is conferred by its ability to interact with Smad1, Dev Cel 8 (4) (2005) 599-610.

K. Miekus, E. Lukasiewicz, D. Jarocha, M. Sekula, G. Drabik, M. Majka, The decreased metastatic potential of rhabdomyosarcoma cells obtained through MET receptor downregulation and the induction of differentiation, Cell Death Disease, 4 (2013).

I. Mikami, L. You, B. He *et al*., Efficacy of Wnt-1 monoclonal antibody in sarcoma cells, BMC Cancer 5 (2005) 53–59.

K.L. Milarski, R.I. Morimoto, Expression of human HSP70 during the synthetic phase of the cell cycle, Proc Natl Acad Sci USA, 83 (24) (1987) 9517-9521.

R.R. Miller, P.G. Okkema, The Caenorhabditis elegans T-Box Factor MLS-1 Requires Groucho Co-Repressor Interaction for Uterine Muscle Specification, PLoS Genet 7 (8)

D.M. Miller, S.D. Thomas, A. Islam, D. Muench, K. Sedoris, c-Myc and Cancer Metabolism, Clin Cancer Res 18 (20) (2012) 5546–5553.

C. Minguillon, M. Logan, The comparative genomics of T-box genes, Briefings Functional Genom Proteom 2 (3) (2003) 224–233.

M. Moghanibashi, F.R. Jazii, Z.S. Soheili, M. Zare, A. Karkhane, K. Parivar, P. Mohamadynejad, Esophageal cancer alters the expression of nuclear pore complex binding protein Hsc70 and eIF5A-1, Funct Integr Genomics 13 (2013) 253–260.

T. Mosmann, Rapid colorimetric assay for cellular growth and survival: application to proliferation and cytotoxicity assays, J Immunol Methods 65 (1983) 55-63.

S. Mowla *et al*., PMA-induced up- regulation of TBX3 is mediated by AP-1 and contributes to breast cancer cell migration, Biochem J, 433 (2011) 145-153.

C.W. Muller, B.G. Herrmann, Crystallographic structure of the T domain-DNA complex of the Brachyury transcription factor, Nature 389 (1997) 884–888.

M. Murakami, M. Nakagawa, E.N. Olson, O. Nakagawa, A WW domain protein TAZ is a critical coactivator for TBX5, a transcription factor implicated in Holt–Oram syndrome, PNAS 102 (50) (2005) 18034–18039.

M.E. Murphy, The HSP70 family and cancer, Carcinogenesis (2013) 1-8.

S. Nagayama, C. Fukukawa, T. Katagiri *et al*., Therapeutic potential of antibodies against FZD 10, a cell- surface protein, for synovial sarcomas, Oncogene 24 (2005) 6201–6212.

L.A. Naiche *et al*., T-box genes in vertebrate development, Ann Rev
Genet 39 (2005) 219-223.

L.A. Naiche, V.E. Papaioannou, Loss of Tbx4 blocks hindlimb development and affects vascularization and fusion of the allantois, Dev 130 (2003) 2681-2693.

M. Nimmakayalu, H. Major, V. Sheffield, D.H. Solomon, R.J. Smith, S.R. Patil, O. Shchelochkov, Microdeletion of 17q22q23.2 encompassing TBX2 and TBX4 in a patient with congenital microcephaly, thyroid duct cyst, sensorineural hearing loss, and pulmonary hypertension, Am J Med Genet, Part A 155A (2011) 418–423.

C. Nardella, J.G. Clohessy, A. Alimonti, P.P. Pandolfi, Pro-senescence therapy for cancer treatment, Nat Rev Cancer

F. Nitzki, N. Cuvelier, J. Dräger, A. Schneider, T. Braun, H. Hahn, Hedgehog/Patched-associated rhabdomyosarcoma formation from delta1-expressing mesodermal cells, Oncogene (2015)

H. Niwa, K. Ogawa, D. Shimosato, K. Adachi, A parallel circuit of LIF signaling pathways maintains pluripotency of mouse ES cells, Nature 460 (2009).

S. Ognjanovic, A.M. Linabery, B. Charbonneau, J.A. Ross, Trends in childhood rhabdomyosarcoma incidence and survival in the United States, 1975-2005, Cancer 115 (2009) 4218-4226.

J.P. O'Neill, M.H. Bilsky, D. Kraus, Head and neck sarcomas: epidemiology, pathology, and management, Neurosurg Clin N Am 24 (2013) 67-78.

L.R., Orrick *et al*., Comparison of Nucleolar Proteins of Normal Rat Liver and Novikoff Hepatoma Ascites Cells by Two-Dimensional Polyacrylamide Gel Electrophoresis, PNAS, 70(5) (1973) 1316-1320.

S.K. Oster, C.S.W. Ho, E.L. Soucie, L.Z. Penn, The myc Oncogene: marvelously complex, Advances Cancer Res 84 (2002) 81-154.

D. Osuna, E. de Alava, Molecular pathology of sarcomas, Rev on recent clinical trials, 4 (2009) 12-26.

Y. Otake *et al.*, Overexpression of nucleolin in chronic lymphocytic leukemia cells induces stabilization of bcl2 mRNA, Blood 109 (7) (2007) 3069-3075.

A.D. Otten, E.J. Firpo, A.N. Gerber, L.L. Brody, J.M. Roberts, S.J. Tapscott,
Inactivation of MyoD-mediated expression of p21 in tumor cell lines, Cell Growth Differ 8 (1997) 1151–1160.

E.A. Packham, J.D. Brook, T-box genes in human disorders, Hum Mol Genet 12 (2003) 37–44.

D. Palmieria, T. Richmonda, C. Piovana, T. Sheetza, N. Zanesia, F. Troiseb, C. Jamesc, D. Wernickea, F. Nyeia, T.J. Gordond, J. Consiglioa, F. Salvatoreb, V. Coppolaa, F. Pichiorrie, C. De Lorenzob, C.M. Croce, Human anti-nucleolin recombinant immunoagent for cancer therapy, PNAS 112 (30) (2015) 9418–9423.

E.M. Pantelouris, Absence of thymus in the mouse, Nat 217 (1968) 370-371.

V.E. Papaioannou, T-box genes in development: From hydra to humans. International Review of Cytology, 207 (2001) 1-70.

V.E. Papaioannou, The T-box gene family: emerging roles in development, stem cells and cancer, Dev 141 (20) (2014) 3819-3833.

D.M. Parham, D.A. Ellison, Rhabdomyosarcoma in adults and children: an update, Arch Pathol Lab Med 130 (2006) 1454-1465.

J.C. Park *et al*., Epigenetic silencing of human T (brachyury homologue) gene in non-small-cell lung cancer, Biochem Biophys Res Comm, 365 (2008) 221–226.

S. Patane, S. Avnet, N. Coltella *et al*., MET over- expression turns human primary osteoblasts into osteosarcomas, Cancer Res 66 (2006) 4750–4757.

V. Paulson, G. Chandler, D. Rakheja, R.L. Galindo, K. Wilson, J.F. Amatruda *et al*., High-resolution array CGH identifies common mechanisms that drive embryonal rhabdomyosarcoma pathogenesis, Genes Chromosomes Cancer 50 (2011) 397–408.

J. Peres, E. Davis, S. Mowla, D.C. Bennett, J.A. Li, S. Wansleben, S. Prince, The highly homologous T-box transcription factors, TBX2 and TBX3, have distinct roles in the oncogenic process, Genes Cancer 1 (2010) 272-282.

J. Peres, S. Prince, The T-box transcription factor, TBX3, is sufficient to promote melanoma formation and invasion, Mol Cancer 12 (2013) 117-121.

J. Peres, S. Mowla, S. Prince, The T-box transcription factor, TBX3, is a key substrate of AKT3 in melanomagenesis, Oncotarget 6 (3) (2015) 1821-1833.

E.A. Perez *et al*., Rhabdomyosarcoma in children: a SEER population based study, J Surg Res 170 (2011) 243–251.

E.F. Petricoin, V. Espina, R.P. Araujo, B. Midura, C. Yeung, X. Wan, G.S. Eichler, D.J. Johann, S. Qualman, M. Tsokos, K. Krishnan, L.J. Helman, L.A. Liotta, Phosphoprotein pathway mapping: Akt/mammalian target of rapamycin activation is negatively associated with childhood rhabdomyosarcoma survival, Cancer Res 67 (2007) 3431-3440.

F., Pichiorri, D., Palmieri D, L., De Luca, J., Consiglio, J., You, A., Rocci, T., Talabere, C., Piovan, A., Lagana, L., Cascione, J., Guan, P., Gasparini, V., Balatti, G., Nuovo, V., Coppola, C.C.,

Hofmeister, G., Marcucci, J.C., Byrd, S., Volinia, C.L., Shapiro, M.A., Freitas, C.M., Croce CM, In vivo NCL targeting affects breast cancer aggressiveness through miRNA regulation, J Exp Med 210 (2013) 951–968.

Y. Pignochino, C. Dell'Aglio, M. Basirico, F. Capozzi, M. Soster, S. Marchio, S. Bruno, L. Gammaitoni, D. Sangiolo, E. Torchiaro, L. D'Ambrosio, F. Fagioli, S. Ferrari, M. Alberghini, P. Picci, M. Aglietta, G. Grignan, The Combination of Sorafenib and Everolimus Abrogates mTORC1 and mTORC2 Upregulation in Osteosarcoma Preclinical Models, Clin Cancer Res (2013) 2117-2131.

N. Platonova, M. Scotti, P. Babich, G. Bertoli, E. Mento, V. Meneghini, A. Egeo, I. Zucchi, G.R. Merlo, TBX3, the gene mutated in ulnar-mammary syndrome, promotes growth of mammary epithelial cells via repression of p19ARF, independently of p53, Cell Tissue Res 328 (2007) 301–316.

J.G. Pressey, J.R. Anderson, D.K. Crossman, J.C. Lynch, F.G. Barr, Hedgehog pathway activity in pediatric embryonal rhabdomyosarcoma and undifferentiated sarcoma: a report from the Children's Oncology Group, Pediatr Blood Cancer 57 (2011) 930–938.

S. Prince, S. Carreirs, K. Vance, Tbx2 Directly Represses the Expression of the p21WAF1 Cyclin-Dependent Kinase Inhibitor, Cancer Res 64 (2004) 1669–1674.

T. Qi, J. Han, Y. Cui, M. Zong, X. Liu, B. Zhu, Comparative proteomic analysis for the detection of biomarkers in pancreatic ductal adenocarcinomas, J Clin Pathol 61 (2008) 49-58.

J. Quesada, R. Amato, The Molecular Biology of Soft-Tissue Sarcomas and Current Trends in Therapy, Sarcoma, 2012, 1-16.

W., Qui, F., Zhou, Q., Zhang, X., Sun, X., Shi, Y., Liang, X., Wang, L. Yue, Overexpression of nucleolin and different expression sites both related to the prognosis of gastric cancer, APMIS 121 (2013) 919–925.

L. Raimondi, R. Ciarapica, M. De Salvo, F. Verginelli, M. Gueguen, C. Martini *et al*., Inhibition of Notch3 signalling induces rhabdomyosarcoma cell differentiation promoting p38 phosphorylation and p21(Cip1) expression and hampers tumour cell growth *in vitro* and *in vivo*, Cell Death Differ 19 (2012) 871–881.

M.L., Rankin et al., A complete nucleolin cDNA sequence from Xenopus laevis, Nucleic Acids Research, 21(1) (1993) 169.

D.D. Rao, J.S. Vorhies, N. Senzer, J. Nemunaitis, siRNA vs. shRNA: Similarities and differences, Advanced drug delivery rev 61 (2009) 746-759.

K.L. Redmond, N.T. Crawford, H. Farmer, Z.C. D'Costa, G.J. O'Brien, N.E. Buckle, R.D. Kennedy, P.G. Johnston, D.P. Harkin, P.B. Mullan, T-box 2 represses NDRG1 through an EGR1-dependent mechanism to drive the proliferation of breast cancer cells, Oncogene 29 (2010) 3252–3262.

T. Reinert, C. Modin, F.M. Castano, Comprehensive Genome Methylation Analysis in Bladder Cancer: Identification and Validation of Novel Methylated Genes and Application of These as Urinary Tumor Markers, Hum Cancer Biol 17 (2011) 5582–5592.

C.A. Renard, C. Labalette, C. Armengol, D. Cougot, Y. Wei, S. Cairo, P. Pineau, C. Neuveut, A. de Reynies, A. Dejean, C. Perret, M.A. Buendia, Tbx3 is a downstream target of the Wnt/beta-catenin pathway and a critical mediator of beta-catenin survival functions in liver cancer, Cancer Res 67 (2007) 901-910.

J. Renshaw, K.R. Taylor, R. Bishop, M. Valenti, A. De Haven Brandon, S. Gowan, S.A. Eccles, R.R. Ruddle, L.D. Johnson, F.I. Raynaud, J.L. Selfe, K. Thway, T. Pietsch, A.D. Pearson, J. Shipley, Dual blockade of the PI3K/AKT/mTOR (AZD8055) and RAS/MEK/ERK (AZD6244) pathways synergistically inhibits rhabdomyosarcoma cell growth in vitro and in vivo. AACR Clini Cancer Res 19 (2013) 5940-5951.

L., Ridley, R., Rahman, M.A., Brundler, D., Ellison, J., Lowe, K., Robson, E., Prebble, I., Luckett, R.J., Gilbertson, S., Parkes, V., Rand, B., Coyle, R.G., Grundy, Children's Cancer and Leukaemia Group Biological Studies Committee: Multifactorial analysis of predictors of outcome in pediatric intracranial ependymoma, Neuro Oncol 10 (2008) 675–689.

L.A.G. Ries, M.A. Smith, J.G. Gurney *et al*., Cancer incidence and survival among children and adolescents: United States SEER Program 1975–1995, NIH PubNCI SEER Program 99 (1999) 4649.

R. Ridzewski, Improving Therapies of Rhabdomyosarcoma (doctoral thesis in molecular medicine),
Georg-August University School of Science (2015) 1-126.

A. Rongvaux, H. Takizawa, T. Strowig, T. Willinger, E.E. Eynon, R.A. Flavell, M.G. Manz, Human hemato
lymphoid system mice: current use and future potential for Medicine, Annu Rev Immunol 31 (2013)
635–674.

J. Roma, A. Almazan-Moga, J. Sanchez de Toledo, S. Gallego, Notch, Wnt, and Hedgehog Pathways in
Rhabdomyosarcoma: From Single Pathways to an Integrated Network, Sarcoma (2012)

M. Rowley, E. Grothey, F.J. Couch, The Role of Tbx2 and Tbx3 in Mammary Development and
Tumorigenesis, J Mammary Gland Biol Neoplasia 9 (2004) 109-118.

A.P. Russ *et al*., Eomesodermin is required for mouse trophoblast development and mesoderm formation, Nature 404 (2000) 95-99.

R. Russell, M. Ilg, Q. Lin, G. Wu, A. Lechel, W. Bergmann, T. Eiseler, L. Linta, P. Kumar, M. Klingenstein, K. Adachi, M. Hohwieler, O. Sakk, S. Raab, A. Moon, M. Zenke, T. Seufferlein, H.R. Scholer, A. Illing, S. Liebau, A. Kleger, A Dynamic Role of TBX3 in the Pluripotency Circuitry, Stem Cell Reports 5 (2015) 1155–1170.

E.A., Said, B., Krust, S., Nisole, J., Svab, J.P., Briand, A.G., Hovanessian, The anti-HIV cytokine midkine binds the cell surface-expressed nucleolin as a low affinity receptor, J Biol Chem 277 (2002) 37492 – 37502.

T. Saito, Y. Oda, A. Sakamoto *et al*., APC mutations in synovial sarcomas. J Pathol 196 (2002) 445–449.

M. Sakabe *et al*., Ectopic retinoic acid signaling affects outflow tract cushion development through suppression of the myocardial Tbx2-Tgfβ2 pathway, Dev 139 (2012) 385–395.

S. Satheesha, G. Manzella, A. Bovay, E.A. Casanova, P.K. Bode, R. Bell, S. Feuchtgruber, P. Jaaks, N. Dogan, E. Koscielniak, B.W. Schäfer, Targeting hedgehog signaling reduces self-renewal in embryonal rhabdomyosarcoma, Oncogene (2015), 1–11.

E.V. Schmidt, The role of c-myc in cellular growth control, Oncogene 18 (1999) 2988-2996.

E. Schmitt *et al*., DNA-damage response network at the crossroads of cell-cycle checkpoints, cellular senescence and apoptosis, J Zhejiang Univ Sci B 8 (6) (2007) 377-397.

S., Schokoroy, D., Juster, Y., Kloog, R., Pinkas-Kramarski, Disrupting the Oncogenic Synergism between Nucleolin and Ras Results in Cell Growth Inhibition and Cell Death, PLoS ONE 8 (9) (2013) 1-12.

C. Schott, U. Graab, N. Cuvelier, H. Hahn, S. Fulda, Oncogenic RAS mutants confer resistance of RMS13 rhabdomyosarcoma cells to oxidative stress-induced ferroptotic cell death, Frontier Oncol 5 (131) (2015) 1-7.

L. Schweigerer, G. Neufeld, A. Mergia *et al*., Basic fibroblast growth factor in human rhabdomyosarcoma cells: implications for the proliferation and neovascularization of myoblast-derived tumors, Proc Natl Acad Sci U S A 84 (1987) 842–846.

A.D. Segni, K. Farin, R. Pinkas-Kramarski, Identification of Nucleolin as New ErbB ReceptorsInteracting Protein, PLoS ONE 3 (6) (2008) 1-.

M.V. Semenov, R. Habas, B.T. Macdonald, X. He, SnapShot: Noncanonical Wnt Signaling Pathways, Cell 131 (2007) 1378.

R. Sharp, J.A. Recio, C. Jhappan *et al*., Synergism between INK4a/ARF inactivation and aberrant HGF/SF signaling in rhabdomyosarcomagenesis, Nat Med 8 (2002) 1276–1280.

N.E. Sharpless, R.A. DePinho, The INK4A/ARF locus and its two gene products**,** Curr Opin Genet Dev 9 (1999) 22-30.

J.F. Shern, L. Chen, J. Chmielecki, J.S. Wei, R. Patidar, M. Rosenberg, L. Ambrogio, D. Auclair, J. Wang, Y.K. Song, C. Tolman, L. Hurd, H. Liao, S. Zhang, D. Bogen, A.S. Brohl, S. Sindiri, D. Catchpoole, T. Badgett, G. Getz, J. Mora, J.R. Anderson, S.X. Skapek, F.G. Barr, M. Meyerson, D.S. Hawkins, J. Khan, Comprehensive genomic analysis of rhabdomyosarcoma reveals a landscape of alterations affecting a common genetic axis in fusion-positive and fusion-negative tumors, Cancer Discov 4 (2014) 216–231.

C.J. Sherr, J.D. Weber, The ARF/p53 pathway*,* Curr Opin Genet Dev 10 (2000) 949-953.

M. Shiota, H. Kusakabe, Y. Izumi, Y. Hikita, Ta. Nakao, Y. Funae, K. Miura, H. Iwao, Heat Shock Cognate Protein 70 Is Essential for Akt Signaling in Endothelial Function, Arterioscler Thromb Vasc Biol, 30 (2010) 491-497.

L.D. Shultz, B.L. Lyons, L.M. Burzenski, B. Gott, X. Chen, S. Chaleff, M. Kotb, S.D. Gillies, M. King, J. Mangada, D.L. Greiner, R. Handgretinger, Human Lymphoid and Myeloid Cell Development in NOD/LtSz-scid IL2Rnull Mice Engrafted with Mobilized Human Hemopoietic Stem Cells, J Immunol 174 (10) (2005) 6477-6489.

J.D. Sims, J. McCready, D.G. Jay, Extracellular heat shock protein (Hsp)70 and Hsp90α assist in matrix metalloproteinase-2 activation and breast cancer cell migration and invasion, PLoS One 6 (2011).

M.K. Singh *et al*., Tbx20 is essential for cardiac chamber differentiation and repression of Tbx2, Dev 132 (2005) 2697–2707.

M.R. Sollazzo, M.S. Benassi, G. Magagnoli, G. Gamberi, L. Molendini, P. Ragazzini, M. Merli, C. Ferrari, A. Balladelli, P. Picci, Increased c-myc oncogene expression in Ewing's sarcoma: correlation with Ki67 proliferation index Tumori 85 (3) (1999) 167-173.

S. Soundararajan, L. Wang, V. Sridharan, W. Chen, N. Courtenay-Luck, D. Jones, E.K. Spicer, D.J. Fernandes, Plasma Membrane Nucleolin Is a Receptor for the Anticancer Aptamer AS1411 in MV4-11 Leukemia Cells, Mol Pharmacol 76 (2009) 984–991.

M., Srivastava *et al*., Cloning and sequencing of the human nucleolin cDNA, FEB 250(1) (1989) 99-105.

M., Srivastava & H.B., Pollard, Molecular dissection of nucleolin's role in growth and cell proliferation: new insights. FASEB J, 13 (1999) 1911 –1922.

D.C. Stefan, D.K. Stones, The South African Paediatric Tumour Registry – 25 years of activity, S Afri Med J 102 (7) (2012)

F.A. Stennard *et al*., Murine T-box transcription factor Tbx20 acts as a repressor during heart development, and is essential for adult heart integrity, function and adaptation, Dev 132 (2005) 2451–2462.

S. Storck, M. Shukl, S. Dimitrov, P. Bouvet, Functions of the histone chaperone nucleolin in diseases, Subcell Biochem 41 (2007) 125-144.

F. Stricher, C. Macri, M. Ruff, S. Muller, HSPA8/HSC70 chaperone protein Structure, function, and chemical targeting, Autophagy 9 (12) (2013) 1937–1954.

S. Sun, Z. Wang, Head neck squamous cell carcinoma c-Met^{+} cells display cancer stem cell properties and are responsible for cisplatin-resistance and metastasis, Int J Cancer 15 (2011) 2337–2348.

X. Sun, W. Guo, J.K. Shen, H.J. Mankin, F.J. Hornicek, Z. Duan, Rhabdomyosarcoma: Advances in Molecular and Cellular Biology, Sarcoma (2015)

A. Suzuki, S. Sekiya, D. Büscher, J. Carlos, I. Belmonte, H. Taniguchi, Tbx3 controls the fate of hepatic progenitor cells in liver development by suppressing p19ARF expression, Dev 135 (2008) 1589-1595.

N. Takebe, P. J. Harris, R. Q. Warren, S. P. Ivy, Targeting cancer stem cells by inhibiting Wnt, Notch, and Hedgehog pathways, Nat Rev Clin Oncol 8 (2) (2011) 97–106.

M., Takagi, M.J., Absalon, K.G., McLure, M.B., Kastan, Regulation of p53 Translation and Induction after DNA Damage by Ribosomal Protein L26 and Nucleolin, Cell 123 (2005) 49–63.

J.K Takeuchi *et al*., Tbx5 and Tbx4 genes determine the wing/leg identity of limb buds, Nature, 398 (1999) 810–814.

J.K Takeuchi *et al.*, Tbx5 and Tbx4 trigger limb initiation through activation of the Wnt/Fgf signaling cascade, Dev 130 (12) (2003) 2729-2739.

H. Takeuchi, A. Bilchik, S. Saha, R. Turner, D. Wiese, M. Tanaka, c-MET expression level in primary colon cancer: a predictor of tumor invasion and lymph node metastases, Clin Cancer Res 9 (2003) 1480–1488.

C.J. Tan, J.L. Yang, P. Crowe, D. Goldstein, Targeted therapy in soft tissue sarcoma—a novel direction in therapeutics, Chin Clin Oncol 2 (3) (2013) 22.

M. Tanaka, S. Mun1, A. Harada, Y. Ohkawa, A. Inagaki, S. Sano, K. Takahashi, Y. Izumi, M. Osada-Oka, H. Wanibuchi, M. Yamagata, T. Yukimura, K. Miura, M. Shiota, H. Iwao, Hsc70 Contributes to Cancer Cell Survival by Preventing Rab1A Degradation under Stress Conditions, PLoS ONE 9 (5) (2014) 1-11.

W.P. Tansey, Mammalian MYC Proteins and Cancer, New J Sci (2014)

R. Taulli, Validation of met as a therapeutic target in alveolar and embryonal rhabdomyosarcoma, Cancer Res, 66 (2006) 4742-4749.

J.G. Taylor, Identification of FGFR4-acivating mutations in human rhabdomyosarcomas that promote metastasis in xenotransplanted models, J Clin Invest 119 (2009) 3395-3407.

B.A. Teicher, Searching for molecular targets in sarcoma, Biochem Pharmacol 84 (1) (2012) 1-10.

J.R. Testa, P.N. Tsichlis, AKT signaling in normal and malignant cells, Oncogene 24 (2005) 7391–7393.

D.M. Thomas, S.A. Savage, G.L. Bond, Hereditary and environmental epidemiology of sarcomas, Clin Saromca Res 2 (13) (2012)

J.D. Thomas, Y. Zhang, Y. Wei, J.H. Cho, L.E. Morris, H.Y. Wang, S. Zheng, Rab1A Is an mTORC1 Activator and a Colorectal Oncogene, Cancer Cell, 26 (5) (2014) 754–769.

Y. Tomita, T. Morooka, Y. Hoshida, B. Zhang, Y. Qiu, I. Nakamichi, K. Hamada, T. Ueda, N. Naka, I. Kudawara, K. Aozasa, Prognostic Significance of Activated AKT Expression in Soft-Tissue Sarcoma, Clin Cancer Res 12 (10) (2006) 3070-3077.

P.N. Tonin, H. Scrable, H. Shimad, W.K. Cavenee, Muscle-specific gene expression in rhabdomyosarcomas and stages of human fetal skeletal muscle development, Cancer Res 51 (19) (1991) 5100-5106.

C.S. Trempus *et al*., A novel role for the T-box transcription factor Tbx1 as a negative regulator of tumor cell growth in mice, Mol Carcinogenesis 50 (2011) 981–991.

H. Tsumura, T. Yoshida, H. Saito, K. Imanaka-Yoshida, N. Suzuki, Cooperation of oncogenic K-ras and p53 deficiency in pleomorphic rhabdomyosarcoma development in adult mice, Oncogene 25 (59) (2006) 7673-7679.

M. Tulchin, G. Chambon, S. Juan, J. Dikman, L. Strauchen, B. Ornstein, N.T. Billack, A.N.A. Woods, A. Monteiro, BRCA1 Protein and Nucleolin Colocalize in Breast Carcinoma Tissue and Cancer Cell Lines, Am J Patho 176 (3) (2010) 1203-.

R., Tuteja & N., Tuteja, Nucleolin: a multifunctional major nucleolar phosphoprotein. Critical Reviews in Biochemistry and Molecular Biology, 33(6) (1998), 407-436.

D.J., Uribe, K., Guo, Y.J., Shin, D., Sun, Heterogeneous nuclear ribonucleoprotein K and nucleolin as transcriptional activators of the vascular endothelial growth factor promoter through interaction with secondary DNA structures, Biochem 50 (2011) 3796- 806.

A. Valkov, T.K. Kilvaer, S.W. Sorbye, T. Donnem, E. Smeland, R.M. Bremnes, L.T. Busund, The prognostic impact of Akt isoforms, PI3K and PTEN related to female steroid hormone receptors in soft tissue sarcomas, J Transla Med 9 (200) (2011) 1-12.

K.W. Vance, S. Carreira, G. Brosch, C.R. Goding, Tbx2 is overexpressed and plays an important role in maintaining proliferation and suppression of senescence in melanomas, Cancer Res 65 (2005) 2260–2268.

A. Van Der Schyff, D.C. Stefan, Clinical characteristics and outcome of rhabdomyosarcoma in South African children, Afr J Haematol Oncol 1 (2) (2010) 40-47.

M.C. Verhoeven, C. Haase, V.M. Christoffels, G. Weidinger, J. Bakkers, Wnt signaling regulates atrioventricular canal formation upstream of BMP and Tbx2, Birth Defects Research, Part A, Clin Mole Teratology 91 (2011) 435–440.

S. Vijayakumar, G. Liu, I.A. Rus, S. Yao, Y. Chen, G. Akiri, L. Grumolato, S.A. Aaronson, Wnt signaling is activated at high frequency and drives proliferation of multiple human sarcoma subtypes through a TCF/β-catenin target gene, CDC25A, Cancer Cell 19 (5) (2011) 601–612.

W.H. Vila-Carriles, Z.H. Zhou, J.K. Bubien, C.M. Fuller, D.J. Benos, Participation of the Chaperone Hsc70 in the Trafficking and Functional Expression of ASIC2 in Glioma Cells, J Biol Chem 282 (47) (2007) 34381–34391.

F. Vitelli *et al*., TBX1 is required for inner ear morphogenesis. Hum Mol Genet 12 (2003) 2041–2048.

M. Wachtel, J. Rakic, M. Okoniewski, P. Bode, F. Niggli, B.W. Schafer, FGFR4 signaling couples to Bim and not Bmf to discriminate subsets of alveolar rhabdomyosarcoma cells, Int J Cancer 135 (2014) 1543–1552.

A. Waghray, N. Saiz, A.D. Jayaprakash, A.G. Freire, D. Papatsenko, C.F. Pereira, D.F Lee, R. Brosh, B. Chang, H. Darr, J. Gingold, K. Kelley, C. Schaniel, A.K. Hadjantonakis, I.R. Lemischka, Tbx3 Controls Dppa3 Levels and Exit from Pluripotency toward Mesoderm, Stem Cell Report 5 (2015) 97-110.

X. Wan, L.J. Helman, Levels of PTEN protein modulate Akt phosphorylation on serine 473, but not on threonine 308, in IGF-II-overexpressing rhabdomyosarcomas cells, Oncogene 22 (2003).

C. Wang, Childhood rhabdomyosarcoma: recent advances and prospective views, J Dent Res 91 (2012) 341–350.

N. Wang, Y.L. He, L.J. Pang, H. Zou, C.X. Liu, J. Zhao, J.M. Hu, W.J. Zhang, Y. Qi, F. Li, Down-Regulated E-Cadherin Expression Is Associated with Poor Five-Year Overall Survival in Bone and Soft Tissue Sarcoma: Results of a Meta-Analysis, PLoS ONE (2015)

T.F. Wang, C.N. Ding, G.S. Wang, S.C. Luo, Y.L. Lin, Y. Ruan, R. Hevner, J.L.R. Rubenstein, Y.P. Hsueh, Identification of Tbr-1/CASK complex target genes in neurons, J Neurochem 91 (2004) 1483–1492.

T., Watanabe, H., Tsuge, T., Imagawa, D., Kise, K., Hirano, M., Beppu *et al*., Nucleolin as cell surface receptor for tumor necrosis factor alpha inducing protein: a carcinogenic factor of Helicobacter pylori, J Cancer Res Clin Oncol 136 (2010) 911-921.

Q. Wei, B.M. Paterson, Regulation of MyoD function in the dividing myoblast, FEBS Lett 490 (2001) 171–178.

K.M. Weidner, M. Sachs, W, Birchmeier, The Met receptor tyrosine kinase transduces motility, proliferation, and morphogenic signals of scatter factor/hepatocyte growth factor in epithelial cells, J Cell Biol 121 (1993) 145–154.

C.E. Weidgang, T. Seufferlein, A. Kleger, M. Mueller, Pluripotency Factors on Their Lineage Move, Stem Cell Int (2016) 1-16.

D.G. Wilkinson, S. Bhatt, B.G. Herrmann, Expression pattern of the mouse T gene and its role in mesoderm formation, Nature 343 (1990) 657-659.

T. Willmer, A. Cooper, D. Sims, D. Govender, S. Prince, The T-box transcription factor 3 is a promising biomarker and a key regulator of the oncogenic phenotype of a diverse range of sarcoma subtypes, Oncogenesis, In press (2016)

T. Willmer, S. Hare, J. Peres, S. Prince, The T-box transcription factor TBX3 represses the expression of the $p21^{WAF1}$ cyclin-dependent kinase inhibitor, Submitted to Cell Division (under review) (IF=3.526) (2016b)

V. Wilson, F.L. Conlon, Protein family review: The T-box family, Genome Biol 3 (2002) 1-7.

C.E. Winbanks, TGF-beta regulates miR-206 and miR-29 to control myogenic differentiation through regulation of HDAC4, J Biol Chem 286 (2011) 13805-13814.

B. Wu, S.P. Crampton, C.C. Hughes, Wnt signaling induces matrix metalloproteinase expression and regulates T cell transmigration, Immunity 26 (2007) 227–239.

D.M. Wu, P. Zhang, R.Y. Liu, Y.X. Sang, C. Zhou, G.C. Xu, J.L. Yang, A.P. Tong, C.T. Wang, Phosphorylation and changes in the distribution of nucleolin promote tumor metastasis via the PI3K/Akt pathway in colorectal carcinoma, FEBS Letters 588 (2014) 1921–1929.

P. Xia, X.Y. Xu, PI3K/Akt/mTOR signaling pathway in cancer stem cells: from basic research to clinical application, Am J Cancer Res 5 (5) (2015) 1602-1609.

F.M. Yakes, J. Chen, J. Tan, K. Yamaguchi, Y. Shi, P. Yu, Cabozantinib (XL184), a novel MET and VEGFR2 inhibitor, simultaneously suppresses metastasis, angiogenesis, and tumor growth, Mol Cancer Ther 10 (2011) 2298–2308.

A., Yang, G., Shi, C., Zhou, R., Lu, H., Li, L., Sun, Y., Jin, Nucleolin Maintains Embryonic Stem Cell Self-renewal by Suppression of p53 Protein-dependent Pathway, J Biol Chem 286 (50) (2011) 43370-43382.

X.R. Yang *et al*., T (brachyury) gene duplication confers major susceptibility to familial chordoma, Nature Genet 41 (2009) 1176–1178.

W. Yarosh *et al*., TBX3 Is Overexpressed in Breast Cancer and Represses p14 ARF by Interacting with Histone Deacetylases, Cancer Res (2008) 693-699.

J. Yu *et al*., Epigenetic inactivation of T-box transcription factor 5, a novel tumour suppressor gene, is associated with colon cancer, Oncogene 29 (2010) 6464–6474.

J. Yuan, C.M. Dutton, S.P. Scully, RNAi mediated MMP-1 silencing inhibits human chondrosarcoma invasion, J Orthop Res 23 (2005) 1467–1474.

M. Zaragoza *et al*., Identification of the TBX5 transactivating domain and the nuclear localization signal, Gene, 330 (2004) 9–18.

D. Zhao, Y. Wu, K. Chen, Tbx3 isoforms are involved in pluripotency maintaining through distinct regulation of Nanog transcriptional activity, Biochem Biophys Res Commun 444 (2014) 411-414.

R. Zhang, W. Chen, P.D. Adams, Molecular Dissection of Formation of Senescence-Associated Heterochromatin Foci, Mol Cel Biol 27 (6) (2007) 2343–2358.

H., Zhao, Y., Huang, C., Xue, Y., Chen, X., Hou, Y., Guo, L., Zhao, Z., Hu, Y., Huang, Y., Luo, L., Zhang, Prognostic Significance of the Combined Score of Endothelial Expression of Nucleolin and CD31 in Surgically Resected Non-Small Cell Lung Cancer, PLoS ONE 8(1) (2013)

B. Zhu B, M. Zhang, E.M. Williams, C. Keller, A. Mansoor, J.K. Davie, TBX2 represses PTEN in rhabdomyosarcoma and skeletal muscle, Oncogene, (2015) 1-13.

B. Zhu B, M. Zhang, S.D. Byrum, A.J. Tackett, J.K. Davie, TBX2 blocks myogenesis and promotes proliferation in rhabdomyosarcoma cells. Int J Cancer 135 (2014) 785–797.

Q.S. Zhu, W. Ren, B. Korchin, G. Lahat, A. Dicker, Y. Lu, G. Mills, R.E. Pollock, D. Lev, Soft Tissue Sarcoma Are Highly Sensitive to AKT Blockade: A Role for p53 Independent Up-regulation of GADD45α, Cancer Res 68 (8) (2008) 2895–2903.

A. Zibat, E. Missiaglia, A. Rosenberger, K. Pritchard-Jones, J. Shipley, H. Hahn *et al.,* Activation of the hedgehog pathway confers a poor prognosis in embryonal and fusion gene-negative alveolar rhabdomyosarcoma, Oncogene 29 (2010) 6323–6330.

M. Zillhardt, J.G. Christensen, E. Lengyel, An orally available small-molecule inhibitor of c-Met, PF-2341066, reduces tumor burden and metastasis in a preclinical model of ovarian cancer metastasis, 10 (2010) 1–10.

M. Zillhardt, S.M. Park, I.L. Romero, K. Sawada, A. Montag, T. Krausz, Foretinib (GSK1363089), an orally available multikinase inhibitor of c-Met and VEGFR-2, blocks proliferation, induces anoikis, and impairs ovarian cancer metastasis, Clin Cancer Re 17 (2011) 4042–4051.

M. Zong, M. Meng, L. Li, Low Expression of TBX4 Predicts Poor Prognosis in Patients with Stage II Pancreatic Ductal Adenocarcinoma, Int J Mol Sci 12 (2011) 4953-4963.

E. Zorzi, P. Bonvini, Inducible Hsp70 in the Regulation of Cancer Cell Survival: Analysis of Chaperone Induction, Expression and Activity, Cancers 3 (2011) 3921-3956.

Chapter 6. Appendix

Recipes, reagents and figures

6.1 Plasmids and DNA constructs

6.1.1 3XFlag-CMV (Addgene):

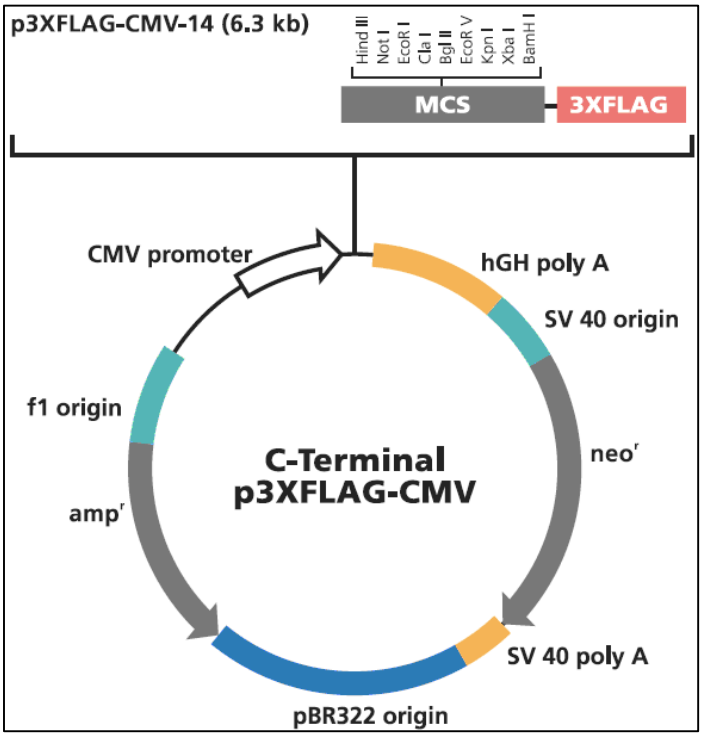

6.1.2 pSuper.neo/GFP (Oligoengine)**:**

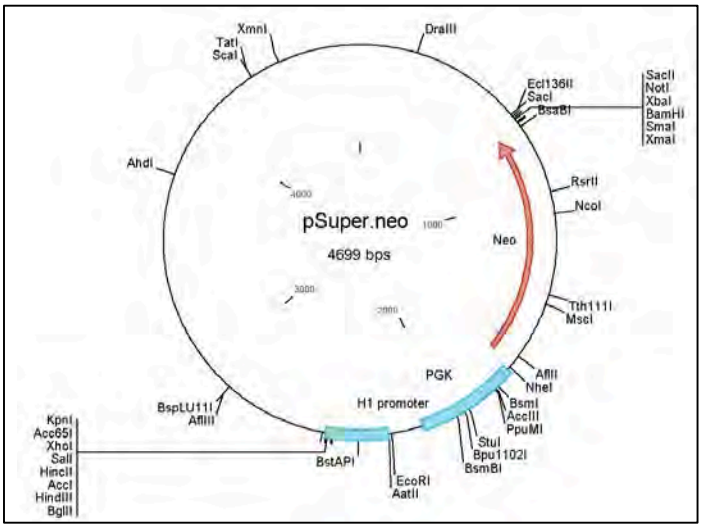

6.1.3 pEGFP-Nucleolin (Addgene)**:**

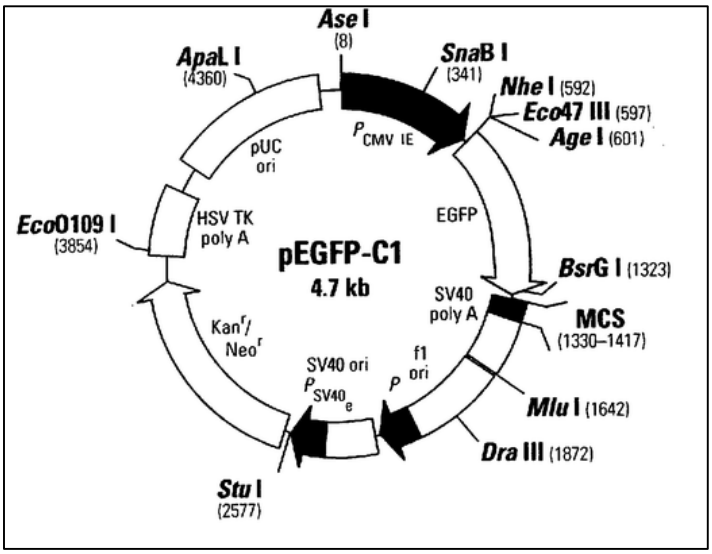

6.2 Cell culture

Mycoplasma test mounting fluid:
20 mM Citric acid
55 mM $Na_2HPO_4.2H_2O$
50% Glycerol
pH to 5.5 and store at 4°C

6.3 Protein isolation and western blotting

Phosphate buffered saline (PBS)/0.1% Tween
10X PBS:
80g NaCl
26.8g $Na_2HPO_4.12H_20$
2g KCl
2.4g KH_2PO_4
Make up to 1L, pH to 6.9 and autoclave
For use dilute to 1 X (100ml 10X PBS; make up to 1L with dH_20)

PBS/0.1% Tween:
For membrane washes, add 0.1% Tween to 1X PBS

2 X Protein loading dye:
125 mM Tris-HCl, pH 6.5

0.4% SDS
10% β-mercaptoethanol
20% glycerol

5 X Protein loading dye:
10% glycerol
1% SDS
0.25M Tris-Cl, pH 6.8
3mg Bromophenol blue

2 X Boiling Blue: 10ml
1M Tris-HCL, pH 6.8
4ml 10% SDS
1ml β-mercaptoethanol
2ml glycerol
1.75ml dH_2O
Pinch of bromophenol blue
Store at -20°C

Sodium Dodecyl Sulphate (SDS)-polyacrylamide gels
Acryl-bisacryl-amide mix (30:08)
29 g acrylamide
1g N,N`-methylenebisacrylamide
Make up to 100 ml, heat at 37°C to dissolve chemicals.
Store at 4°C, protected from light

10% Sodium docecyl sulphate (SDS)
100g SDS
Make up to 1L with dH_20, pH to 7.2
Store at RT

10% Ammonium persulphate (APS)
0.1g ammonium persulphate
Make solution up to 1ml with dH_20
Store at 4°C

Resolving gel:
Acryl-bisacryl-amide mix (30:08) (percentage depending on size of protein of interest) 0.375 M Tris (pH 8.8)
0.1% SDS
0.01% TEMED

0.1% Ammonium persulphate

Stacking gel:
5% Acryl-bisacryl-amide mix (30:08)
0.192 M Tris (pH6.8)
0.1% SDS
0.01% TEMED
0.1% Ammonium persulphate

10X Running buffer:
10g SDS
30g Tris
144g Glycine pH to 8.3 and make solution up to 1L with dH_20
For use dilute to 1 X (100ml 10X PBS; make up to 1L with dH_20)

10X Transfer buffer:
38g Tris
144g Glycine
Make solution up to 1L with dH20 and store at 4°C
For use dilute 1 X (100ml 10 X Transfer Buffer, 200ml Isopropanol and 700ml dH_20)
Store at 4°C

5% PBS/T milk
5% powder milk (w/v)
Make up to 100ml with 1 XPBS/0.1% Tween-20
Store at 4°C

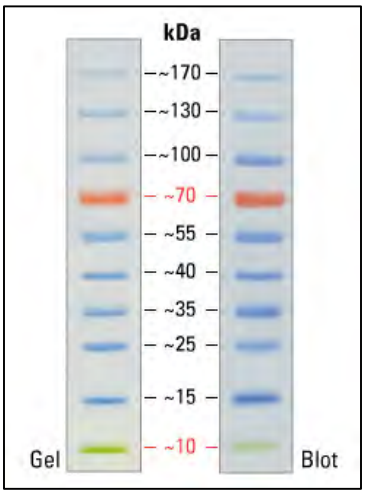

Figure 6.1: PageRuler Pre-stained Protein Marker

6.4. Affinity purification assays

FLAG-lysis buffer
50 mM Tris HCl, pH 7.4
150 mM NaCl
1 mM EDTA
1% TRITON X-100
Protease inhibitors were added before use:
2 µg/ml aprotinin
0.7 µg/ml pepstatin A
2 mM NaF
0.2 mM phenylmethanesulphonyl fluoride (PMSF)

Co-immunoprecipitation assays
RIPA-IP buffer
0.05 M Tris-HCl, pH 8
0.15 M NaCl
0.1% NP-40
0.1% sodium deoxycholate
0.1% SDS
5 mM EDTA
1 mM DTT
Protease inhibitors were added before use:
1µg/ml aprotinin
1µg/ml pepstatin
10 mM NaF
0.5mM PMSF
0.01 mM sodium orthovanadate
2 complete proteinase inhibitor tablets

preferences

turnitin
Originality Report

Processed on: 11-Apr-2016 13:50 SAST
ID: 657631628
Word Count: 19275
Submitted: 1

smtdan013:MScMed_for
By Nici Smuts

Similarity Index
25%

Similarity by Source
Internet Sources: 5%
Publications: 9%
Student Papers: 22%

Document Viewer

include quoted | include bibliography | excluding matches < 12 words

mode: show highest matches together

Cancer remains one of the leading causes of death worldwide due to late diagnosis and ineffective treatment options. To address this problem requires the elucidation of the molecular mechanisms, including the signaling pathways and transcription factors that drive cancer initiation and progression. In this regard, our laboratory has been particularly interested in the embryonically importantly

T-box family of transcription factors which has been heavily **implicated in** 25

promoting initiation and progression of a long list of cancers. For example, the

overexpression of the T-box factor TBX3, has been reported to function **in** 3

promoting immortalization, migration, invasion and tumour formation in a number of epithelial-derived malignancies. Furthermore, our laboratory recently reported that TBX3 is also overexpressed in a wide range of sarcoma subtypes including rhabdomyosarcomas which suggests that TBX3 may also contribute to the development and/or progression of sarcomas and potentially may serve as a biomarker for their diagnosis and targeted therapy. This is exciting because sarcomas are diverse and heterogeneous cancers with varying clinical behaviours, high rates of metastasis and recurrence and are notoriously resistant to current chemotherapies. However whether TBX3 is a molecular driver of these mesenchymal-derived cancers remains to be determined. This project therefore aimed to elucidate the role of TBX3 overexpression in emrbyonal rhabdomyosarcomas (ERMS) which

is the most common soft tissue sarcoma in children and adolescents. 15

Using ERMS

cell culture models in which TBX3 was either stably knocked down **or overexpressed** this study shows **that TBX3** promotes ERMS **cell proliferation,** anchorage independent growth **and** 1

cell migration in vitro and tumour formation in vivo. Furthermore,

nucleolin and TBX3 interact and **co-operate to promote proliferation and migration of** ERMS **cells** 1

1 16% match (student papers from 14-Oct-2015)
Submitted to University of Cape Town

2 2% match (student papers from 29-Oct-2011)
Submitted to University of Cape Town

3 1% match (student papers from 04-Mar-2016)
Submitted to University of Cape Town

4 1% match (student papers from 11-Oct-2015)
Submitted to University of Cape Town

5 1% match (publications)
Willmer, T, A Cooper, D Sims, D Govender, and S Prince. "The T-box transcription factor 3 is a promising biomarker and a key regulator of the oncogenic phenotype of a diverse range of sarcoma subtypes", Oncogenesis, 2016.

6 < 1% match (publications)
Willmer, Tarryn, Jade Peres, Shaheen Mowla, Amaal Abrahams, and Sharon Prince. "The T-Box factor TBX3 is important in S-phase and is regulated by c-Myc and cyclin A-CDK2", Cell Cycle, 2015.

7 < 1% match (student papers from 30-Oct-2013)
Submitted to University of Cape Town

8 < 1% match (publications)
Wansleben, Sabine, Jade Peres, Shannagh Hare, Colin R. Goding, and Sharon Prince. "T-